

A100422558

U.S. DEPARTMENT OF COMMERCE  
National Technical Information Service

PB-264 019

# Fracture Behavior of Fiberglass Reinforced Plastics Suitable for Hull Materials

Massachusetts Inst of Tech, Cambridge. Sea Grant Program

DISTRIBUTION STATEMENT A  
Approved for public release  
Distribution Unlimited

DEPARTMENT OF DEFENSE  
PLASTICS TECHNICAL EVALUATION CENTER  
PICATINNY ARSENAL, DOVER, N. J.

Prepared for

National Oceanic and Atmospheric Administration, Rockville, Md Office of  
Sea Grant

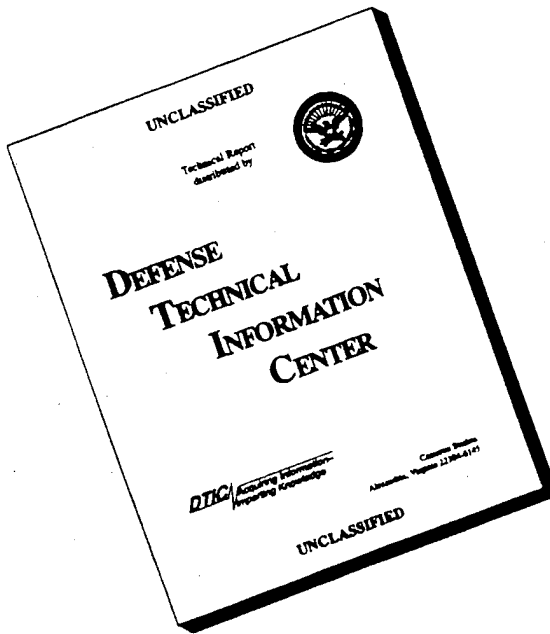
Dec 76

*2-3 Dec 1976*  
PLASTEC *2-3 Dec 1976*

19960227 032

DTIC QUALITY INSPECTED 1

# DISCLAIMER NOTICE



THIS DOCUMENT IS BEST  
QUALITY AVAILABLE. THE  
COPY FURNISHED TO DTIC  
CONTAINED A SIGNIFICANT  
NUMBER OF PAGES WHICH DO  
NOT REPRODUCE LEGIBLY.

77011906

PB 264 019

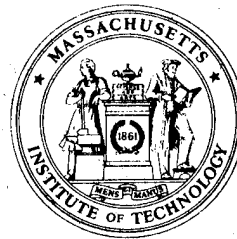


MIT  
SEA  
GRANT  
PROGRAM

# **FRACTURE BEHAVIOR OF FIBERGLASS REINFORCED PLASTICS SUITABLE FOR HULL MATERIALS**

by

**John F. Mandell  
Frederick J. McGarry**



Massachusetts Institute of Technology

Cambridge, Massachusetts 02139

REPRODUCED BY  
**NATIONAL TECHNICAL  
INFORMATION SERVICE**  
U. S. DEPARTMENT OF COMMERCE  
SPRINGFIELD, VA. 22161

Report No. MITSG 75-25

December 1976

## BIBLIOGRAPHIC DATA SHEET

1. NOAA ACCESSION NUMBER NOAA-77011906	2.	3. RECIPIENT'S ACCESSION NUMBER
4. TITLE AND SUBTITLE Fracture Behavior of Fiberglass Reinforced Plastics Suitable for Hull Materials		5. REPORT DATE Dec 1976
7. AUTHOR(S) John F. Mandell and Frederick J. McGarry		6.
9. PERFORMING ORGANIZATION NAME AND ADDRESS Massachusetts Institute of Technology, Cambridge, MA 02139 Department of Materials Science		8. REPORT NO. MITSG 75-25
12. SPONSORING ORGANIZATION NAME AND ADDRESS NOAA, Washington, DC, 20235 Office of Sea Grant		10. PROJECT/TASK NO. SG=04-6-158-44007
		11. CONTRACT/GRANT NO.
		13. TYPE OF REPORT AND PERIOD COVERED
		14.
15. PUBLICATION REFERENCE Massachusetts Institute of Technology Sea Grant Report No. MITSG-75-25, /December 1976. 120 p. 44 fig, 8 tab, 61 ref.		
16. ABSTRACT This report summarizes research done under the project, "Fracture Mechanics of Fiberglass Reinforced Plastic Composites Suitable for Hull Materials," which was completed in June 1975. The study was divided into three areas: (1) the effects of material and geometric variables, time and temperature on the fracture toughness of the fiberglass laminates; (2) cyclic fatigue crack propagation; and (3) marine environment effects. In each case, the mechanisms of fracture in fiberglass hull materials have been studied with a view toward preventing catastrophic failures. (Author modified)		
17. KEY WORDS AND DOCUMENT ANALYSIS		
17A. DESCRIPTORS Fiberglass reinforced plastics, Hulls (structures), Fractures (materials), Fatigue (Materials), Composite materials, Reinforced plastics		
17B. IDENTIFIERS/OPEN-ENDED TERMS Marine environment, Sea Grant Program		
17C. COSATI FIELD/GROUP 11D, 11I, 14G		
18. AVAILABILITY STATEMENT Released for distribution: <i>Sarah J. Kroll</i>	19. SECURITY CLASS ( <i>This report</i> ) UNCLASSIFIED	21. NO. OF PAGES
	20. SECURITY CLASS ( <i>This report</i> ) UNCLASSIFIED	

FRACTURE BEHAVIOR OF FIBERGLASS REINFORCED  
PLASTICS SUITABLE FOR HULL MATERIALS

by

John F. Mandell  
Frederick J. McGarry

Report No. MITSG 75-25  
Index No. 75-325-Ifn

1a)

Authors

John F. Mandell and Frederick J. McGarry are professors in M.I.T.'s Department of Materials Science.

Acknowledgements

This report describes the results of research done as part of the M.I.T. Sea Grant Program with support from the Office of Sea Grant in the National Oceanic and Atmospheric Administration, U.S. Department of Commerce, through grant number 04-6-158-44007, and from the Massachusetts Institute of Technology.

Related Reports

Mandell, John, Frederick McGarry, Reiichiro Kashiwara, and William Bishop. ENGINEERING ASPECTS OF FRACTURE TOUGHNESS: FIBER REINFORCED LAMINATES. MITSG 73-9, NTIS COM-74-10365. Cambridge: Massachusetts Institute of Technology, June 1973. 50 pp.

Demchick, Robert P., John F. Mandell, and Frederick McGarry. MARINE ENVIRONMENT EFFECTS ON FATIGUE CRACK PROPAGATION IN GRP LAMINATES FOR HULL CONSTRUCTION. MITSG 73-16. Cambridge: Massachusetts Institute of Technology, November 1973. 72 pp.

Mandell, John F. FATIGUE CRACK PROPAGATION RATES IN WOVEN AND NON-WOVEN FIBERGLASS LAMINATES. MITSG 74-21, NTIS COM-74-11257/AS. Cambridge: Massachusetts Institute of Technology. April 1974. 20 pp.

Snyder, Paul G., John F. Mandell, and Frederick McGarry. THE IMPACT RESISTANCE OF MODIFIED FERRO-CEMENT PANELS. MITSG 74-18, NTIS COM-74-11248/AS. Cambridge: Massachusetts Institute of Technology, March 1974. 74 pp.

Note: The preceding publications may be ordered from the National Technical Information Service, U.S. Department of Commerce, Springfield, Virginia 22151. Use the NTIS number when ordering; prices are variable.

TABLE OF CONTENTS

	<u>Page</u>
Summary.....	1
Section I      FRACTURE TOUGHNESS.....	2
Introduction.....	2
Materials and Test Methods.....	3
Characteristics of Fracture.....	6
Notch Geometry Effects.....	9
Fracture Criteria and Specimen Size Effects.....	12
Laminate Thickness Effects.....	15
Strain Rate and Temperature Effects.....	17
Effects of Material Composition.....	18
Conclusion.....	19
References.....	21
Tables.....	23
Figures.....	25
Section II      FATIGUE CRACK GROWTH.....	51
Introduction.....	51
Theory.....	51
Materials and Test Methods .....	53
Results and Discussion.....	55
Conclusions.....	59
References.....	60
Tables.....	61
Figures.....	62
Section III      EFFECTS OF MARINE ENVIRONMENT....	71
Introduction.....	71
Experimental Methods.....	74
Theoretical Prediction.....	77
Results.....	80
Discussion.....	84
Conclusions.....	92
References.....	93
Tables.....	96
Figures.....	101

## ABSTRACT

This report summarizes research done under the project, "Fracture Mechanics of Fiberglass Reinforced Plastic Composites Suitable for Hull Materials," which was completed in June 1975. The study was divided into three areas: 1. the effects of material and geometric variables, time and temperature on the fracture toughness of the fiberglass laminates, 2. cyclic fatigue crack propagation, and 3. marine environment effects. In each case, the mechanisms of fracture in fiberglass hull materials have been studied with a view toward preventing catastrophic failures. A more detailed description of the work presented in this report may be found in the following Sea Grant reports: fracture toughness--MITSG 73-9, 74-10, and 74-18; fatigue crack growth--MITSG 73-14 and 74-21; marine environment effects--MITSG 73-16 and 75-18.

## SECTION I: FRACTURE TOUGHNESS

### INTRODUCTION

Numerous investigators have studied the fracture resistance of fiber reinforced plastics in recent years, particularly from the viewpoint of the applicability of linear elastic fracture mechanics (LEFM). Results of tests on a variety of laminate types, such as those given by Owen and Bishop [1]\*, indicate that the fracture behavior may or may not be consistent with the basic concepts of LEFM theory, depending upon the style of reinforcement used. The extreme examples of behavior are observed for unidirectional composites, where a crack introduced parallel to the fibers will propagate colinearly with the original crack, in a brittle fashion consistent with the assumptions of LEFM [2], while a crack introduced normal to the fibers will usually deflect and propagate parallel to the fibers, contrary to the assumptions of LEFM [3].

Previous studies [4,5,6] have shown that the initial response of a laminate to a load in the presence of a sharp stress concentration is the propagation of subcracks parallel to the local fiber direction at any point. For practical composites such as the crossplied, woven fabric, or chopped fiber mat styles, this results in numerous subcracks extending in several directions at the tip of a main, through-thickness notch. These subcracks, which also accompany main crack extension, apparently serve to blunt the main crack tip as originally envisioned by Cook

\*Numbers in brackets refer to list of references at the end of each section.

and Gordon [7]. The length of subcrack extension has been related directly to the fracture toughness of the laminate [4,5].

Although progress has been made in characterizing the applicability of LEFM and in understanding the origins of the toughness, few data are available to characterize effects such as thickness, strain rate, and temperature which have been major considerations in brittle service failures of homogeneous materials. In addition to continuing the investigation of fracture criteria, origins of toughness, and variations in material characteristics such as fiber orientation, the work reported in this paper also considers the influence of these other variables.

#### MATERIALS AND TEST METHODS

The following are the principal materials investigated in this study:

1. Scotchply Type 1002 unidirectional-ply E-glass/epoxy (3M Co.) in various ply configurations.
2. Laminac 4155 polyester matrix with MEK peroxide catalyst (American Cyanamid Co.) reinforced with 18 oz/yd<sup>2</sup> E-glass woven-roving Style 779 (J.P. Stevens Fiberglass Co.) and Style 61 (Uniglass Industries), and 1.5 oz/ft<sup>2</sup> random chopped fiber mat using approximately two inch E-glass strands (Ferro Corp.), or combinations thereof.

3. Laminac 4173 polyester matrix with MEK peroxide catalyst (American Cyanamid Co.) reinforced with 8.9 oz/yd<sup>2</sup> Style 181 E-glass woven fabric (J.P. Stevens Fiberglass Co.).

Material (1) was compression molded in accordance with manufacturer's instructions; Materials (2) were fabricated by hand lay-up, and Material (3) was compression molded using a vacuum bag. The fiber volume fraction for each material tested is given in Table 1 while the fiber orientation will be given later for each case.

The laminates were machined to the specimen shapes indicated in Figure 1 using a diamond-edged wheel and a TensilKut router; notches were cut with a thin diamond-edged wheel. The particular shape of the unnotched tensile specimen was determined by trial and error to give the highest stress at failure without breaking in the grips; despite these efforts, fractures originated in some cases in the transition region rather than in the gage section.

The value of the critical stress intensity factor,  $K_Q$ , was determined from available K-calibrations for isotropic materials.\* For the DEN specimen  $K_Q$  is

---

\*The subscript Q used with  $K_Q$  indicates the candidate opening mode critical stress intensity factor as suggested by ASTM [8]; the candidate value is distinct from  $K_{Ic}$  as the latter satisfies certain validity requirements which are not available yet for composites.

determined from [9] as:

$$K_Q = \sigma_f Y \sqrt{C} \quad (1)$$

where  $\sigma_f$  is the applied stress at fracture and  $Y$  is given by:

$$Y = 1.98 + 0.36\left(\frac{2c}{w}\right) - 2.12\left(\frac{2c}{w}\right)^2 + 3.42\left(\frac{2c}{w}\right)^3$$

For the cleavage specimen  $K_Q$  is given in [10] as:

$$K_Q = \frac{P_f}{tH}^{1/2} \left(\frac{c}{H} + 0.7\right) \quad (2)$$

where  $P_f$  is the applied load at fracture,  $t$  is the thickness and  $H$  is the half-width; for the specimen shown in Figure 1, Equation (2) reduces to:

$$K_Q = P_f (8.72c + 9.13)$$

where  $P_f$  is the applied load at fracture. Although the  $K$ -calibration for the cleavage specimen assumes infinite length, it is in good agreement with the finite element data given by Kanninen [11] for this specimen size in crack lengths of practical interest. Unpublished finite element and experimental results which consider the effects of anisotropy indicate a maximum deviation from the isotropic  $K$ -calibrations of approximately ten percent.

The critical strain energy release rate (fracture work or energy),  $G_Q$ , can be measured directly for the cleavage specimen as described in Reference [4]. Assuming the validity of LEFM,  $G_Q$  is related to  $K_Q$  for an orthotropic material with coincident structural and material principal directions by [12]:

$$G_Q = K_Q^2 \left[ \frac{A_{11}A_{22}}{2} \right]^{1/2} \left[ \left( \frac{A_{22}}{A_{11}} \right)^{1/2} + \frac{2A_{12} + A_{66}}{2A_{11}} \right]^{1/2} \quad (3)$$

where the  $A_{ij}$  terms are from the stress-strain relations

$$[\varepsilon] = [A][\sigma]$$

The procedure for measuring the fracture toughness was to load the specimen until fracture occurred, noting the maximum load. In most cases the load-deflection curve was approximately linear to fracture, so the load used in calculating  $K_Q$  was clearly defined as the maximum load. Fracture of the cleavage specimen proceeded in a stable fashion down the length of the specimen, with an increasing deflection necessary to keep the crack moving; the load to cause initial crack extension from the precut notch was used in calculating  $K_Q$  for this case. An Instron universal testing machine was used for all tests, with a displacement rate of 0.05 inches/minute and laboratory temperature and humidity unless otherwise noted. The replication factor for most experiments was three, with a minimum of two in some cases. All results are calculated using an average ply thickness for all specimens of a given series; thicknesses for each material are given in Table 1.

#### CHARACTERISTICS OF FRACTURE

The characteristics of crack propagation in crossplied, woven fabric, and chopped fiber mat reinforced polyester and epoxy have been described previously for glass and

graphite fiber reinforcement [4,5,6]. When a crack propagates so as to cause failure of the fibers in at least one direction, the growth of subcracks parallel to the fibers results in a ligamented appearance of the fracture region, with the typical subcracks extending a tenth of an inch on both sides of the main fracture plane. Figure 2 indicates the ligamented appearance of the fracture region for a crack growing normal to the unidirectional 0° fibers of a 0°/90° crossplied E-glass/epoxy laminate; the crack tip is blunted by the split parallel to the fibers.

The blunting of the main crack is even more distinct in the case of a partial through-thickness crack, as shown in Figures 3 and 4. In this case the crack was introduced into the Scotchply laminate during fabrication by cutting the prepreg tape with a razor blade. During cure of the laminate the cut filled with epoxy, which, upon loading of the specimen, fractured at a low stress level, forming a sharp surface crack. At higher stress levels the usual subcracks formed in the cut 0° and 90° plies and a zone of delamination formed between the last cut ply and the first uncut ply (Figure 4a). Crack extension occurred by growth of the crack in the cut plies, in the manner indicated in Figure 2, with the delamination zone simultaneously spreading over a large area as shown in Figure 4b. Finally the cut plies may separate completely from the uncut plies before total failure of the laminate.

Fracture of a laminate containing a surface crack is different from fracture of a homogeneous material in which the crack propagates through the specimen to form a through-thickness crack. The role of delamination between plies is clearly evident in Figure 3; delamination may also play an important role in the fracture of certain angle-plied laminates containing a through-thickness crack. As shown in Figure 5, taken from Reference [6], fracture may occur by the propagation of a delamination zone accompanied by buckling of the fibers which cross the zone, with the major deformation being shear parallel to the crack rather than opening of the crack. In this case the interlaminar strength and toughness, rather than the fiber strength, will determine the fracture resistance.

Almost without exception the fracture characteristics of woven fabric, woven roving and chopped fiber mat reinforced composites is in the opening mode, displaying the ligamentated fracture region shown in Figure 2 [4,5]. Since such a material may contain randomly oriented strands, and warp and fill yarns of various size and direction, the growth of subcracks and yarn debonding zones [4] at the main crack tip are very complex and difficult to delineate. Figure 6 shows a stationary crack in such a laminate, consisting of woven roving and chopped mat.

## NOTCH GEOMETRY EFFECTS

Experience with metals which fail by brittle fracture indicates that the dominant features of a notch are its length and tip radius [13]. In an otherwise uniform stress field in a large specimen, the introduction of an elliptical notch produces a maximum stress at the notch tip of [14]:

$$\sigma_{\max} = \sigma(1 + 2\sqrt{c/\rho}) \quad (4)$$

where  $\rho$  is the notch radius,  $c$  is the notch half-length, and  $\sigma$  is the applied stress. Experience also indicates that below some critical radius  $\rho_0$ , the fracture stress is insensitive to further reduction in radius, so that

$$\sigma_{\max} = \sigma(1 + 2\sqrt{c/\rho_0}) \quad (5)$$

for  $\rho \leq \rho_0$ . For typical high strength metals  $\rho_0$  is in the range of  $10^{-4} - 10^{-2}$  inches [15,16], and is proportional to the plastic zone size of a natural crack [17].

A meaningful value of  $K_Q$  can be obtained only if the radius of the notch introduced into the specimen is less than  $\rho_0$ . In the derivation of the classical stress field about a sharp crack which leads to the definition of  $K_Q$ , it is assumed that the crack tip is infinitely sharp, and that any zone of inelastic behavior is very small compared to the crack length [18]. The stress field at the tip of a sharp crack in a typical anisotropic material is shown, in Reference [6], to deviate significantly from the classical  $1/\sqrt{r}$  singularity at a distance ahead of the

crack equal to a small fraction of the total crack length. Thus, the existence of a zone of inelastic behavior at the crack tip, which is of the same order of magnitude in size as the crack length, would be expected to destroy the classical stress singularity and render the calculated value of  $K_Q$  meaningless. However, the nominal stress at fracture might still vary with  $\sqrt{C}$  as in Equation (4) if most of the specimen remained elastic.

Figure 7 gives the variation in fracture stress with notch radius for a Style 61 woven roving/chopped mat reinforced laminate. Designating a roving ply as R and a mat ply as M, the ply configuration of the material is M/R/M/R/M which will be the case for all 5 ply roving/mat laminates discussed; in this case the roving is oriented with the  $0^\circ$ , or fill direction parallel to the load, and the warp direction at  $90^\circ$ , perpendicular to the load. In all of the following cases the angle given for the roving represents the angle between the load direction and the fill direction. The results in Figure 7, which are similar to those in Reference [6] for graphite/epoxy, indicate that the applied stress at fracture is relatively constant or even decreases slightly as the notch tip radius increases up to approximately 0.10 inches, and then increases as the radius becomes larger. The effective stress concentration of the sharpest notch is relatively low, as the average stress on the net cross-section between notches is approximately 60% of the ultimate tensile strength

for the one inch notch length.

The value of  $\rho_0$  implicit in Figure 7 is approximately 0.10 inch, one to three orders of magnitude greater than that reported for high strength metals, and consistent with the dimensions of the subcracking zone in Figure 6. Although it is desireable to have the inherent bluntness of a natural crack in any material be as great as possible, the applicability of LEFM must be questioned for such a case. Despite the brittle character of the fracture, which occurs catastrophically with the entire sample behaving elastically except for the small damage region near the crack tip, the existence of a classical stress singularity at the crack tip seems unlikely.

Figure 8 presents the effect of the notch shape on the fracture stress; as expected, the notch flank angle has little influence on the fracture stress over a broad range. The data in Figures 7 and 8 indicate that for a notch several tenths of an inch long, the fracture stress is almost completely insensitive to the shape of the notch, even to the extreme case of a circular hole, as was indicated in Reference [5] for a 181-style fabric reinforced laminate. The length of the notch is of great importance, however, as will be indicated in the next section. The relative insensitivity of the fracture stress to notch radius is convenient, since no difficulty is encountered in introducing a naturally sharp crack into the sample for testing. This is contrary to experience with homogeneous materials.

## FRACTURE CRITERIA AND SPECIMEN SIZE EFFECTS

The preceding comments and data have raised doubts about the applicability of classical LEFM and the meaning of  $K_Q$  for fiber reinforced plastics. The difficulty in measuring the stresses immediately local to the crack tip precludes direct evidence to clarify the question; however, the practical utility of any fracture criterion can be determined by testing specimens of varying size and crack length to determine whether the fracture stress is accurately predicted by the criterion for all cases.

The data given in the previous section suggests another brittle fracture criterion which is not based on the classical stress singularity. Following the concept originally suggested by Neuber [17] and Kuhn [19] for metals, a generalized version of Equation (5) may be used for cracks with  $\rho \leq \rho_0$  given by:

$$\sigma_{UTS} = \sigma_f (1 + q\sqrt{c}) \quad (6)$$

where  $\sigma_{UTS}$  is the ultimate tensile strength, and  $q$  is a generalized stress concentration parameter which includes the effects of inherent radius,  $\rho_0$ , specimen shape (analogous to  $Y$  in Equation (1)), and, for anisotropic materials, the effect of modulus. For high strength metals  $q\sqrt{c} \gg 1$ , and Equation (6) reduces to a simple criterion where the fracture stress is inversely proportional to  $\sqrt{c}$  as in the classical Equation (1). The two criteria are not identical

for many composite materials, however, since  $q\sqrt{c}$  is of the same order of magnitude as unity.

Figures 9(a) - 9(h) give the results of notched tension tests on laminates constructed of Style 779 woven roving/chopped mat, woven roving alone, and chopped mat alone, with various orientations of the woven roving. Specimens of 2, 4 and 6 inch width were tested with  $2c/w$  ratios of 0.25 and 0.50. In each case the solid line represents the classical LEFM criterion, while the dashed line represents the generalized stress concentration criterion, with the average of  $K_Q$  or  $q$  for all specimen sizes used to obtain the equation of the line.

From the results in Figures 9(a) - 9(h), it appears that either criterion fits the data reasonably well for large cracks, although the generalized stress concentration criterion appears to be in agreement with the data over a broader range of crack lengths, particularly for short cracks, as would be expected.

Figure 10 gives the variation of  $K_Q$  and  $q$  with woven roving orientation for the roving/mat laminates. Since the woven roving is not balanced in the warp and fill directions (it has more fibers in the warp), the data are not symmetric about  $45^\circ$ . The variation in toughness with roving orientation for this five ply, M/R/M/R/M material is not great, however, and the fracture surface appearance was similar in all cases. The only noticeable effect of roving orientation was on the direction of crack propagation:

the crack typically propagated at approximately half of the orientation angle. For example, the crack deviation from the original notch direction was approximately  $22^\circ$  for the  $45^\circ$  roving orientation. The deviation from colinear crack growth further violates the assumptions of Equation (1) for LEFM.

Figure 11 shows the two extreme cases observed for sensitivity to notches: woven roving oriented at  $90^\circ$  and at  $45^\circ$ . For all specimen sizes, the  $45^\circ$  case fails at a stress on the net cross-sectional area of almost precisely the ultimate strength, while even small cracks reduce the net section strength considerably for the  $0^\circ$  case. The behavior in the  $45^\circ$  case is unique among the materials tested in this study, and was apparently the result of severe inelastic deformation and cracking across the entire specimen prior to fracture. Similar behavior is reported for  $\pm 45^\circ$  graphite/epoxy laminates as well as for higher fiber orientations such as  $\pm 75^\circ$  in Reference [6].

The variation of  $K_Q$  with specimen width is plotted for several materials in Figure 12 using the data given in Figure 9. As described by Owen and Bishop [1] for similar laminates, the value of  $K_Q$  is found to increase with the width of the specimen. Following the procedure used with metals [18], which has also been employed by Owen and Bishop, it is possible to reduce or eliminate this variation with width by correcting the crack length used in the calculation of  $K_Q$ , as indicated in Figure 13. The

crack length correction,  $\Delta c$ , is added to the actual crack length in Equation (1) to obtain the corrected  $K_Q$ . Although the value of  $\Delta c$  used with metals is based on the effect of the plastic zone size on the elastic stress field, the procedure takes on the characteristics of simple curve fitting in the case of composites, and the correction factors may become unrealistically large.

The generalized stress concentration criterion, while providing good agreement with the data, is difficult to interpret. Figure 10 indicates a value for  $q$  in the range of 1.6 - 2.1 for the roving/mat laminates; neglecting the effects of anisotropy, this results in an unrealistically high value of  $\rho_0$  when  $q$  is compared to Equation (5). While the reasons for this discrepancy are not clear at this time, it is thought that the generalized stress concentration concept may be more consistent with the fracture characteristics of composite materials than is the  $K_Q$  concept, and should be further explored.

#### LAMINATE THICKNESS EFFECTS

The fracture toughness of metals is known to be a strong function of thickness [20]; thin specimens under plane stress conditions yield more readily at the crack tip and display higher toughness, while for thick specimens yielding is constrained under plane strain conditions, resulting in lower toughness. In earlier descriptions of the origins of toughness for fiber reinforced plastics [4,5], crack propagation even for very thin specimens was characterized as blunting of the main crack by subcracking, and brittle tensile failure of

the ligaments at the crack tip so that no thickness effects due to variations in the triaxial stress field constraint on plastic flow are anticipated.

Figures 14 and 15 indicate that the value of  $K_Q$  obtained for 181-style fabric and roving/mat reinforced composites is almost completely insensitive to thickness over a broad range (see Reference [21] for more details on the 181-style fabric tests). The roving/mat laminates were of the ply configuration M/R/M/R/M/..../R/M, and the orientation for both materials was  $0^\circ$ .

The results in Figures 14 and 15 suggest that the complications which thickness effects incur on fracture toughness testing of metals are not to be expected for this class of composites. Figure 16 indicates, however, that thickness complications can exist for some composites, particularly those with unidirectional plies. In this case the origins of the effect are clearly indicated in Figure 17. When the plies on the outside surfaces are oriented with fibers in the load ( $0^\circ$ ) direction, the split length is excessive, measuring several inches compared to the usual tenth of an inch when each  $0^\circ$  ply is constrained by a  $90^\circ$  ply on either side (the outside plies are oriented at  $90^\circ$ ). In the case with each  $0^\circ$  ply constrained by a  $90^\circ$  ply on either side, the value of  $K_Q$  decreases only slightly with thickness, perhaps because of problems in curing the thicker sections. The interior  $0^\circ$  plies of the specimens with  $0^\circ$  surface plies are also under con-

straint from a 90° ply on either side, so only the surface plies display different behavior. If a value of  $K_Q^0$  for the surface 0° plies is obtained from the 3 ply (0°/90°/0°) case, and a value of  $K_Q^0$  is obtained for constrained 0° plies from the cases with 90° surface plies, then a simple rule of mixtures formula gives the expected value of  $K_Q^0$  normalized to consider the effect of 0° plies only,  $K_Q^0$ , as:

$$K_Q^0 = \frac{2(K_Q^0)_{\text{surface}} + (n-2)(K_Q^0)_{\text{interior}}}{n} \quad (7)$$

where

$$K_Q^0 = K_Q^0 \left( \frac{\text{total number of plies}}{\text{number of } 0^\circ \text{ plies}} \right)$$

and  $n$  is the number of 0° plies.

Figure 16 indicates fair agreement between Equation (7) and the measured results, with most of the deviation for thicker specimens probably due to the curing problems which lower the toughness of both types of laminates. The effect of thickness on other ply configurations, particularly those which fail in a shear buckling mode, are not known, but may also be significant.

#### STRAIN RATE AND TEMPERATURE EFFECTS

The effects of strain rate and temperature have been investigated for Scotchply and roving/mat laminates, and the results are found to be contrary to experience with metals. Figure 18 shows that  $K_Q$  for (0°/90°) Scotchply

and  $K_Q$  and  $G_Q$  for roving/mat increase steadily with deflection rate. Figure 19 shows a similar increase with decreasing temperature for the same materials, as well as for  $(45^\circ/-45^\circ/0^\circ/-45^\circ/45^\circ)$  Scotchply, which fails in the shear buckling mode. Variations with rate and temperature appear to be similar to the published variations for strength and modulus of  $0^\circ/90^\circ$  Scotchply [22], and, more meaningfully, the data indicate similar rate effects to those measured for E-glass fibers alone [23]. The apparent close dependence of the laminate toughness on the fiber modulus and strength is consistent with the toughening mechanism described earlier, and suggests a more efficient use of composites in low temperature, high rate applications than under the reverse conditions which tend to favor the application of metals.

#### EFFECTS OF MATERIAL COMPOSITION

The data presented in earlier sections of this paper indicate that the style and orientation of reinforcement may have a significant effect on the toughness, and Reference [6] indicates that an order of magnitude variation in  $K_Q$  with fiber orientation is possible. Figure 16 also indicates that the arrangement of plies may have a significant effect, particularly in the case of unidirectional plies, and earlier work has indicated that an order of magnitude increase in  $G_Q$  is possible by varying the ply

stacking configuration [5].  $K_Q$  and  $G_Q$  have also been shown [4,5] to increase in proportion to the fiber volume fraction as do the strength and modulus.

Table 2 indicates that the properties of the matrix material have very little effect on the toughness of the composite. The various matrices represent a difference of approximately a factor of 40 in fracture surface work between polyester and CTBN modified epoxy [24], with only a minor effect on composite toughness detectable. This again indicates that the fiber properties determine the toughness of the composite. Apparently the growth of subcracks which blunt the main crack is controlled more by the constraint of adjacent plies than by the toughness and adhesion properties of the matrix.

#### CONCLUSIONS

The toughness of FRP laminates derives from the growth of subcracks which blunt the main crack and reduce the concentration of stress. The validity of classical linear elastic fracture mechanics is doubtful due to the inherent bluntness of the crack, and a generalized stress concentration criterion may provide a conceptually sound and practical alternative. The fracture toughness of FRP laminates tends to increase with decreasing temperature and increasing strain rate, and is insensitive to thickness in many cases; each of these characteristics is contrary to experience with metals.

Fracture toughness is also sensitive to fiber orientation and ply stacking arrangement, increases in proportion to fiber volume fraction and is insensitive to matrix toughness.

REFERENCES FOR SECTION I

1. M.J. Owen and P.T. Bishop, "Critical Stress Intensity Factor Applied to Glass Reinforced Polyester Resin," *J. Composite Materials*, Vol. 7, (April 1973), p. 146.
2. E.M. Wu and R.C. Reuter, Jr., "Crack Extension in Fiberglass Reinforced Plastics," *Univ. of Illinois, TAM Report 275* (1965).
3. D.B. Hiatt, "Fracture of Prenotched Unidirectional Glass Fiber Reinforced Composites," *S.M. Thesis, MIT Dept. of Mech. Engr.* (1970).
4. F.J. McGarry and J.F. Mandell, "Fracture Toughness of Fibrous Glass Reinforced Plastic Composites," *Proc. 27th Reinforced Plastics/Composites Div., SPI* (1972), Section 9A.
5. F.J. McGarry and J.F. Mandell, "Fracture Toughness Studies of Fiber Reinforced Plastic Laminates," *Proc. Special Discussion of Solid-Solid Interfaces, Faraday Division of The Chemical Society, Nottingham, England* (1972).
6. J.F. Mandell, S.S. Wang, and F.J. McGarry, "Fracture of Graphite Fiber Reinforced Composites," *Air Force Materials Laboratory Report AFML-TR-73-142* (July 1973).
7. J. Cook and J.E. Gordon, "A Mechanism for the Control of Crack Preparation in All Brittle Systems," *Proc. Roy. Soc. A282* (1964), p. 508.
8. W.F. Brown, Jr. and J.E. Srawley, "Commentary on Present Practice," *Review of Developments in Plane Strain Fracture Toughness Testing, ASTM STP 463*, American Society for Testing and Materials, 1970, p. 216.
9. D.L. Bowie, "Rectangular Tensile Sheet with Symmetric Edge Cracks," *Paper 64-APM-3, ASME* (1964).
10. B. Gross and J.E. Srawley, "Stress Intensity Factors by Boundary Collocation for Single-Edge Notch Specimens Subject to Splitting Forces," *NASA Technical Note D-3295* (1966).
11. M.F. Kanninen, "An Augmented Double Cantilever Beam Model For Studying Crack Propagation and Arrest," *Int. J. of Fracture*, Vol. 9, (1973), p. 83.
12. G.R. Irwin, "Analytical Aspects of Crack Stress Field Problems," *TAM Report 213, Univ. of Illinois* (1962).

13. A. Kelly, *Strong Solids*, Clarendon, Oxford (1966).
14. C.E. Ingliss, *Trans. Naval Arch.*, Vol. 55, No. 1, p. 219.
15. J.H. Malherin, D.F. Armiento, and H. Marcess, "Fracture Characteristics of High Strength Aluminum Alloys Using Specimens with Variable Notch-Root Radii," Paper presented to Am. Soc. Mech. Engr. meeting, Philadelphia (1963).
16. "Fracture Testing of High-Strength Sheet Materials," *Materials Research Standards*, Vol. 1, (1966), p. 716.
17. H. Neuber, "Kerbspannungslehre," Berlin, Julius Springer (1937).
18. G.R. Irwin, "Analysis of Stresses and Strains Near the Tip of a Crack Traversing a Plate," *Trans. ASME, J. App. Mech.* (1957), p. 361.
19. P. Kahn, "Colloquim on Fatigue; Stockholm, May 1955," (Ed. W. Weibull and F.K.G. Odquist) Berlin (Springer-Verlag) (1956), p. 131.
20. G.R. Irwin, "Fracture Mode Transition for a Crack Traversing a Plate," *Transactions, Am. Soc. Mech. Engr.*, Vol. 32, Series D (1960), p. 417.
21. W.J. Schulz, et al, "Fracture Toughness of FRP Laminated Plates," *MIT Civil Engr. Report R70-1-* (1970).
22. 3M Co., Technical Data Sheet for Type 1002 Scotchply (1963).
23. N.M. Cameron, "An Investigation into the Effects of Environmental Treatments on the Strength of E-Glass Fibers," *TAM Report 274*, Univ. of Illinois (1965).
24. G.B. McKenna, J.F. Mandell, and F.J. McGarry, "Inter-laminar Strength and Toughness of Fiberglass Laminates," *Proc. 29th Reinforced Plastics Technical and Management Conf.*, SPI, (February 1974), Paper 13-D.

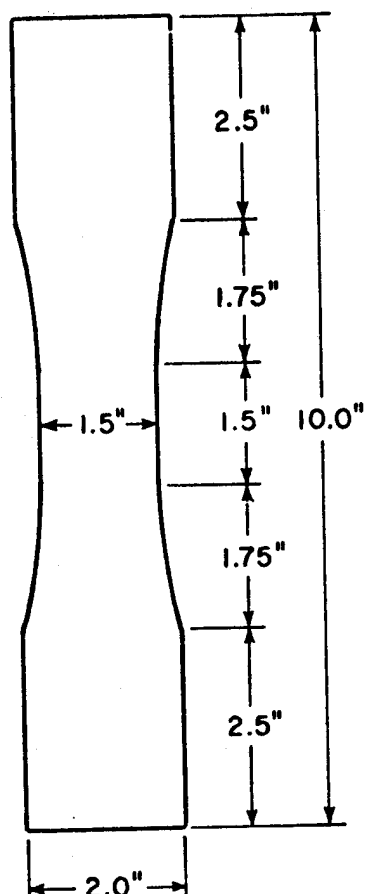
**TABLE I**  
**FIBER VOLUME FRACTION AND PLY THICKNESS**

<u>Reinforcement or Material</u>	<u>Nominal Thickness per ply (in.)</u>	<u>Nominal Fiber Volume Fraction</u>
Scotchply	0.010	0.50
Woven Roving	0.020	0.40
Chopped Mat	0.036	0.20
5 ply Roving/Mat	0.024	0.32
Variable Thickness Roving/Mat (Fig.15)	0.030	0.24
181-Style Fabric	0.0085	0.50

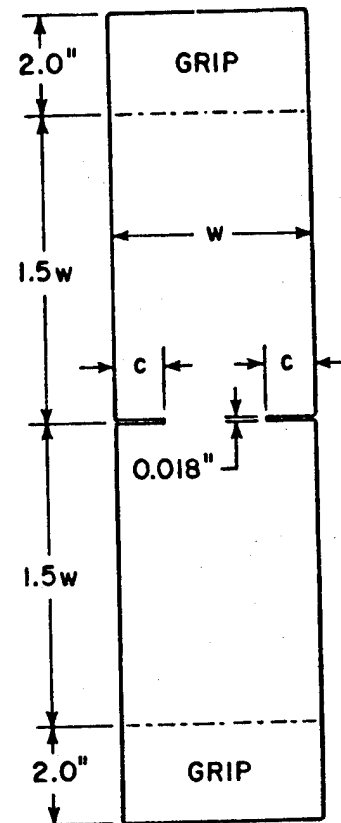
TABLE II

FRACTURE TOUGHNESS FOR SEVERAL MATRICES  
 REINFORCED WITH 9 PLIES OF 181 STYLE FABRIC  
(DEN Specimens, 50% Fiber Volume Fraction)

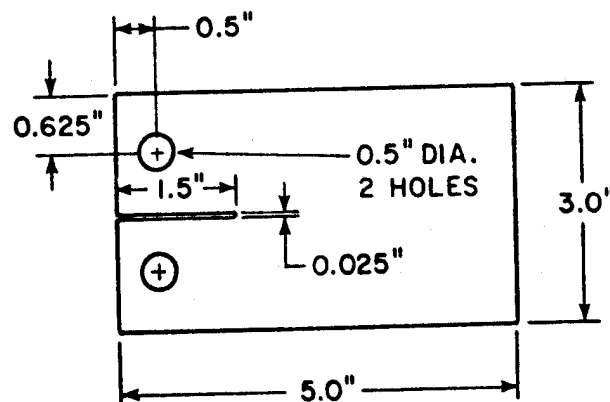
<u>Matrix</u>	<u>Fiber Orientation</u> <u>(Degrees)</u>	<u>Average <math>K_Q</math></u> <u>(Ksi/in)</u>
Polyester (Laminac 4173) (American Cyanamid Co.)	0° 45°	18.3 16.0
Vinylester (Derakane 411-45) (Dow Chemical Co.)	0° 45°	16.6 12.1
Epoxy (Epon 828/CAD) (Shell Chemical Co.)	0° 45°	16.5 12.8
Epoxy + 10% CTBN Elastomer (B.F. Goodrich Co.)	0° 45°	17.8 14.2



UNNOTCHED TENSION

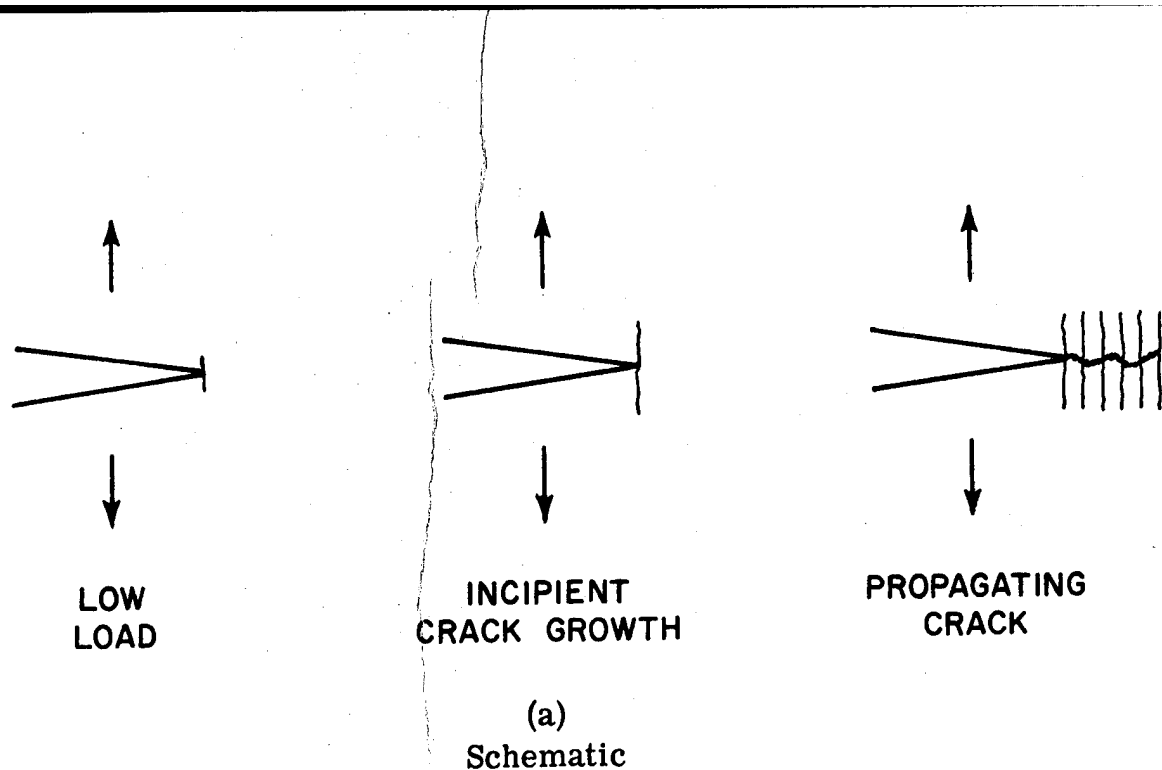


DOUBLE-EDGE-NOTCHED  
TENSION  
(DEN)

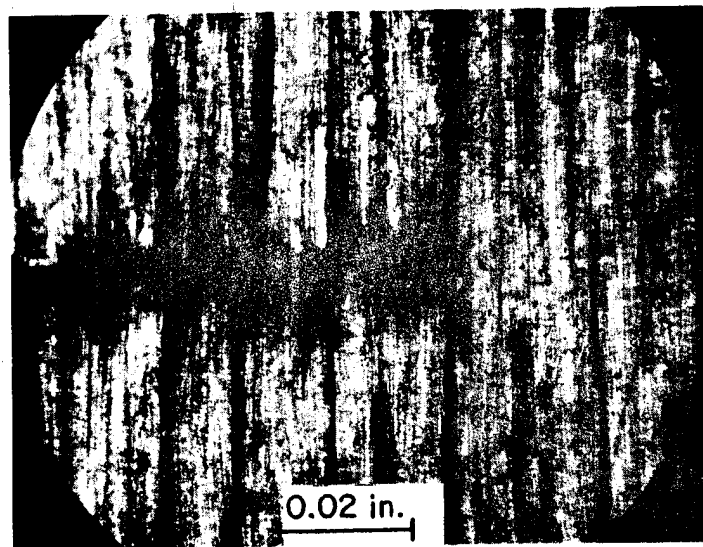


CLEAVAGE

FIGURE 1.  
TEST SPECIMENS.

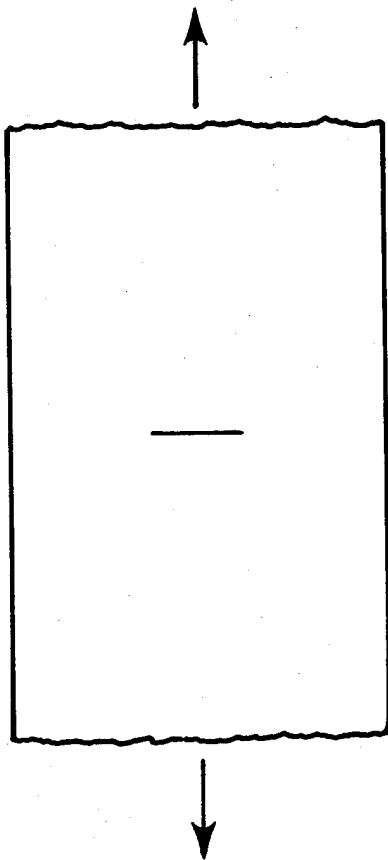


(a)  
Schematic



(b)  
Crack Tip in  $0^{\circ}/90^{\circ}$  Scotchply Laminate  
(Transmitted Light)

**FIGURE 2.**  
**CRACK EXTENSION NORMAL TO FIBERS OF  $0^{\circ}/90^{\circ}$  LAMINATE.**



FRONT VIEW

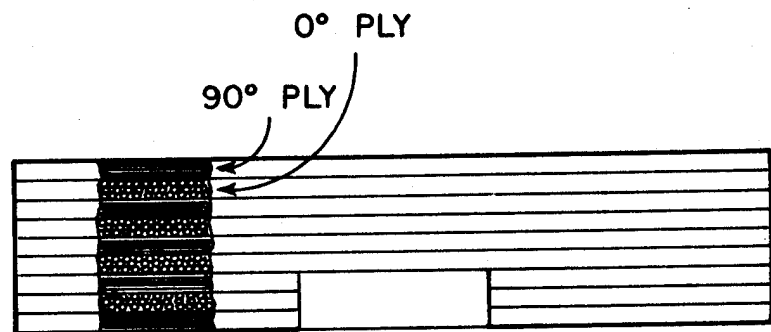
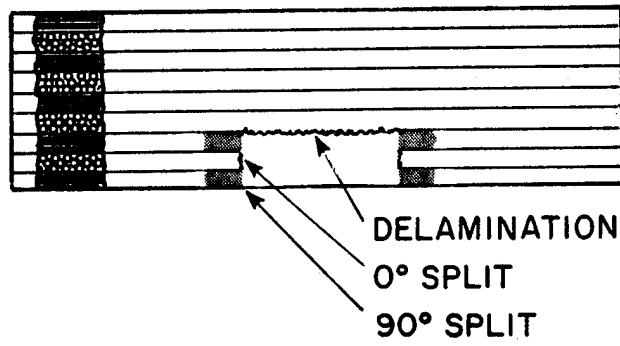
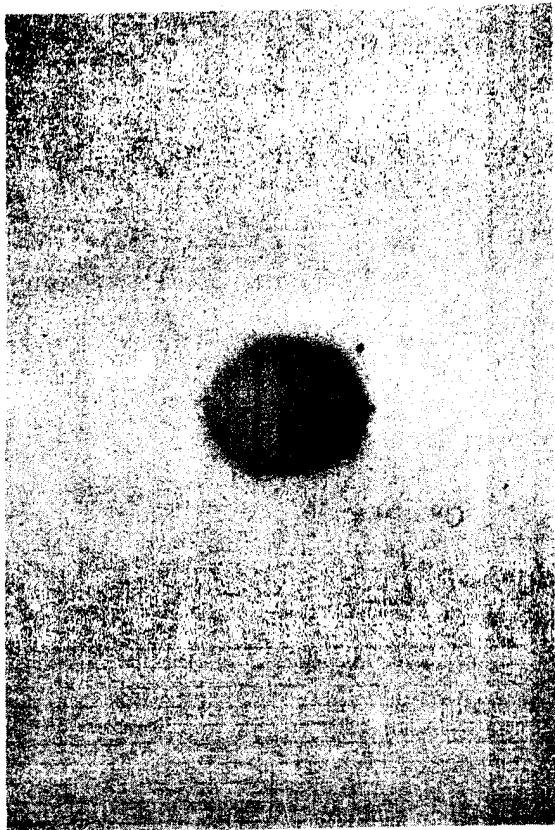
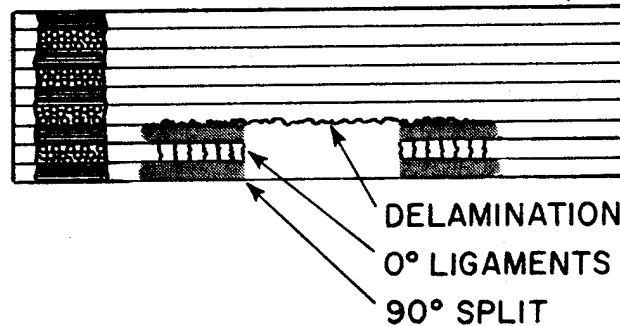
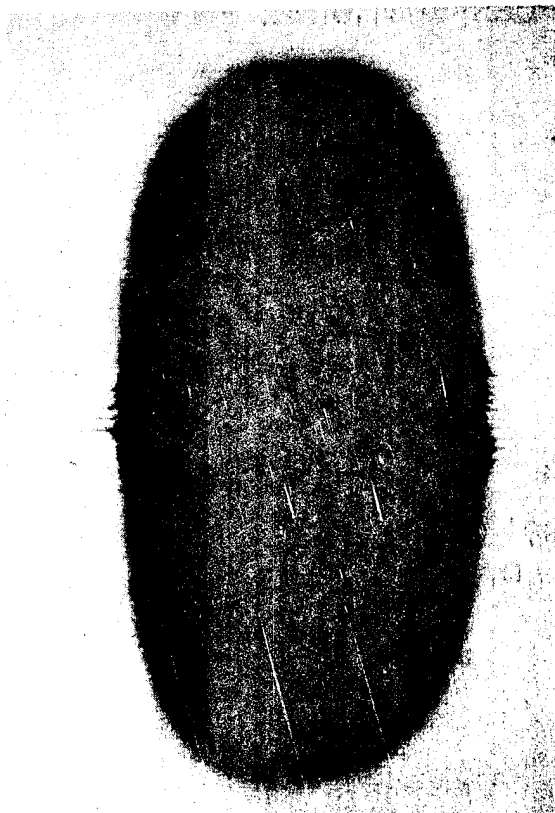


FIGURE 3.

SCHEMATIC OF 9 PLY,  $0^\circ/90^\circ$  SPECIMEN WITH SURFACE CRACK, BEFORE LOADING.



(a) Low Load



(b) Propagating Crack

FIGURE 4.

CROSS-SECTIONAL SCHEMATICS AND FRONT VIEW PHOTOGRAPHS OF INK-STAINED, SURFACE-CRACKED 0°/90° SCOTCHPLY SPECIMENS AFTER LOADING.

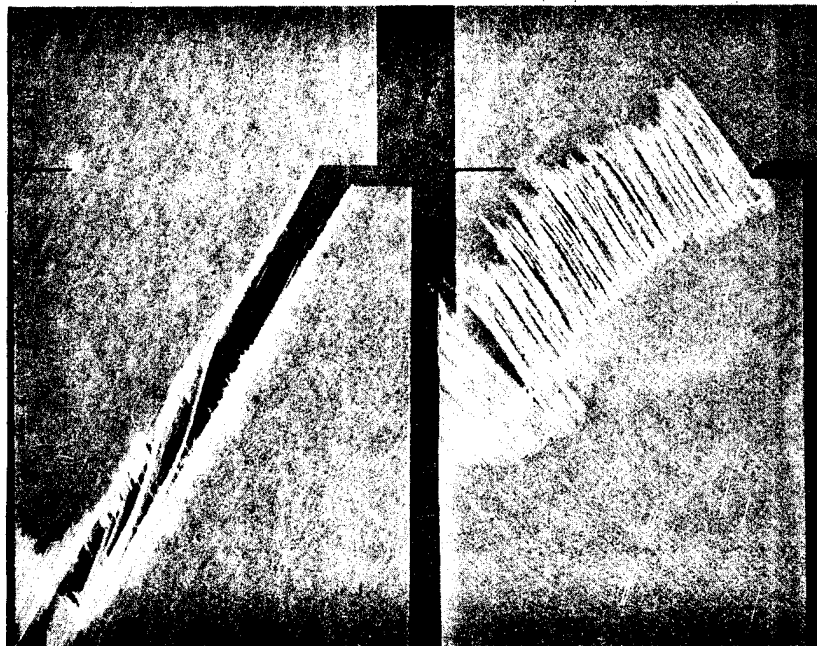
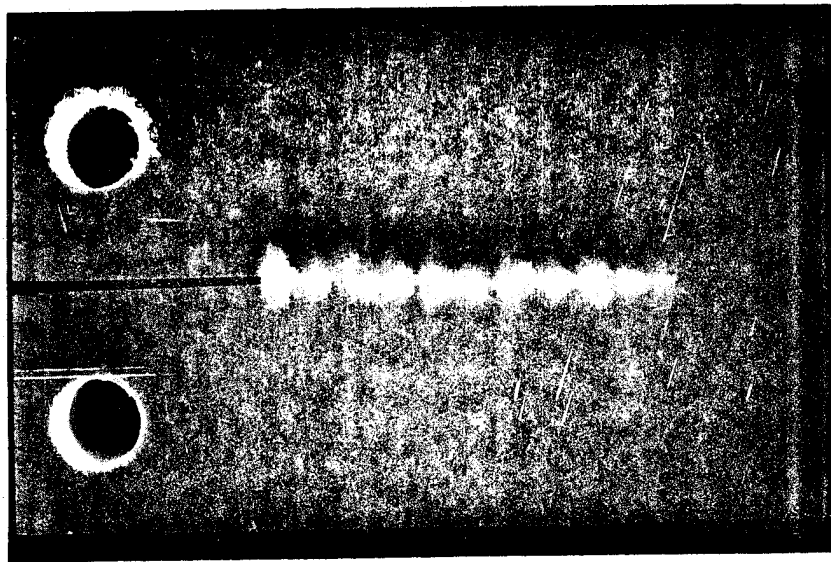


FIGURE 5.

FRACTURED SCOTCHPLY SPECIMENS INDICATING OPENING MODE FOR (30/-30/30/-30/30) LAMINATE (LEFT) AND SHEAR BUCKLING MODE FOR (-45/45/0/45/-45) LAMINATE (RIGHT).



**FIGURE 6.**  
**CRACK PROPAGATION IN E-GLASS/POLYESTER  
DOUBLE CANTILEVER BEAM SPECIMEN.**

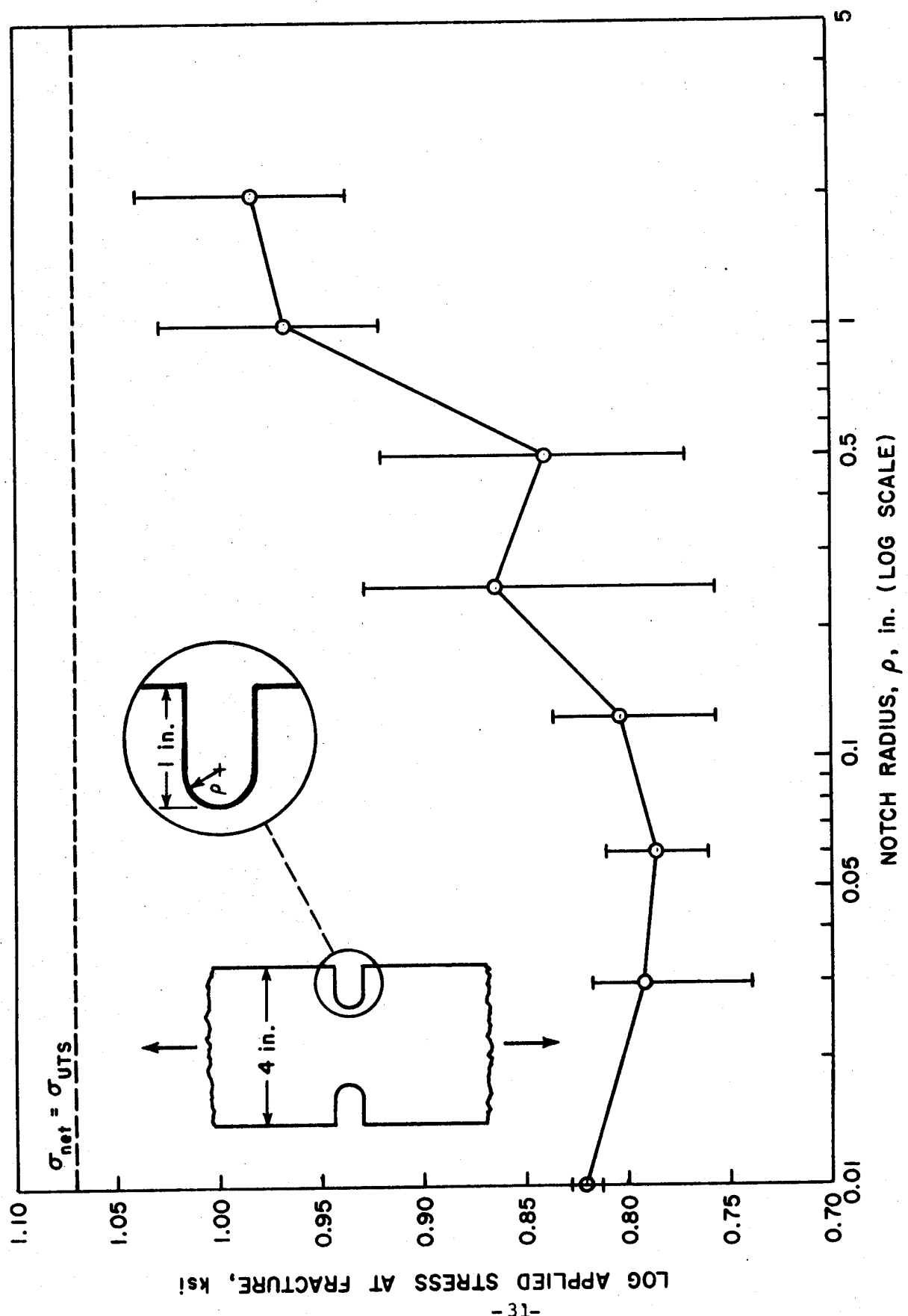


FIGURE 7.  
EFFECT OF NOTCH RADIUS ON FRACTURE STRESS  
FOR 5 PLY, 0° ROVING/MAT/POLYESTER.

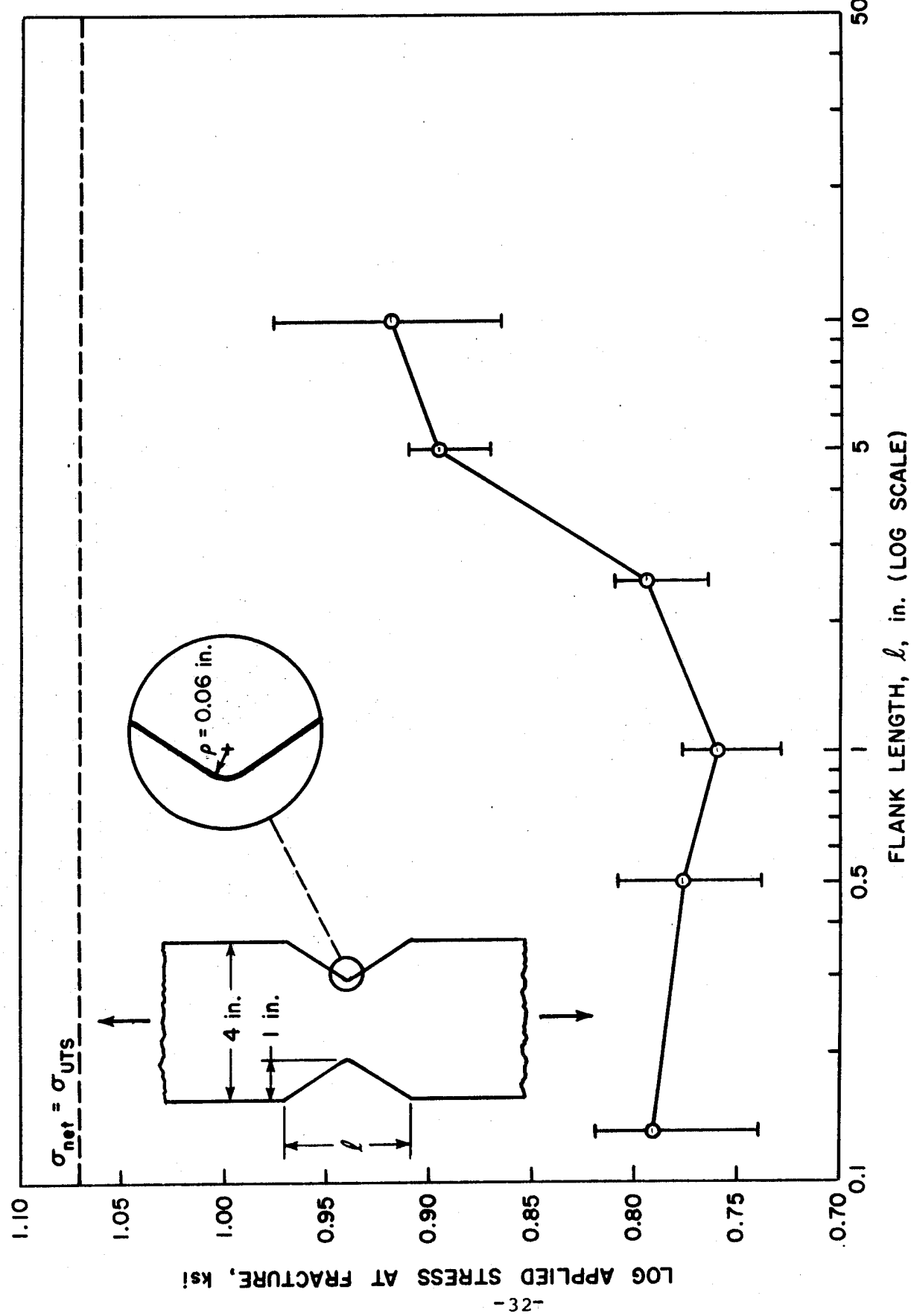
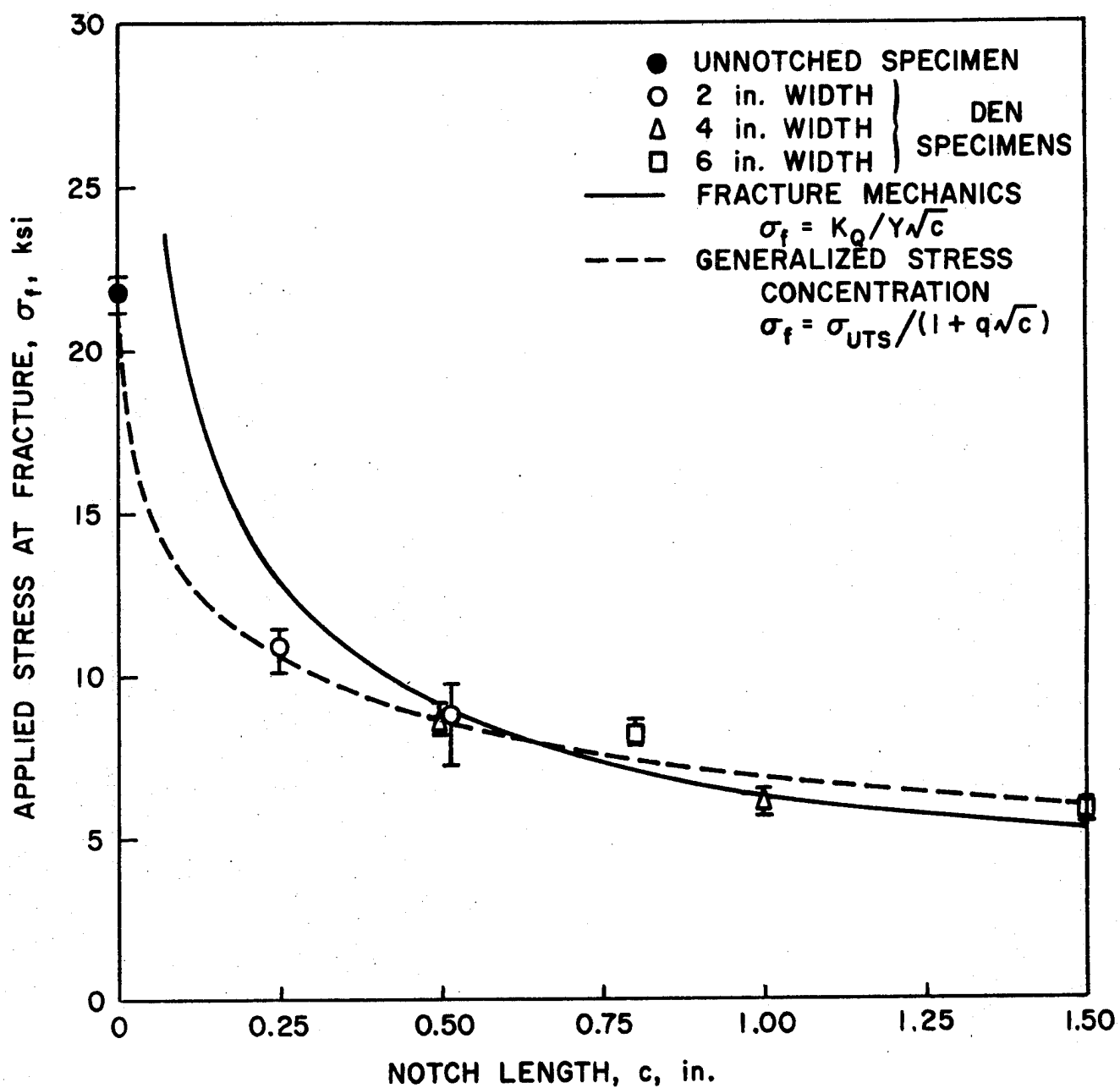


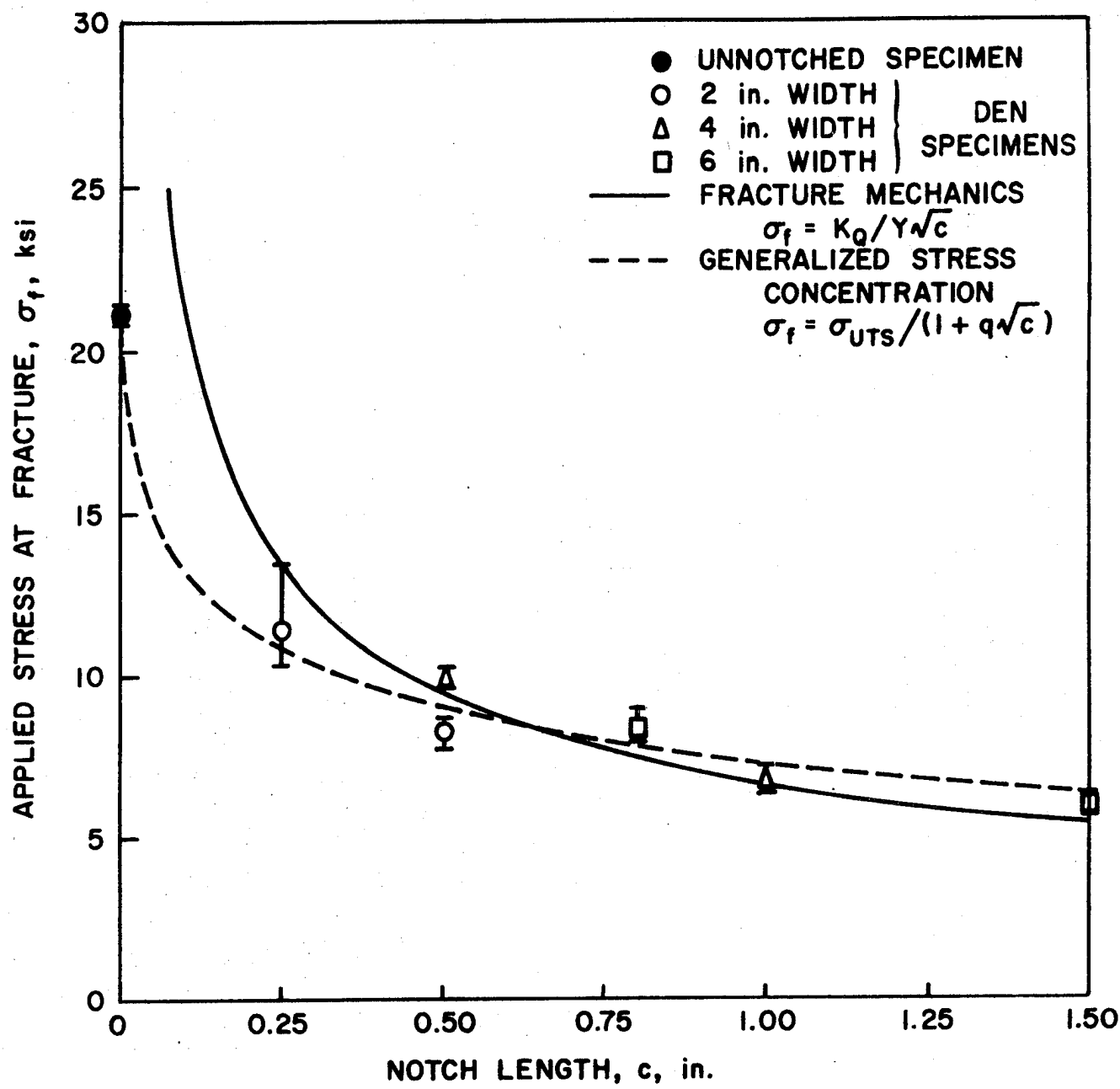
FIGURE 8.  
EFFECT OF NOTCH FLANK LENGTH ON FRACTURE STRESS  
FOR 5 PLY, 0° ROVING/MAT/POLYESTER.



(a) 5 Ply, 0° Roving/Mat/Polyester

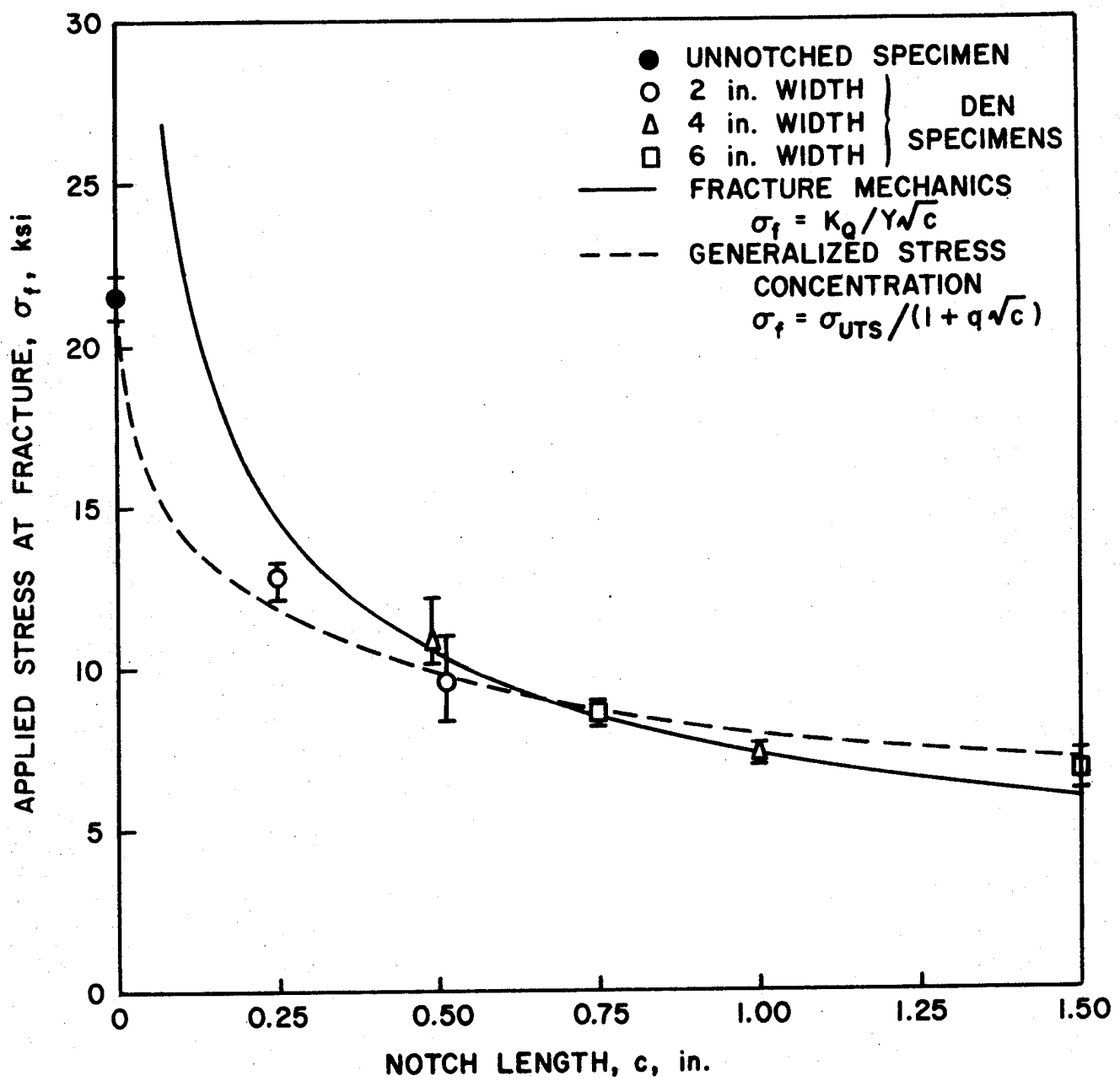
FIGURE 9.

VARIATION OF APPLIED STRESS AT FRACTURE WITH  
NOTCH LENGTH INDICATING ACCURACY OF FIT FOR  
FRACTURE TOUGHNESS AND STRESS CONCENTRATION  
CRITERIA, VARIOUS MATERIALS, DEN TEST.



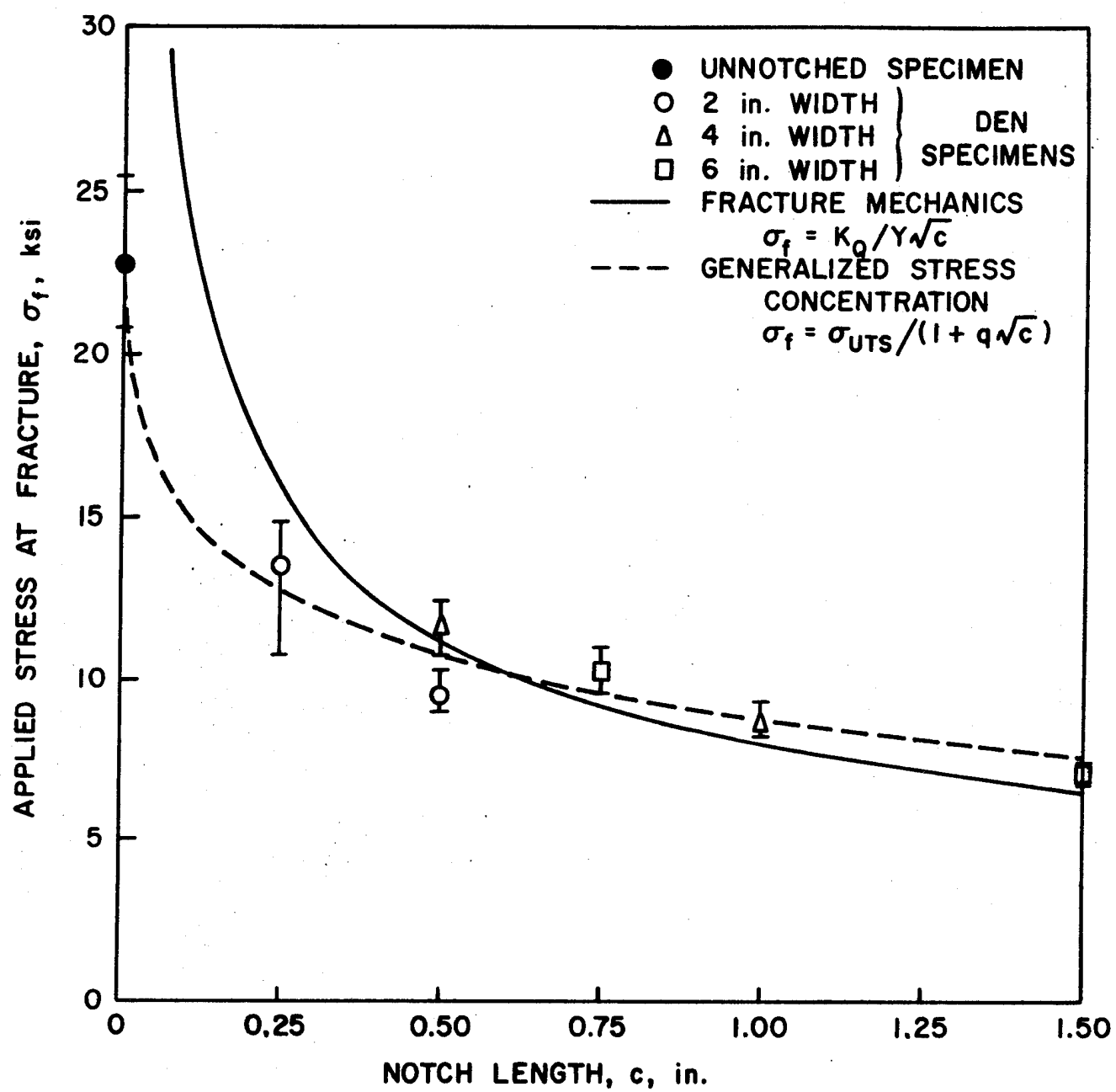
(b) 5 Ply, 30° Roving/Mat/Polyester

FIGURE 9. (continued).



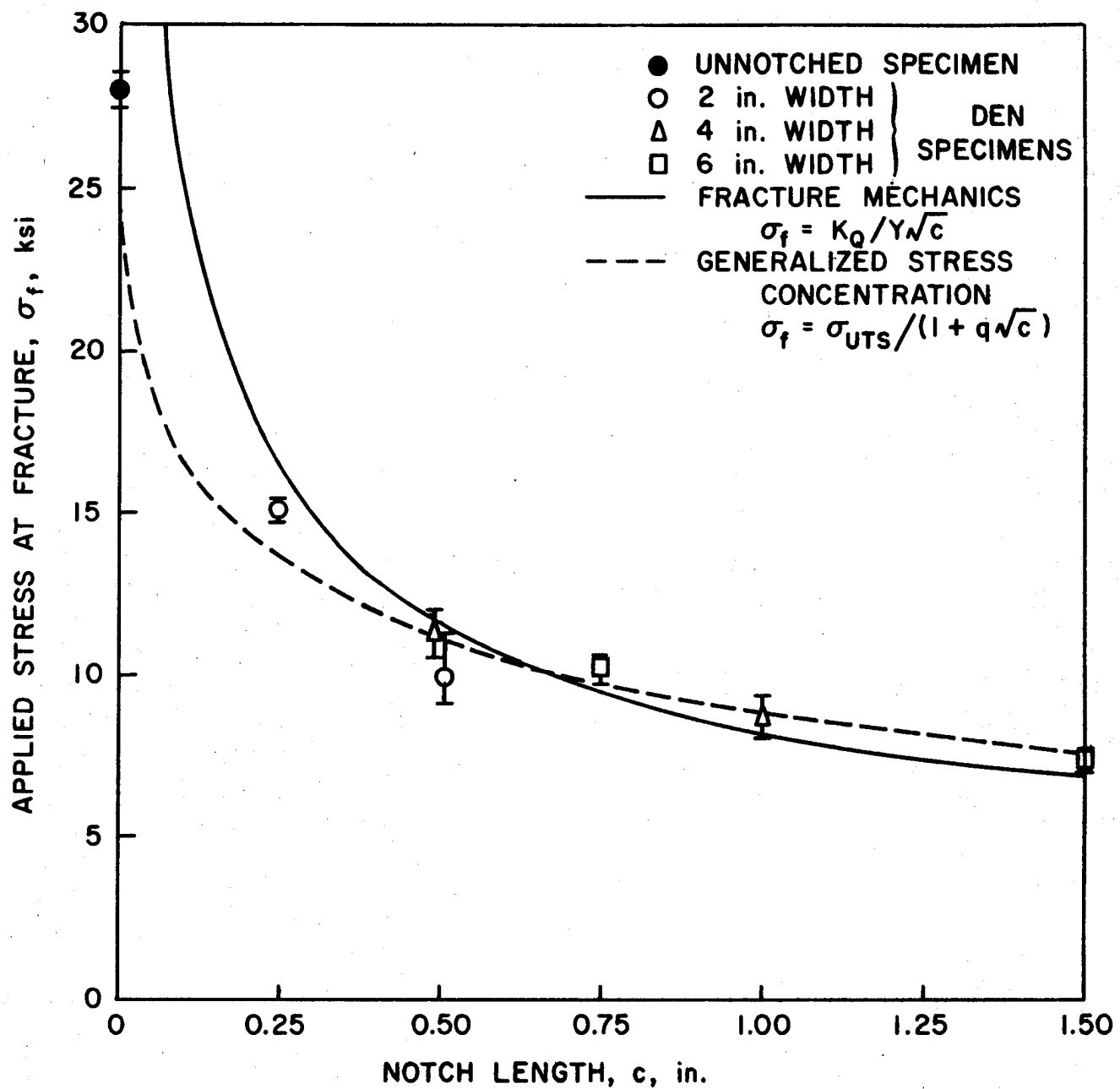
(c) 5 Ply, 45° Roving/Mat/Polyester

FIGURE 9. (continued).



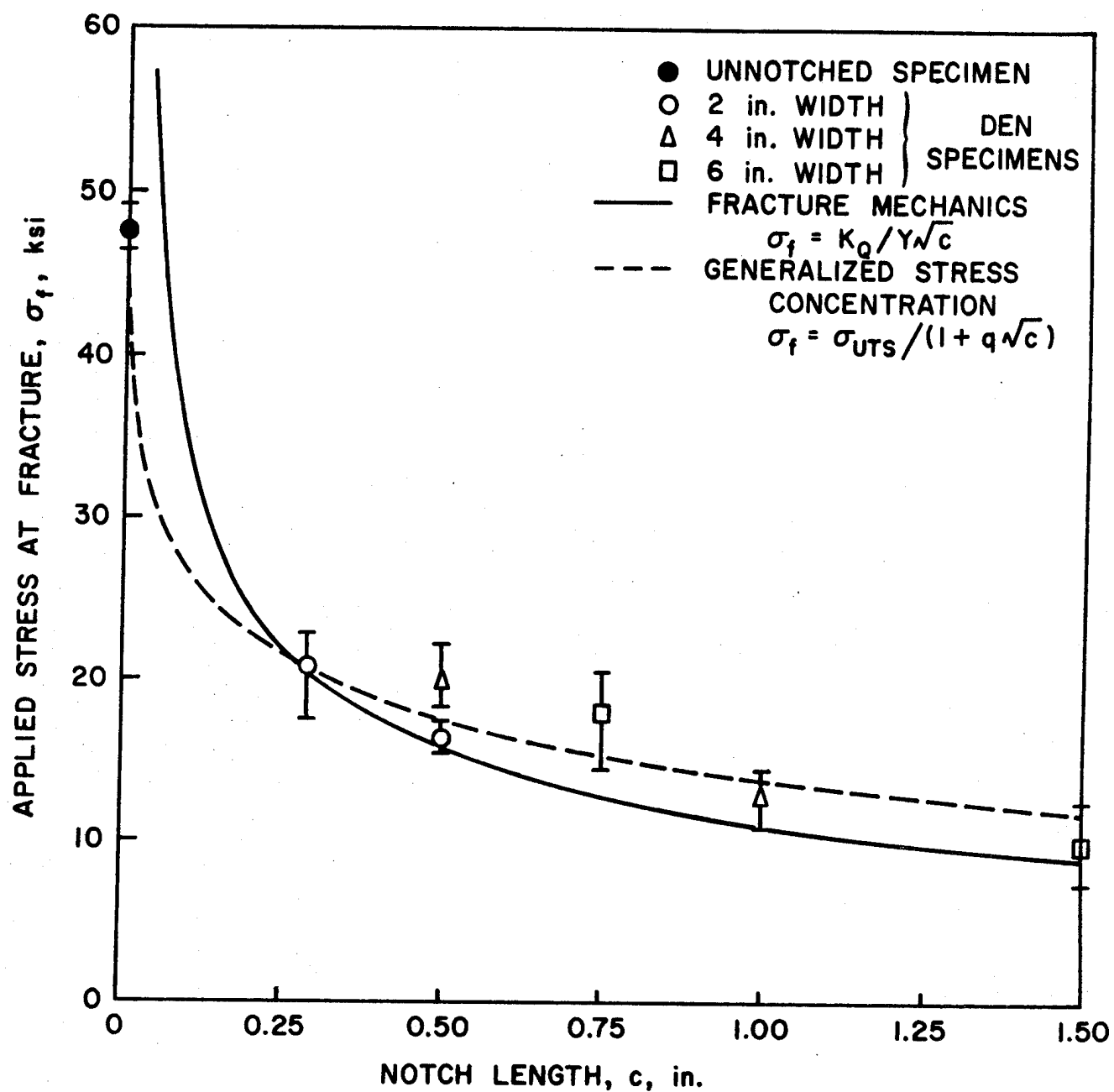
(d) 5 Ply, 60° Roving/Mat/Polyester

FIGURE 9. (continued).



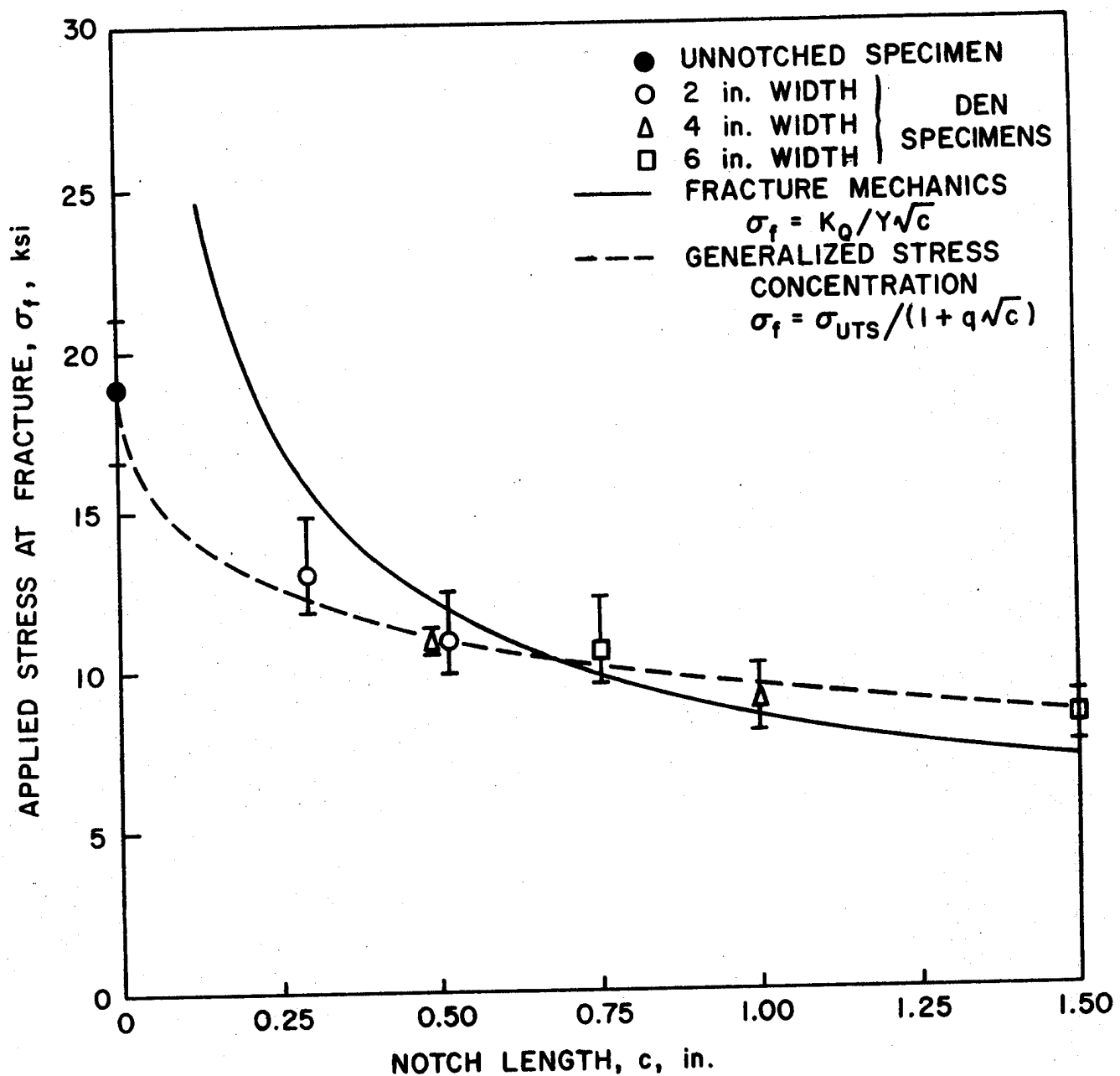
(e) 5 Ply, 90° Roving/Mat/Polyester

FIGURE 9. (continued).



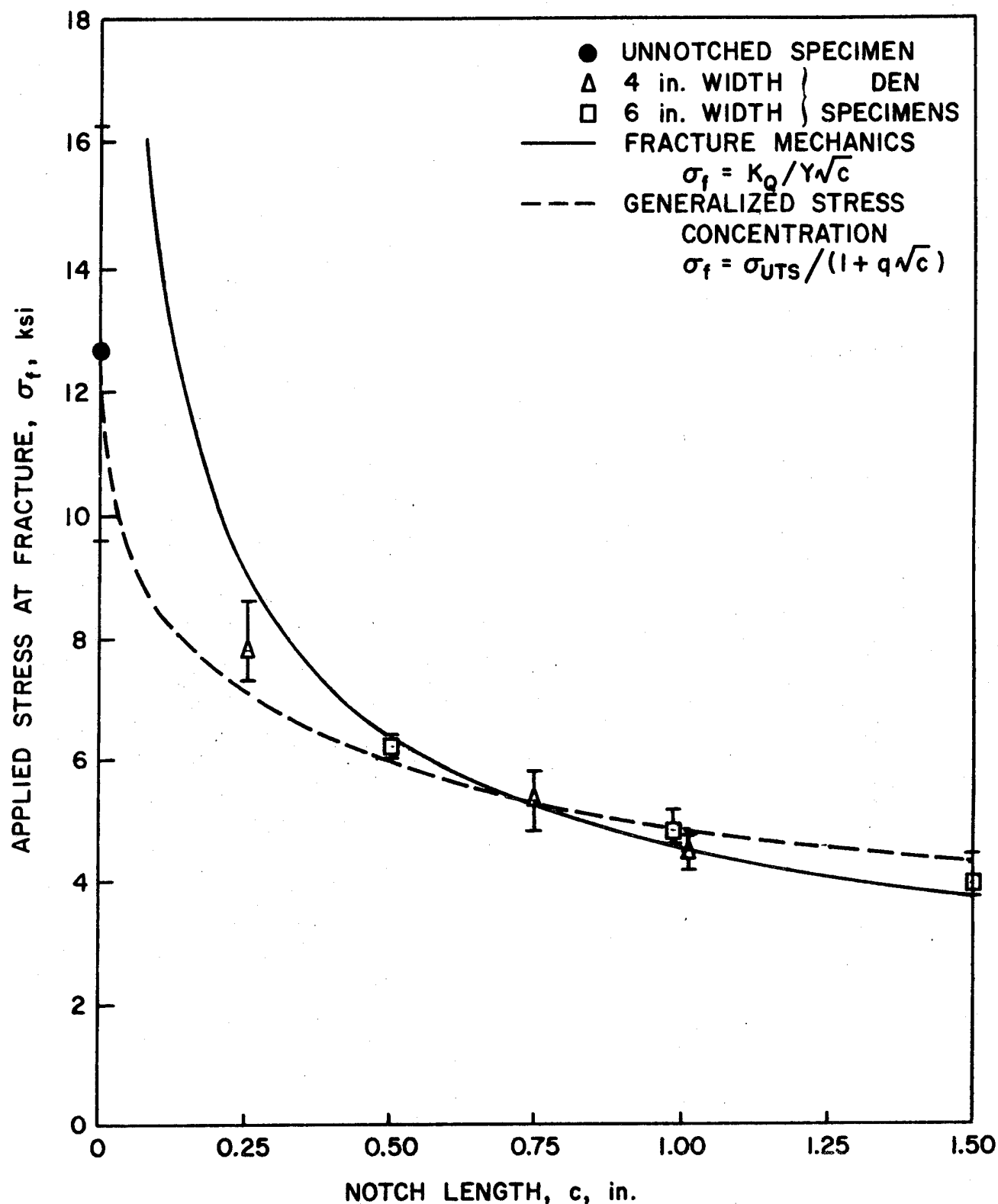
(f) 3 Ply, 90° Woven Roving/Polyester

FIGURE 9. (continued).



(g) 3 Ply, 45° Woven Roving/Polyester

FIGURE 9. (continued).



(h) 5 Ply Chopped Mat/Polyester

FIGURE 9. (continued)..

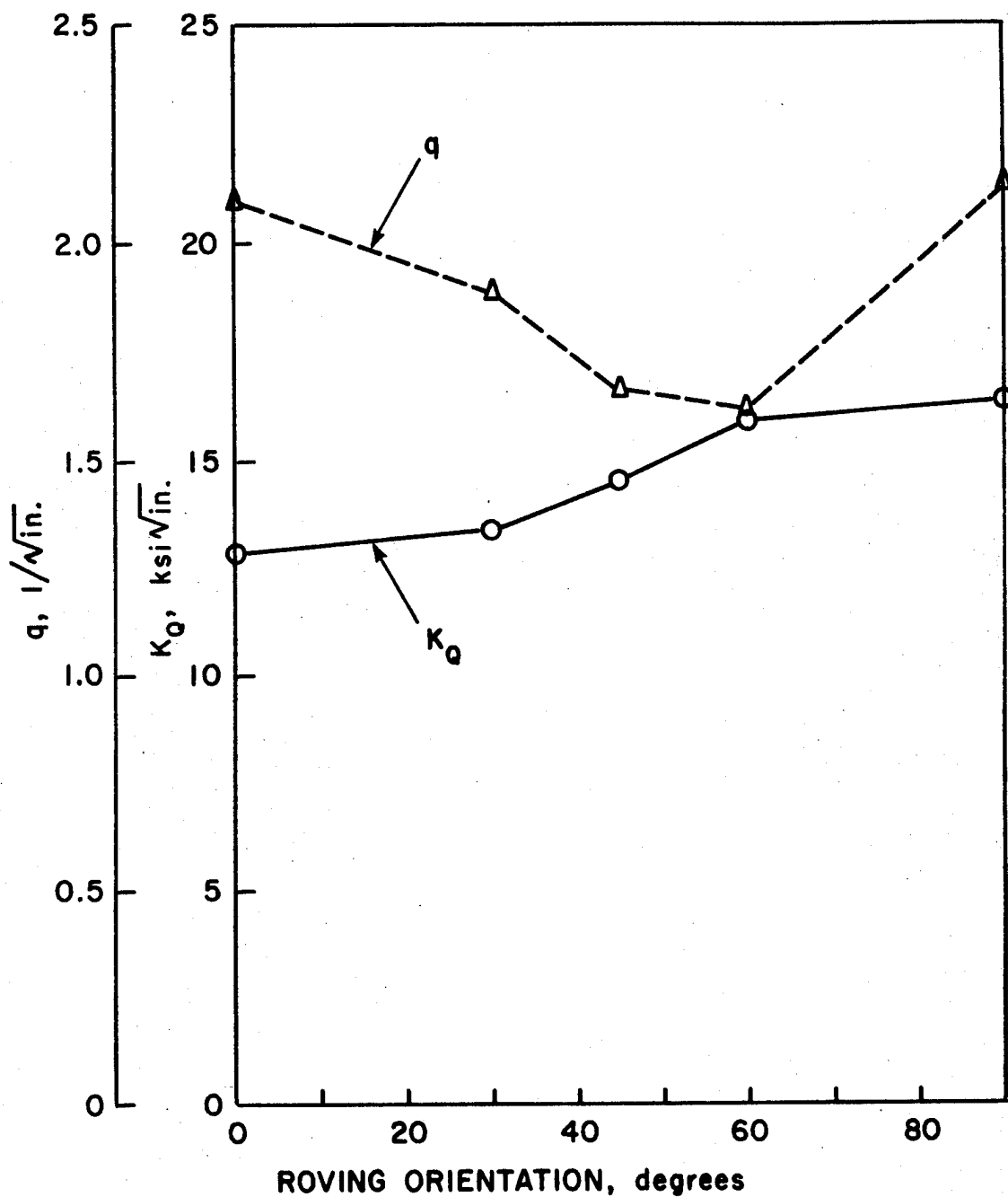


FIGURE 10 .

VARIATION OF FRACTURE TOUGHNESS,  $K_Q$ , AND GENERALIZED STRESS CONCENTRATION PARAMETER,  $q$ , WITH ROVING ORIENTATION FOR ROVING/MAT/POLYESTER MATERIAL, DEN TEST, ALL SIZES.

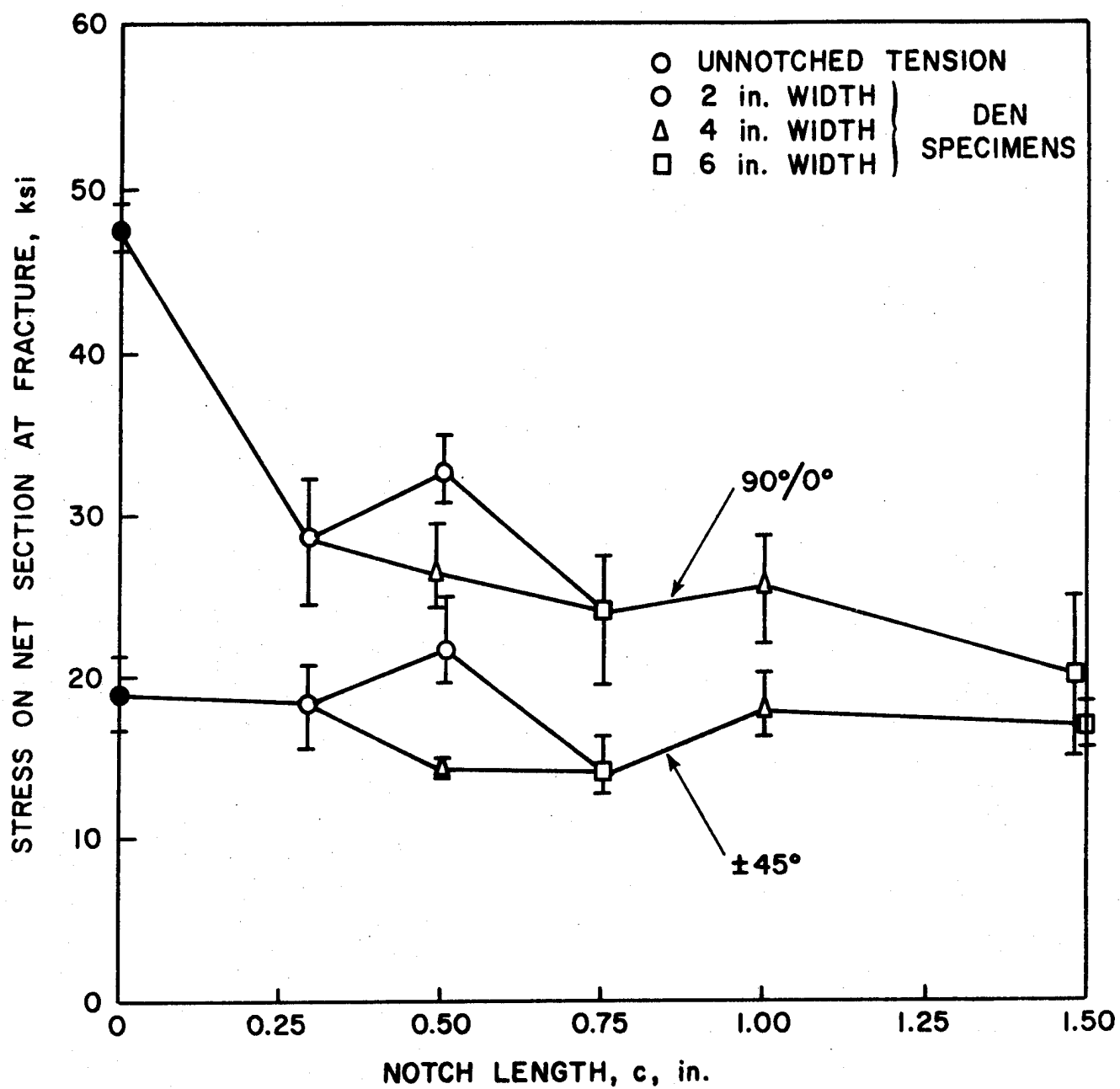


FIGURE 11.

VARIATION OF THE STRESS ON THE NET CROSS-SECTION BETWEEN NOTCHES AT FRACTURE WITH NOTCH LENGTH FOR 3 PLY 90° AND 45° WOVEN ROVING/POLYESTER, DEN TEST.

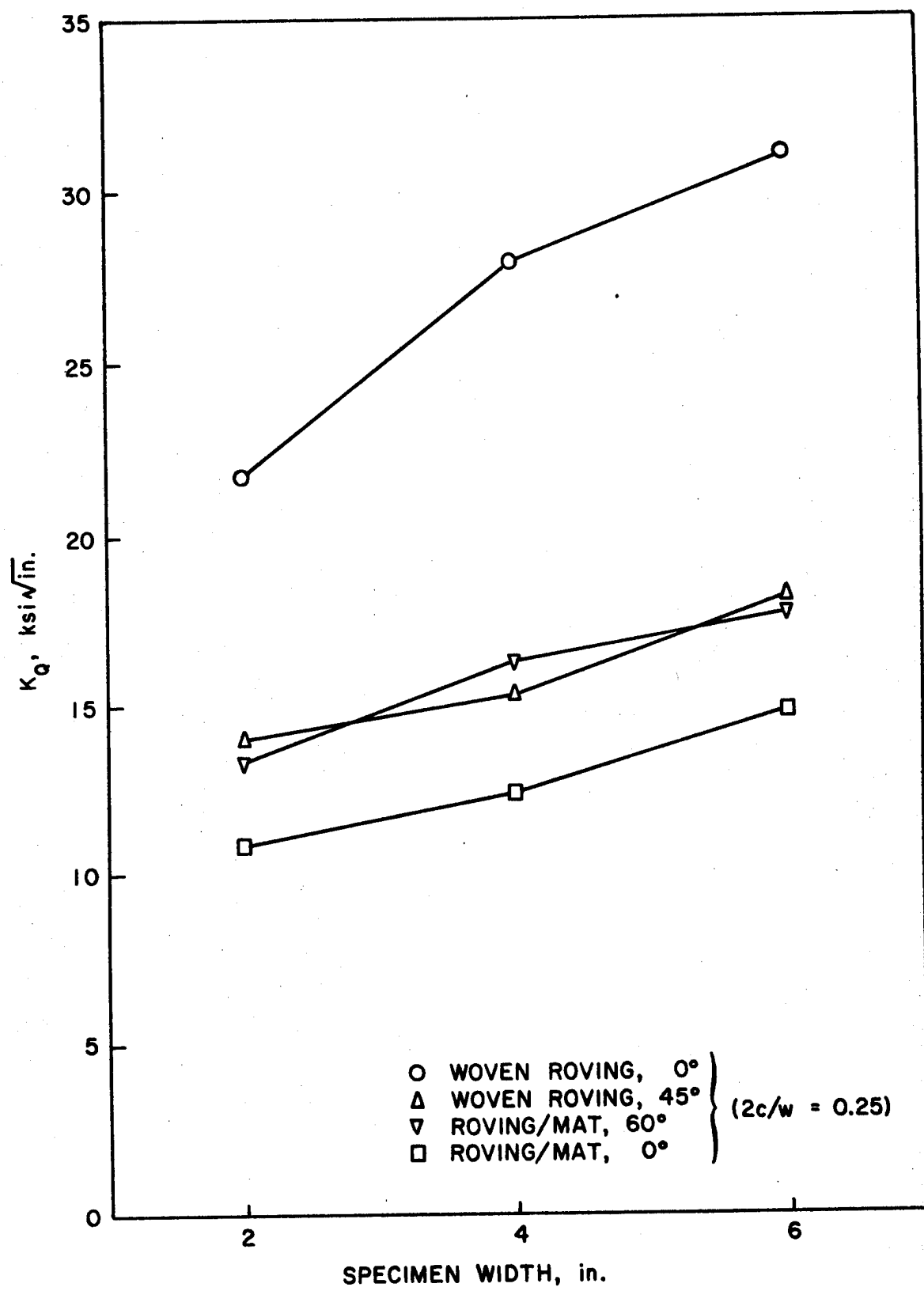


FIGURE 12.  
FRACTURE TOUGHNESS vs. SPECIMEN WIDTH FOR  
VARIOUS MATERIALS, DEN TEST ( $2c/w = 0.25$ ).

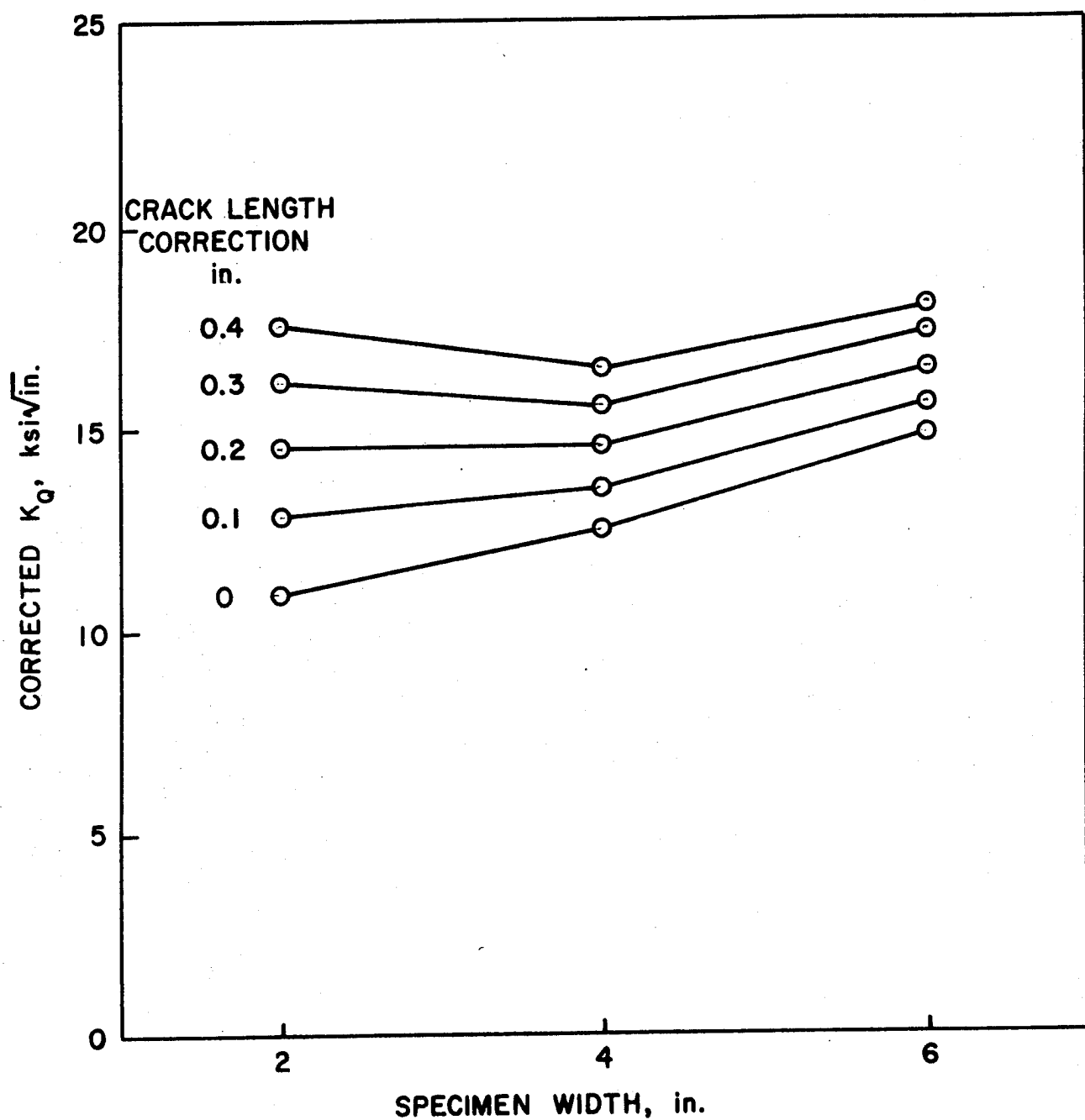


FIGURE 13.

CRACK LENGTH CORRECTION CURVES FOR FRACTURE TOUGHNESS OF ROVING/MAT/POLYESTER MATERIAL WITH 0° ROVING, DEN TEST ( $2c/w = 0.25$ ).

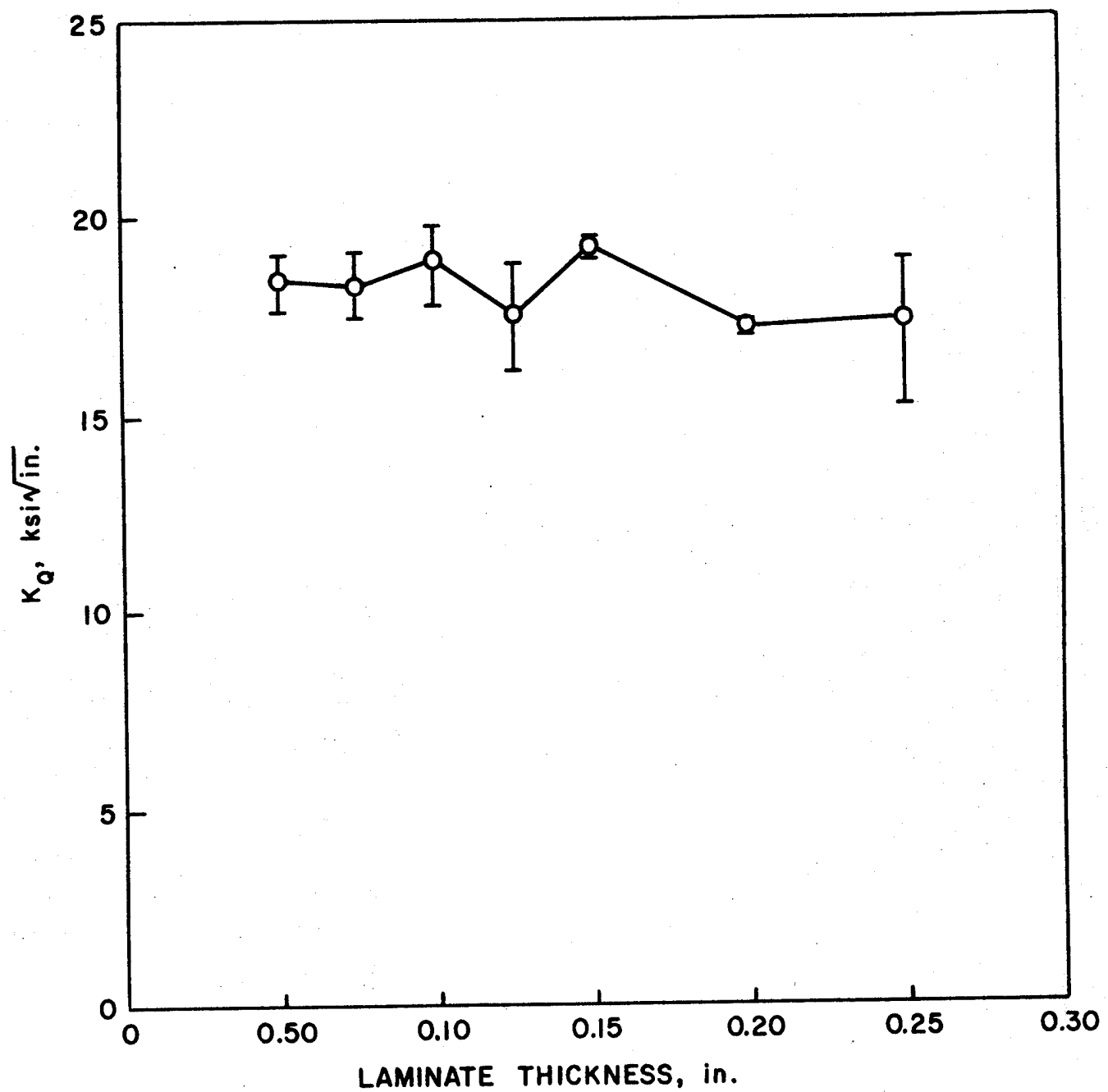


FIGURE 14.  
FRACTURE TOUGHNESS vs. LAMINATE THICKNESS,  
181 FABRIC/POLYESTER, DEN TEST ( $2c/w = 0.50$ ).

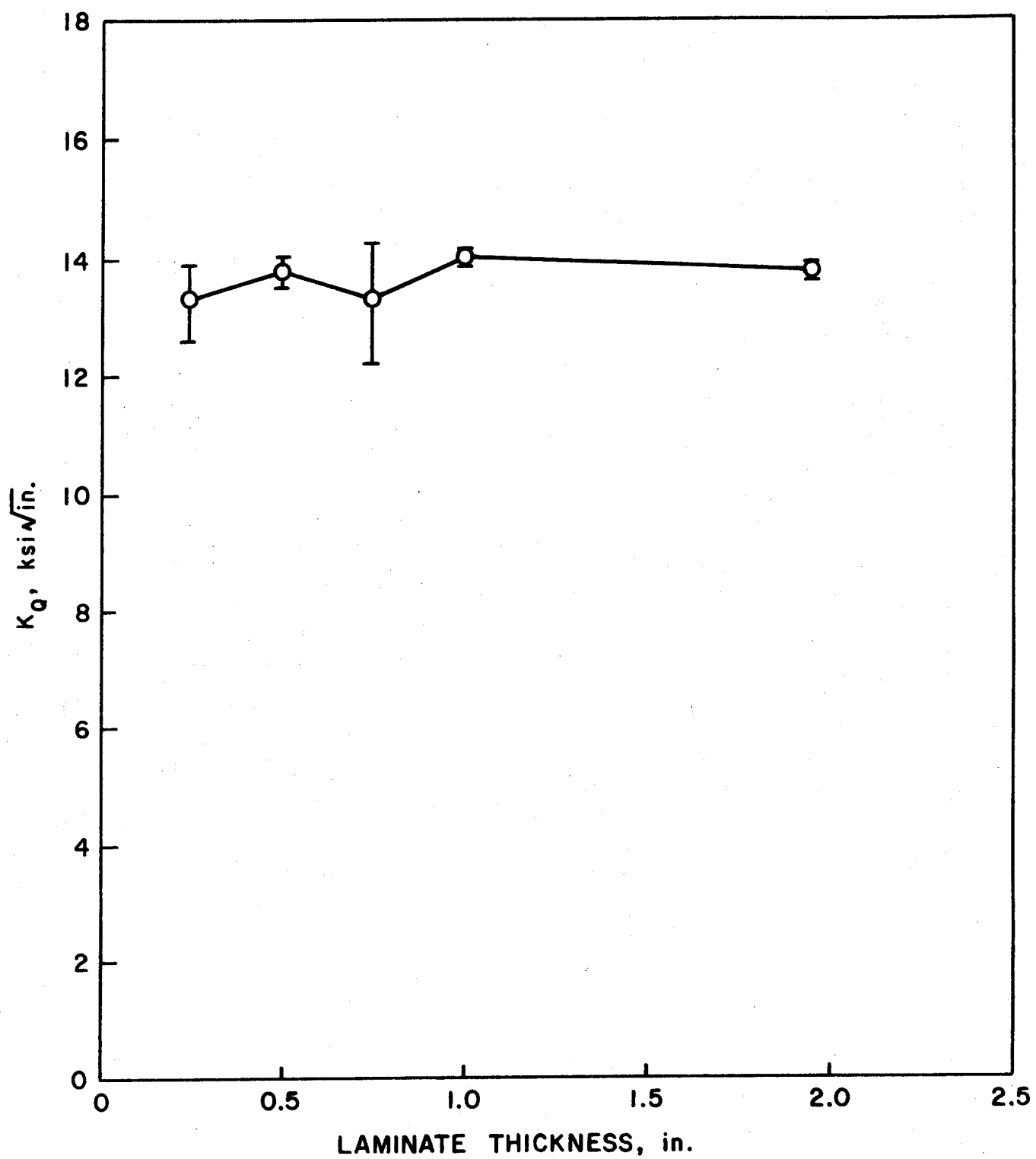


FIGURE 15.

FRACTURE TOUGHNESS vs. LAMINATE THICKNESS, ROVING/MAT/  
POLYESTER MATERIAL WITH 0° ROVING, CLEAVAGE TEST.

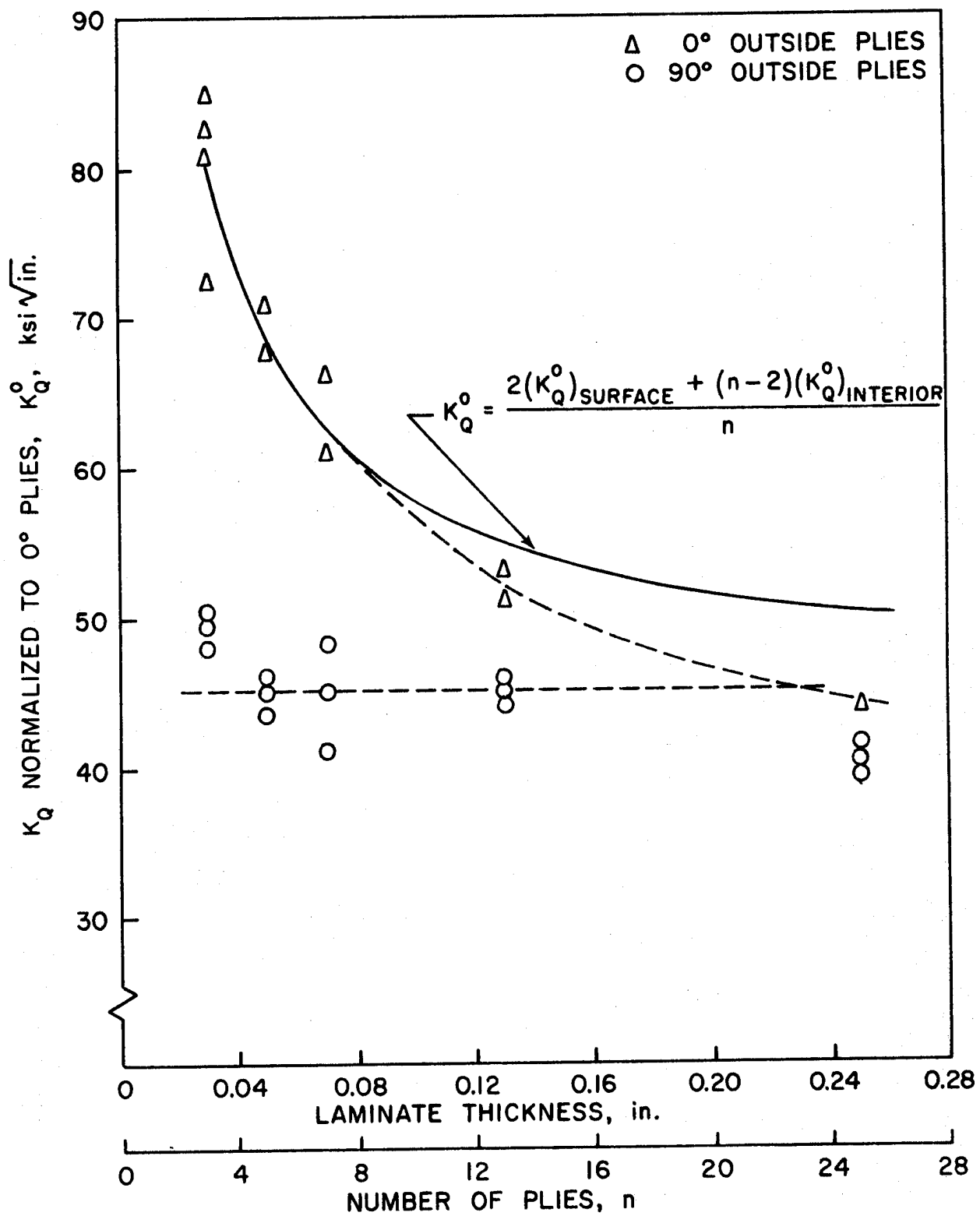


FIGURE 16.  
FRACTURE TOUCHNESS vs. LAMINATE THICKNESS FOR  
90/0/90/0/.../90 AND 0/90/0/90/.../0 SCOTCHPLY  
GLASS/EPOXY LAMINATES, DEN TEST ( $2c/w = 0.25$ ).

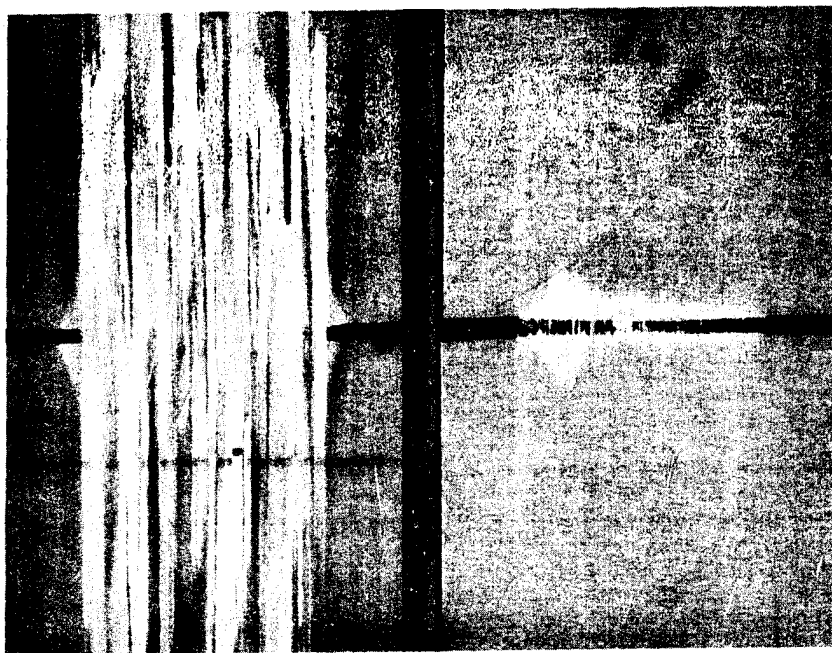


FIGURE 17.

FRACTURED SPECIMENS OF 90/0/90/0/..../90 (RIGHT)  
AND 0/90/0/90/..../0 (LEFT) SCOTCHPLY GLASS/EPOXY  
LAMINATE.

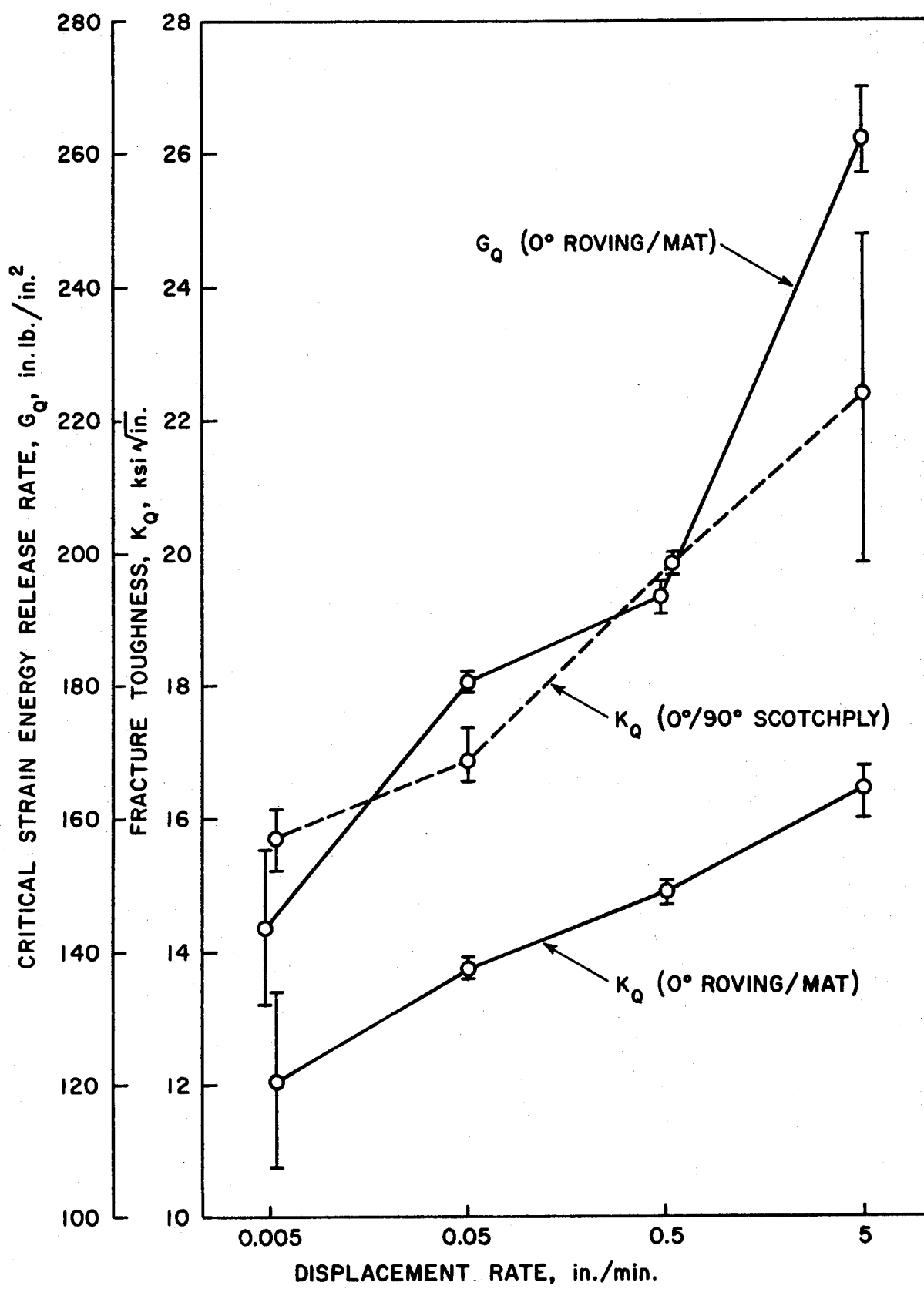


FIGURE 18.

EFFECT OF DISPLACEMENT RATE ON FRACTURE TOUGHNESS AND CRITICAL STRAIN ENERGY RELEASE RATE FOR 0° ROVING/MAT/POLYESTER (CLEAVAGE TEST), AND (90/0/90/0/90) SCOTCH-PLY (DEN TEST), AT 75°F.

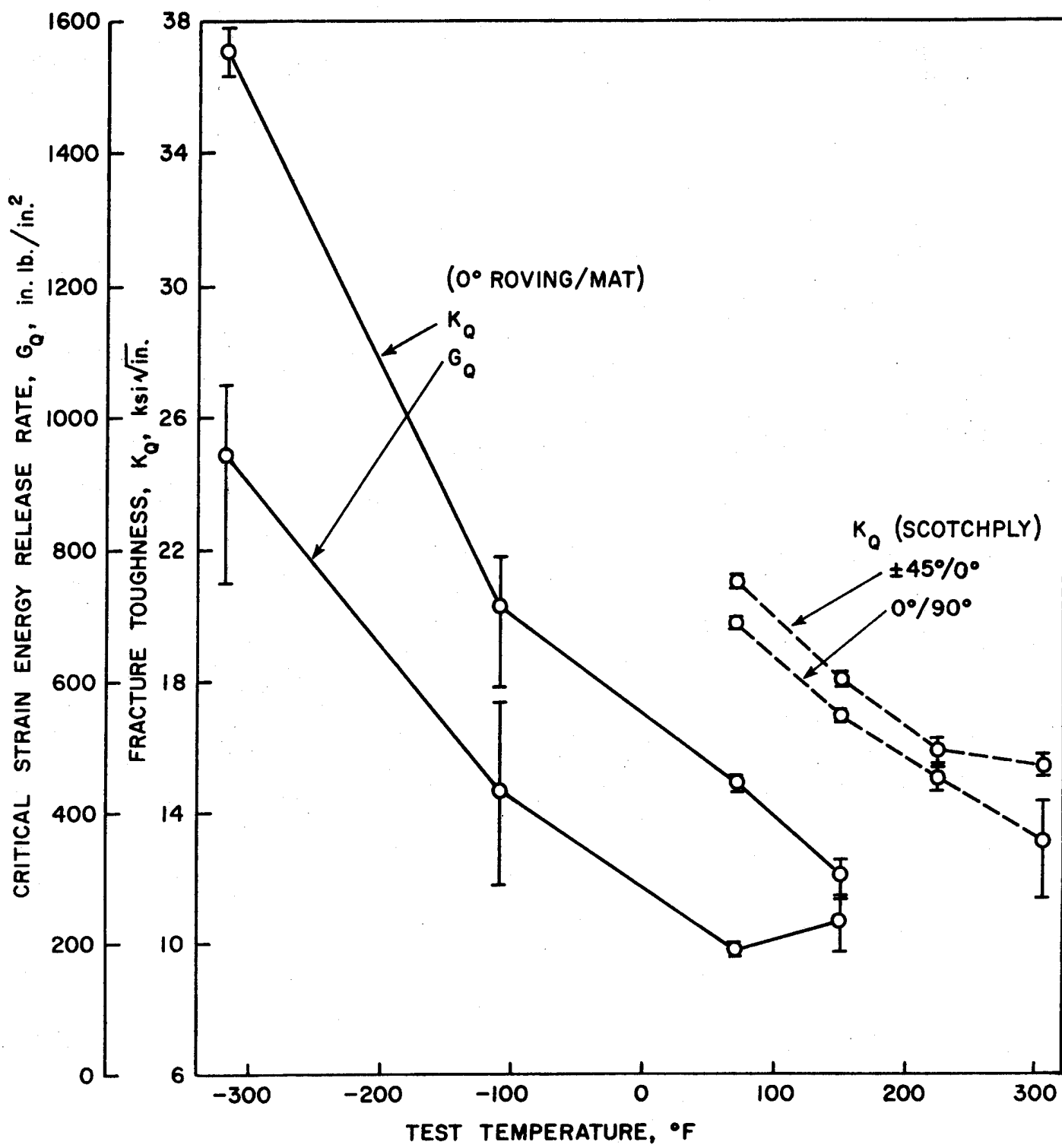


FIGURE 19.

EFFECT OF TEST TEMPERATURE ON FRACTURE TOUGHNESS AND CRITICAL STRAIN ENERGY RELEASE RATE FOR 0° ROVING/MAT/POLYESTER (CLEAVAGE TEST), AND (90/0/90/0/90) AND (45/-45/0/-45/45) SCOTCHPLY (DEN TEST), AT 0.5 in./min. DISPLACEMENT RATE.

## SECTION II FATIGUE AND CRACK GROWTH

### INTRODUCTION

The rate of fatigue crack growth in metals has been the topic of numerous studies which have, in most cases, established a linear relationship between the rate of crack growth,  $dc/dN$ , and some power of the range of the stress intensity factor,  $K_I$  [1]. A recent study of fatigue crack propagation in a  $0^\circ/90^\circ$  crossplied glass/epoxy laminate [2] indicates an exponential relationship between  $dc/dN$  and  $K_I$  which can be predicted by an approximate theory. The present paper describes the development of an improved test specimen for measuring fatigue crack growth in certain composites and compares theoretical and experimental crack growth rates for several important classes of fiberglass laminates typical of marine applications.

### THEORY

The mode of fatigue crack propagation in crossplied  $0^\circ/90^\circ$  glass/epoxy has been described previously [2] as a series of ligament failures. As depicted in Figure 1, the crack tip in the  $0^\circ$  plies (plies having fibers perpendicular to the crack) remains stationary in a given position for a number of cycles of stress until a ligament of material fails, whereupon the crack extends by one ligament width,  $d$ , and the process is repeated. Thus, the main crack extends in a stepwise fashion and the crack growth rate is taken as the ligament width divided by the number of cycles

necessary to fail the ligament. For purposes of discussion, crack extension is defined as extension of the main crack in its original direction as distinct from extension of the subcrack parallel to the fibers.

The rate of crack growth may be predicted by an approximate theory which assumes that the ligament of material at the crack tip fails according to the fatigue life curve of an unnotched strip of material, but at the local crack tip stress level [2]. If the stress vs. log cycles to failure (S-N) curve for the material can be approximated as linear over the stress domain of interest, then the fatigue life of the ligament will be given by

$$\log N = \frac{\sigma_f - \sigma_\ell}{S} \quad (1)$$

where  $\sigma_f$  is the ultimate tensile strength at the appropriate strain rate,  $\sigma_\ell$  is the local stress in the ligament, and  $S$  is the slope of the S-N curve. The value of  $\sigma_\ell$  is determined by assuming a linear increase in local stress with  $K_I$  up to the critical stress intensity factor,  $K_Q$ , at which point  $\sigma_\ell$  must equal  $\sigma_f$ , so that

$$\sigma_\ell = \sigma_f \left( \frac{K_I}{K_Q} \right) \quad (2)$$

Substituting (2) into (1), the crack growth rate for a ligament width  $d$  will be

$$\frac{dc}{dn} = d / \exp [2.3 \frac{\sigma_f}{S} (1 - K_I/K_Q)] \quad (3)$$

Although Equation (3) neglects cumulative damage effects for ligaments ahead of the crack tip, Ref. [2] has indicated that for ligament widths of 0.25 mm. and greater, such effects are negligible because of the high stress gradients in the crack tip region.

#### MATERIALS AND TEST METHODS

The four types of E-glass reinforcement used in the study are described in Figure 2 and Table 1; in each case the fibers were supplied with a polyester compatible finish by the manufacturer (Uniglass Ind.). The matrix used in all cases was Laminac 4155 (American Cyanamid Co.) with 0.5% MEK peroxide. Laminates were fabricated by hand lay-up followed by compression molding at  $0.35 \text{ MN/m}^2$  and room temperature for one day, then postcure at  $100^\circ\text{C}$  for two hours.

Test specimens were machined to the sizes indicated in Figures 4 and 6 using a diamond-edged wheel and TensilKut router; the initial crack was cut with a 0.63 mm. thick diamond-edged wheel. Unnotched tension specimens for woven roving laminates were machined to a larger size, 3.8 cm. wide in the gage section, due to the increased material heterogeneity. Ultimate strength and  $K_Q$  values were obtained at the displacement rates indicated in Table 1 using an Instron universal or Model 1251 machine; because of the strain rate dependence of strength and toughness [3], tests

were conducted at a similar strain rate to that used in the fatigue tests. Fatigue crack growth data were obtained on an Instron Model 1211 dynamic cycler at constant load amplitude with an approximately sinusoidal load vs. time variation at a frequency of 4-7 Hz. All fatigue loading was approximately 0-tension, with a minimum load of 0.5 MN to avoid gripping problems. Tests were conducted in an uncontrolled laboratory environment using wedge-action grips for unnotched specimens and pin loading for crack growth specimens. A replication factor of four was used in all monotonic tests.

The value of stress intensity factor was determined from the relationship [4]

$$K_I = \frac{3.46 P \left( \frac{C}{H} + 0.7 \right)}{B H^{1/2}} \quad (4)$$

where P is the applied force in MN and B is the thickness (B, C, and H are in meters). This relationship was derived for isotropic constants and is in slight error when applied to anisotropic materials, but has been found to give invariant toughness results for various crack lengths in laminates similar to those used in this study [5]. In all cases the crack was propagated parallel to the warp direction of fabric reinforced samples to reduce instances of deviation of the crack from the intended direction of propagation.

## RESULTS AND DISCUSSION

The ligament by ligament nature of crack propagation was observed for all materials tested in this study. The ligament width,  $d$ , was clearly evident from polished cross-sections for the woven reinforcements as shown in Figure 3; the ligament width for the random chopped mat laminates was less definite, and an approximate value was determined from crack length vs. time curves.

Figure 4 indicates that the S-N curves for unnotched samples were typically linear down to some low stress level, where a knee in the curve was evident for woven fabrics. The approximately linear portions of the S-N curves in Figures 4 and 5 were fit by a least squares program to obtain values for  $\sigma_f$  and  $S$  to be used in the  $dc/dN$  prediction for each material. The relatively steep S-N curves for the woven materials apparently result from the development of cracks at the crossover points of the weave [6]; such cracks are clearly observable (see Figure 9), and are quickly followed by failure in the case of the unnotched samples. Table 1 gives the experimentally determined values for  $d$ ,  $\sigma_f$ ,  $S$ , and  $K_Q$  to be used as material properties in Equation (3).

Figures 6 and 7 indicate approximate agreement between experimental and predicted crack growth data for all four materials. Figure 8 indicates that all data along with previous data for glass/epoxy [2] can be normalized to fall

along one of two lines when plotted  $K_I/K_Q$  vs.  $\log (dc/dN)/d$ . All of the woven reinforcement data fall along a line given by Equation (3) with  $\sigma_f/S = 6$ , while data from the non-woven materials fall along a line given by  $\sigma_f/S = 10$ . The scale for  $(K_I)_{\max}$  in Figures 6 and 7 was expanded because of the steepness of the curves; in conventional metals technology  $dc/dN$  varies with  $K_I$  to some power, typically in the range of 3-6 [1], while the results in Figures 6 and 7 indicate approximate exponents between 9 for the woven roving and 13 for the chopped fiber mat if the data are approximated by a straight line.

Several problems were encountered in the development of the fatigue crack growth test. The cleavage-type sample without side-grooving is useful only for materials in which the crack has a strong tendency to propagate down the length of the specimen; if the woven roving, for example, were oriented with the warp direction perpendicular to the specimen length, the crack would still propagate parallel to the warp, perpendicular to the desired direction. Heating of the crack growth specimens at high frequencies was also a problem. Although preliminary tests did not indicate a significant dependence of  $dc/dN$  on frequency below 10 Hz, some specimens, particularly the woven roving, became warm to the touch near the crack tip; however, the heating problem was not studied in detail. Difficulty was also encountered in measuring the crack length because of the stepwise nature of the crack growth and the extensive

damage region associated with the crack tip. The lack of any fatigue striations typical of homogeneous materials [1] made it necessary to estimate the position of the crack tip on the specimen surface by optical inspection at low magnification.

The reduction of the test data by classical fracture mechanics techniques may have introduced some inaccuracy. Although fundamental aspects of the applicability of classical fracture mechanics to similar materials have been questioned in the past [3], recent unpublished analytical modeling of subcracking of the type shown in Figure 1 indicates that the  $r^{-1/2}$  stress singularity is maintained for inplane stresses outside of a very local region at the immediate crack tip. Other studies [3,7] have suggested that a crack length correction factor should be applied to account for subcracking at the crack tip, but results for the cleavage-type sample with its longer crack length suggest that such a correction factor is unnecessary [5]. The use of an isotropic K-calibration introduces some error which will vary with the degree of anisotropy [5] as discussed previously, and the combined effects of microcracking for significant distances away from the crack tip and near the loading points, evident in Figure 3, and the effects of time on the modulus in regions of high stress may further alter the K-calibration. Another possible complication is the use of specimens of different thickness for the unnotched and crack growth tests; however, previous results have indicated no significant

effect of laminate thickness on  $K_Q$  over a broad range for similar materials [3].

The results in Figures 5-8 provide convincing evidence that the fatigue crack growth rate for these specific materials and testing conditions can be deduced from the fracture toughness and S-N parameters combined with microstructural observations. The underlying mechanisms which lead to the fatigue failure are contained in the S-N curve, and the results suggest that no additional mechanisms are introduced by the sharp crack. Other investigators have associated the fatigue failure of unnotched material with the extension of microcracks [8] and the formation of cracks at the weave crossover points [6]. The absence of macroscopic heating in the unnotched specimens suggests that fatigue failure may result from local stress concentrations in the vicinity of microcracks or the abrasion of the exposed fibers as the microcracks open and close in fatigue; the latter explanation appears to be particularly likely in the case of the woven fabric where the crack formed at the weave crossovers is relatively large and significant friction is to be expected during cycling.

Analytical procedures are not yet available for the prediction of the ligament size, but it is observed to be approximately 0.025 to 0.050 cm. in all cases except for the random chopped mat. The apparent ligament size for the random chopped mat samples appears to be more a function of statistical point to point variations in fiber content

and orientation rather than any fundamental mechanism which may be operable in the other cases.

### CONCLUSIONS

It appears that the relationship between the fatigue crack growth rate and the stress intensity factor can be predicted by Equation (3) for a variety of fiberglass laminates using the S-N curve as material property, for the simple case of pulsating opening mode loading. The crack growth rate curves can be normalized to a single relationship for all woven reinforcements tested, and to a second relationship for non-woven reinforcements.

REFERENCES FOR SECTION II

1. Tetelman, A.S. and McEvily, A.J., Jr., Fracture of Structural Materials, Wiley, 1967.
2. Mandell, J.F. and Meier, U., "Fatigue Crack Propagation in 0°/90° E-Glass/Epoxy Composites," presented at the ASTM/AIME Symposium on the Fatigue of Composite Materials, Bal Harbour, Fla., December 1973.
3. Mandell, J.F., McGarry, F.J., Kashihara, R., and Bishop, W.O., "Engineering Aspects of Fracture Toughness: Fiber Reinforced Laminates," Proc. 29th Reinforced Plastics/Composites Div., SPI, 1974, paper 17D.
4. Gross, B. and Srawley, J.E., "Stress Intensity Factors by Boundary Collocation for Single-Edge Notch Specimens Subject to Splitting Forces," NASA Technical Note D-3295, 1966.
5. Mandell, J.F., McGarry, F.J., Wang, S.S., and Im, J., "Stress Intensity Factors for Anisotropic Fracture Test Specimens of Several Geometries," J. Composite Materials (to be published).
6. McGarry, F.J. and Desai, M.B., "Failure Mechanisms in Fiberglass Reinforced Plastics," Proc. 14th Conf., Reinforced Plastics Div., SPI, 1959, Section 16-E.
7. Owen, M.J. and Bishop, P.T., "Critical Stress Intensity Factor Applied to Glass Reinforced Polyester Resin," J. Composite Materials, Vol. 7, 1973, p. 141.
8. Broutman, L.J. and Sahu, S., "A New Theory to Predict Cumulative Fatigue Damage in Fiberglass Reinforced Plastics," 24th Annual Tech. Conf., Reinforced Plastics/Composites Div., SPI, 1969, Paper 11D.

TABLE 1 - PHYSICAL AND MECHANICAL PROPERTIES<sup>a</sup>

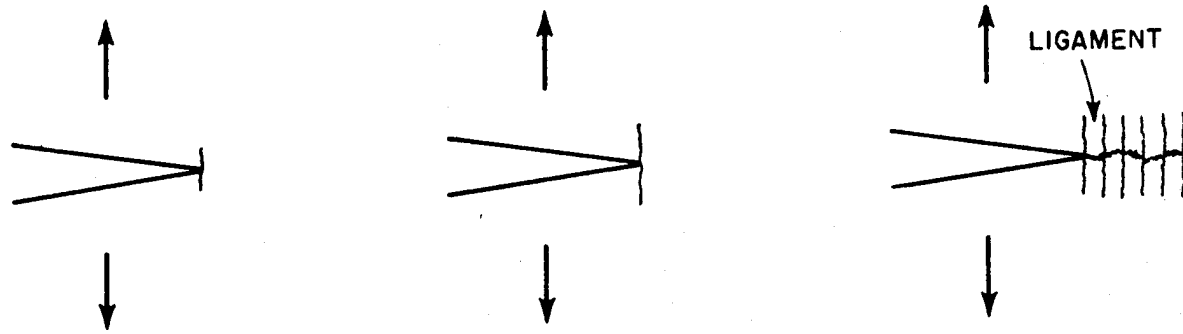
Reinforcement (E-glass)		Woven			Non-Woven	
		Fabric Style	181	1800	Woven Roving Style 61	Chopped Fiber Mat
Matrix		poly- ester	poly- ester	poly- ester	poly- ester	epoxy
Yarn Count Yarns/cm	Warp	22.5	6.3	1.6 <sup>b</sup>	--	--
	Fill	21.3	5.5	1.6	--	--
Fabric Weave		satin	plain	plain	--	--
Fabric Weight (Kg/m <sup>2</sup> )		0.303	0.329	0.611	0.458	--
No. Plies/ Thickness (cm)	Specimen					
	Unnotched	10/0.254	9/0.254	5/0.229	5/0.303	5/0.127
	Crack Growth	36/0.915	33/0.915	20/0.915	15/0.915	5/0.127
Fiber Volume Fraction		0.47	0.47	0.52	0.29	0.50
Ultimate Tensile Strength, $\sigma_f$ (MN/m <sup>2</sup> ) <sup>d</sup>		429	339	450	134	418
Slope of S-N Curve, S [ (MN/m <sup>2</sup> ) / decade ]		70.8	58.0	71.9	12.9	42.5
$K_Q$ (MN/m <sup>3/2</sup> ) <sup>d</sup>		32.3	26.7	45.4	14.0	26.4
Ligament Width, d (cm)		0.05	0.05	0.05	0.32	0.025

a - Fabric description is from manufacturer's data, thickness, fiber volume fraction and mechanical properties are average values, and ligament width is estimated as described in the text.

b - Although yarn count is balanced, the amount of fiber is approximately in the ratio of 5:8 in the fill:warp directions.

c - Scotchply Type 1002 unidirectional ply, 3M Co.

d - Monotonic tests were conducted at a displacement rate of 0.85 cm/s.



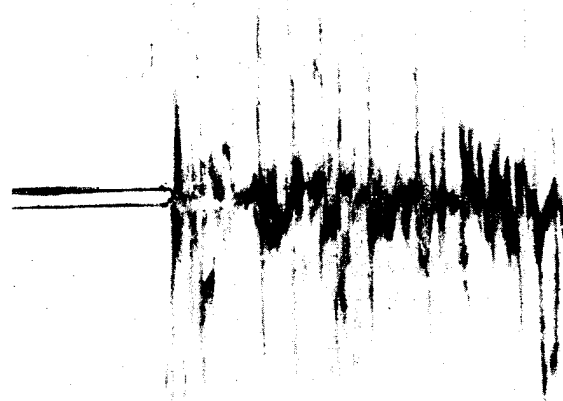
After first cycle

After many cycles

Stationary crack after  
5 ligament failures

(a)

Schematic



2 mm

(b)

Photograph of fatigue crack propagating from notch at left

**FIGURE 1.**  
**FATIGUE CRACK PROPAGATING IN 0° PLY OF**  
**[90/0/90/0/90] GLASS/EPOXY LAMINATE.**

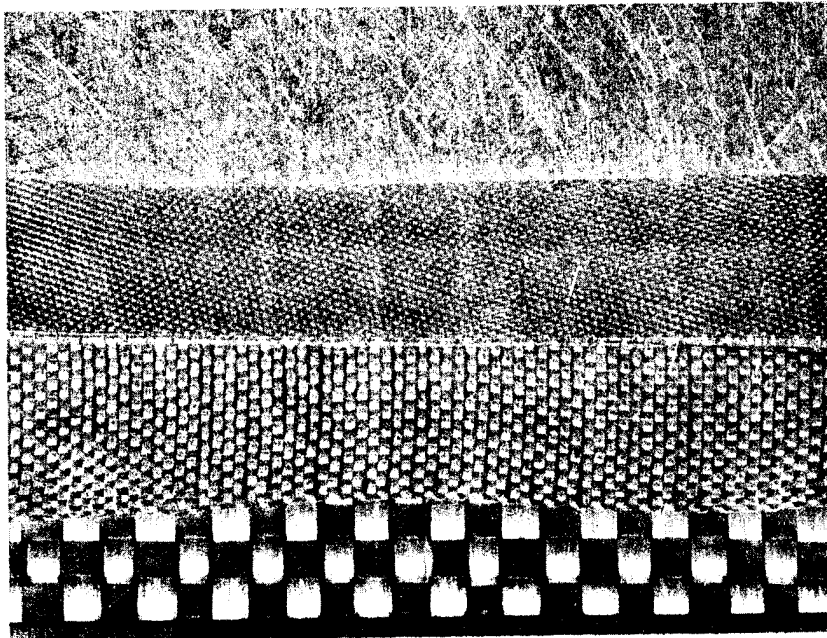
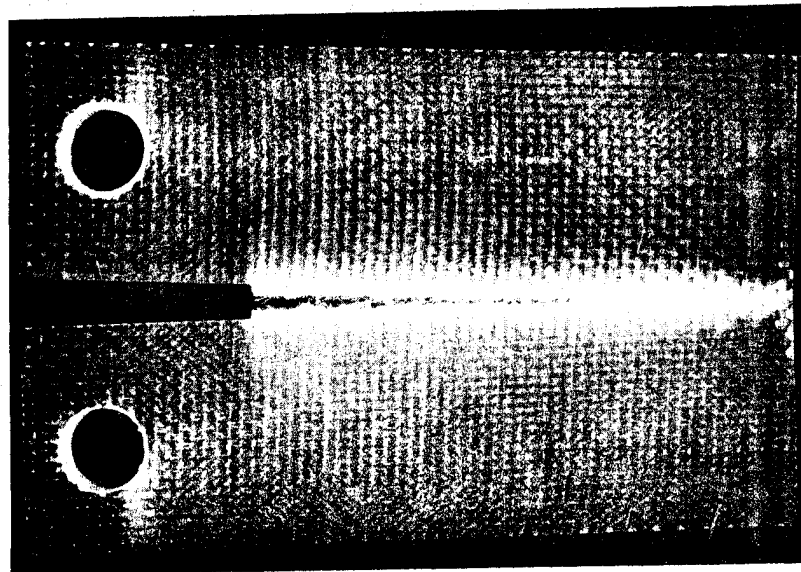


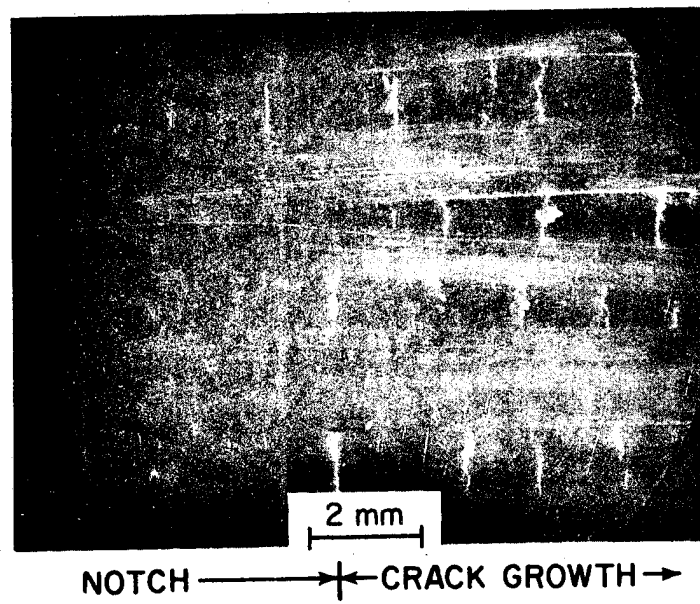
FIGURE 2.

**TYPES OF E-GLASS FIBER REINFORCEMENT (TOP TO BOTTOM: RANDOM CHOPPED FIBER MAT, STYLES 181 AND 1800 WOVEN FABRIC, AND STYLE 61 WOVEN ROVING WITH CENTIMETER SCALE).**



(a)

Fractured specimen, style 1800 fabric



(b)

Cross-section of woven roving specimen taken parallel to the main crack plane, showing sub-critical splits.

FIGURE 3.  
FRACTURED SPECIMEN AND CROSS-SECTION  
THROUGH LIGAMENTS.

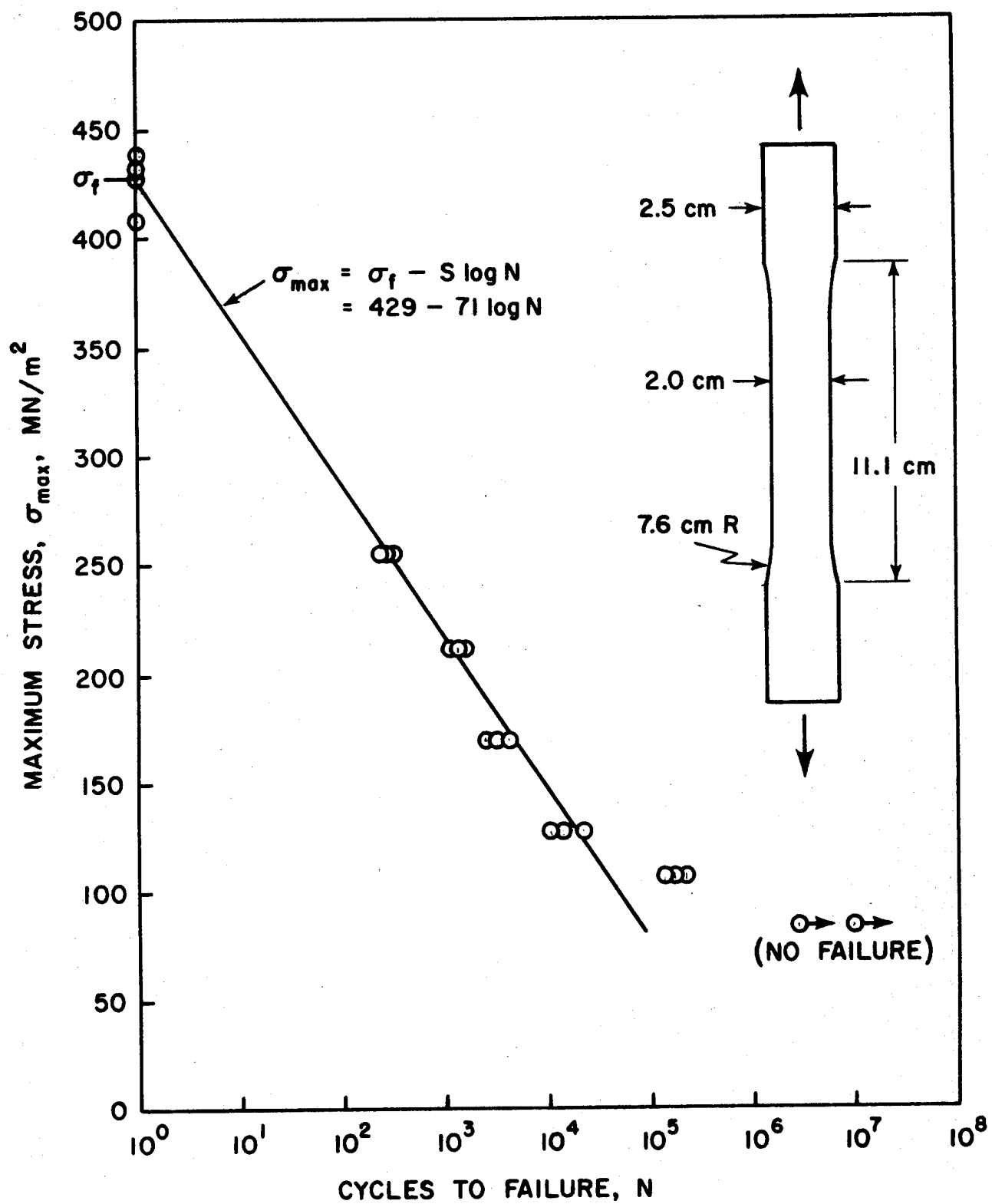


FIGURE 4.

UNNOTCHED STRESS vs. FATIGUE LIFE FOR STYLE 181  
WOVEN FABRIC/POLYESTER MATRIX.

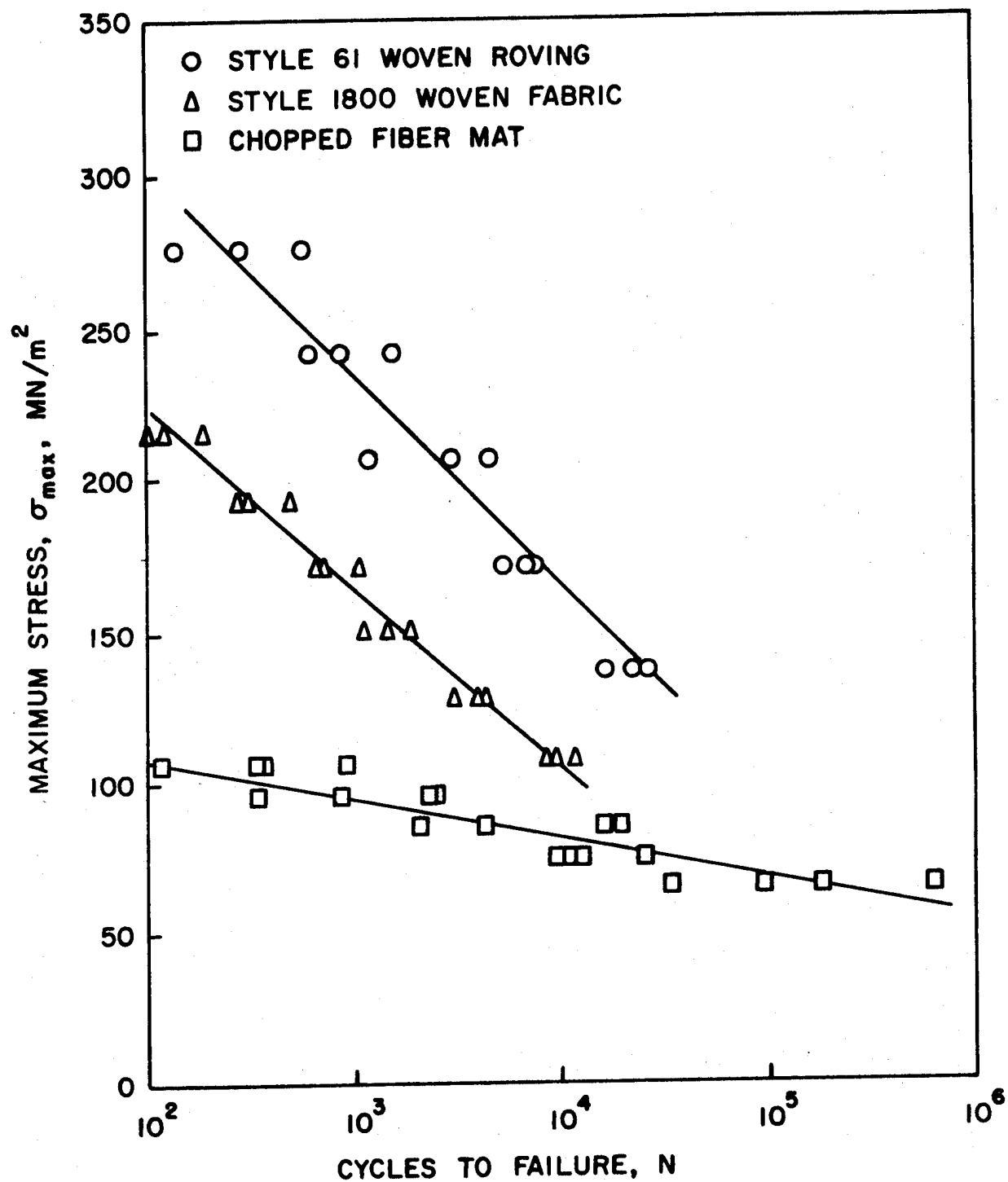


FIGURE 5.

UNNOTCHED STRESS vs. FATIGUE LIFE CURVES FOR  
VARIOUS REINFORCEMENTS/POLYESTER MATRIX.

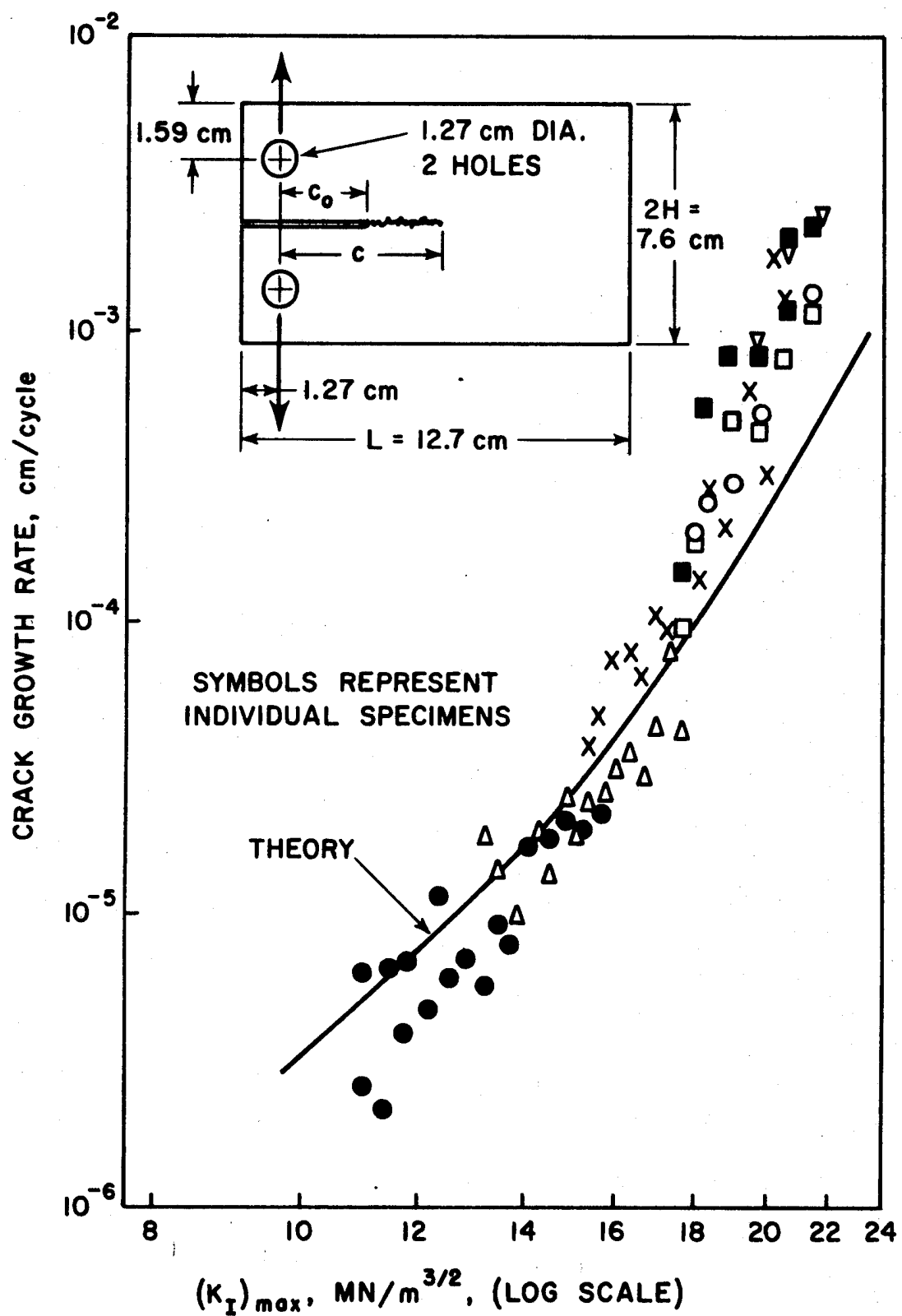


FIGURE 6.

THEORETICAL vs. EXPERIMENTAL FATIGUE CRACK GROWTH RATES FOR STYLE 181 E-GLASS WOVEN FABRIC WITH POLYESTER MATRIX.

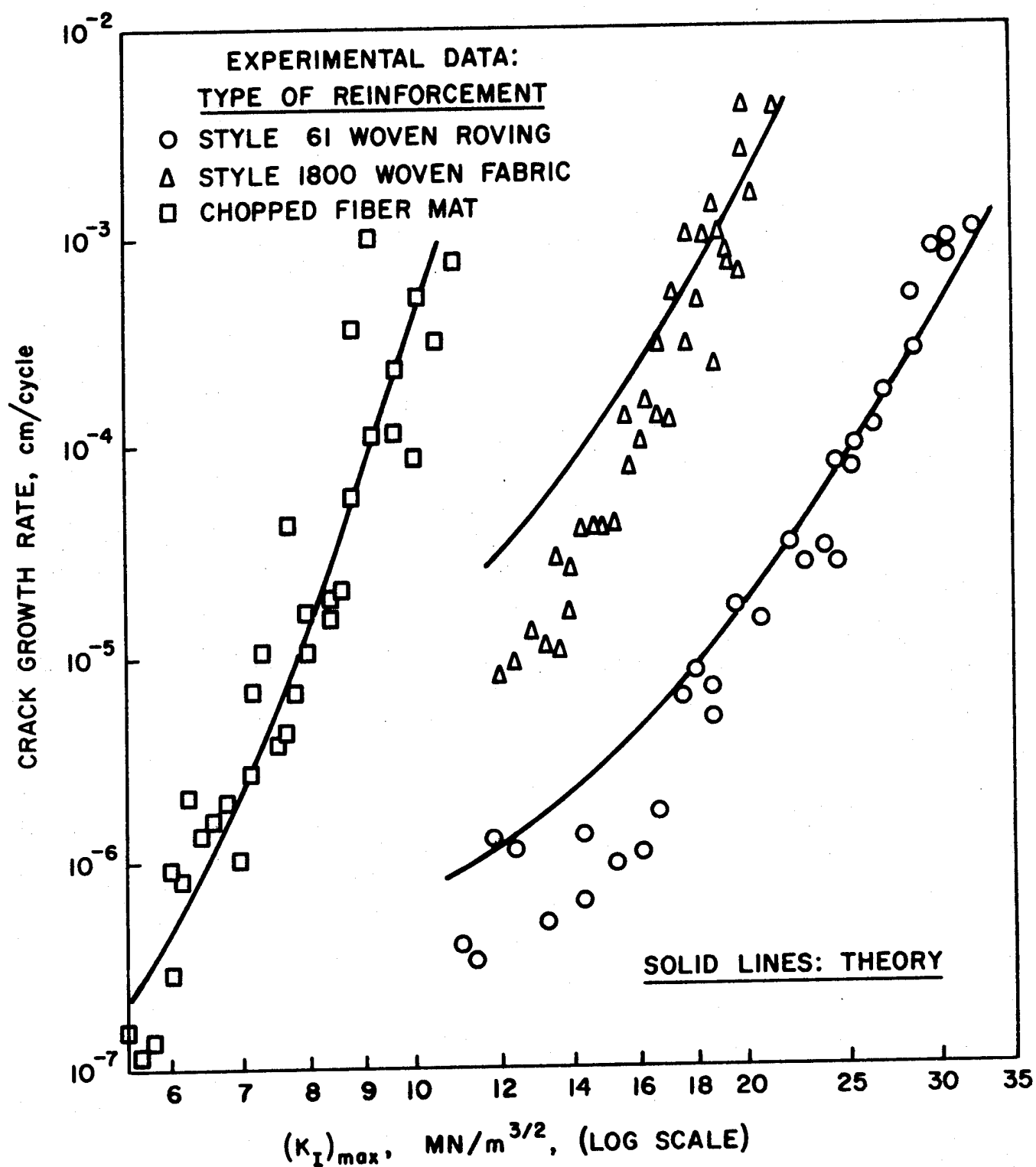


FIGURE 7.

THEORETICAL vs. EXPERIMENTAL FATIGUE CRACK GROWTH RATES FOR POLYESTER MATRIX WITH VARIOUS FORMS OF E-GLASS REINFORCEMENT.

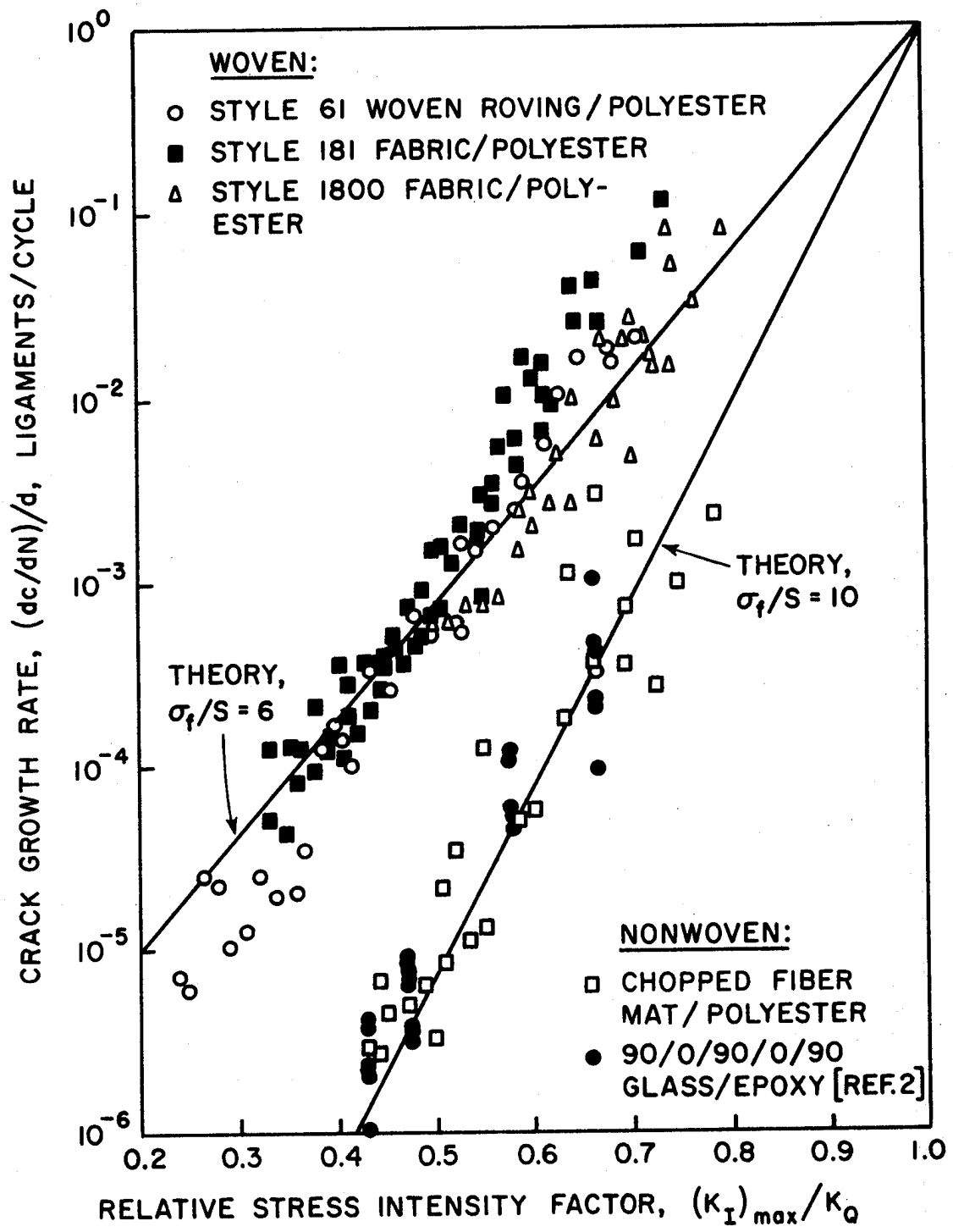


FIGURE 8.

NORMALIZED FATIGUE CRACK GROWTH RATE CURVES  
FOR FIVE MATERIALS.

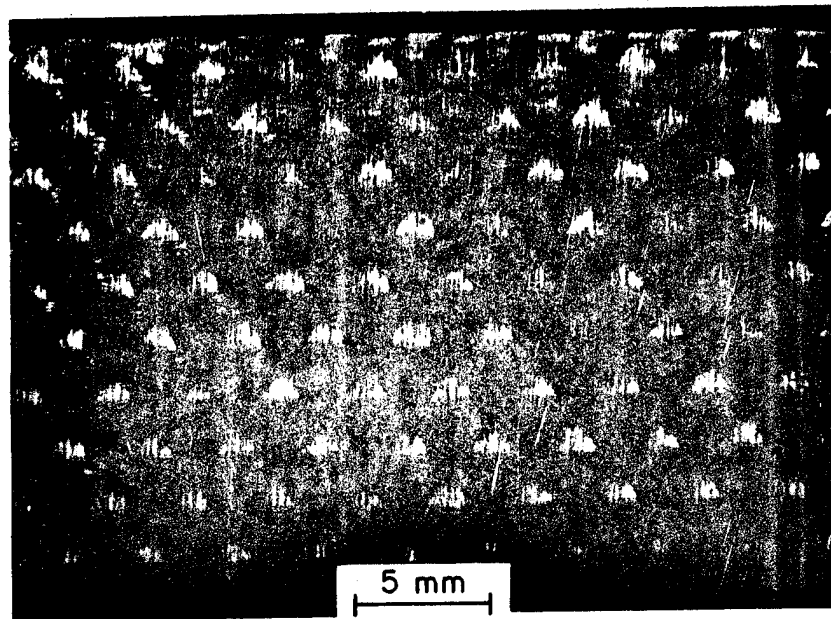


FIGURE 9.

FORMATION OF CRACKS AT WEAVE CROSS-OVER POINTS  
IN UNNOTCHED STYLE 1800 WOVEN FABRIC/POLYESTER  
SPECIMEN.

### SECTION III EFFECTS OF MARINE ENVIRONMENT

#### INTRODUCTION

The tendency to fail in a notch-sensitive, brittle fracture mode is characteristic of a variety of fiberglass laminates, including those based on chopped strand mat, woven fabric, woven roving, and  $0^\circ/90^\circ$  cross-ply [1-3]. These laminates are also known to be sensitive to static fatigue [4] as well as dynamic (cyclic) fatigue [5], both of which are considerably more severe in the presence of a water environment [6]. The application of fiberglass, particularly in the marine and transportation industries, is likely to lead to combinations of these geometric/loading/environmental factors as cracks slowly propagate under the influence of a particular load history, to eventually cause failure of the structure. The lifetime of structures in such situations depends primarily upon the rate at which cracks extend prior to reaching a critical length necessary for catastrophic fracture.

The various fatigue and environmental effects of interest in this study occur in the localized context of a propagating crack tip, so that the mechanisms of crack extension and crack resistance are of primary importance. The resistance to crack extension may be described from either an energetic [7, 8] or stress intensity point of view; the latter approach will be taken in this paper. The crack resistance of multi-directional laminates is found to derive from the extension of a damage zone at the crack tip, which serves, in effect, to blunt the crack and relax the locally high stresses [9, 10]. The mechanisms of stress transfer and the effect of the damage zone in relaxing the stresses tending to break the fibers in a  $0^\circ/90^\circ$  laminate have been demonstrated analytically [11]. The damage zone size is a function of the stress intensity factor,  $K_I$ , for notch-sensitive laminates, and larger crack-tip damage zones lead to

higher values of fracture toughness [9, 10, 12].

The tensile strength of fiberglass laminates is found to decrease with log time under stress in an approximately linear manner [4]. The origins of this effect have been related to stress-corrosion of the fibers and the time-dependent nature of the resin [13]. In addition to the cumulative effects of time under stress, the cycling of the stress with time has a separate and usually severe effect [14], which is associated with cumulative debonding and matrix cracking damage [15]. Comparisons of static and dynamic fatigue results under dry and wet conditions indicate that water immersion tends to reduce the strength and increase the rate of reduction of strength with time [4, 6, 13].

A limited amount of information is available on the effects of fatigue and environment on the fracture toughness of fiberglass. The fracture toughness of 0°/90° glass/epoxy and woven roving/mat reinforced polyester was found to decrease with decreasing strain rate and increasing temperature to a similar degree as did the strength [2]. Cyclic fatigue loading was found to increase the residual fracture toughness in some cases [9, 15] due to enlargement of the damage zone and associated blunting of the crack. However, continued cyclic loading resulted in extension of the crack and eventual failure, even at relatively low stress intensity levels [17, 18]. The rate of crack extension has been studied for a variety of fiberglass laminates, and good agreement has been demonstrated with a theory which predicts an exponential relationship between the cyclic crack growth rate and the stress intensity factor [17, 18], as will be described later.

The purpose of the present study was two-fold: 1) to investigate the previously unexplored topic of crack extension under sustained static load

conditions, and (2) to investigate the effects of water immersion on the rate of crack extension for both static and cyclic loading. The initial part of the study was concerned with the effects of seawater on the rate of crack extension under cyclic loading; a laminate composed of alternate layers of woven roving and chopped strand mat with a polyester matrix was chosen for this work. While satisfactory results were obtained with this material, the scatter in the results was greater than is commonly observed with more finely woven fabrics. The increased scatter became impractical in the second part of the study, which was concerned with crack extension under static loads. Crack extension under static loads is so sensitive to the test parameters that it was necessary to switch to a fine woven fabric laminate which displayed more consistent properties. At the same time, the water environment was switched to distilled water which has an almost identical effect on laminate mechanical properties [19]. To provide a consistent set of results and to confirm the findings of the first two parts of the study, a subsequent series of experiments was conducted on a crossplied glass/epoxy material with both static and dynamic tests in air and in distilled water.

## EXPERIMENTAL METHODS

### Materials

The materials used in this study were chosen to represent those laminates common to marine applications which have been demonstrated to fail in a notch-sensitive manner [2]. These include chopped strand mat, woven roving, and woven fabric reinforced polyester; additionally, laminates of 0°/90° unidirectional-ply glass/epoxy were used to confirm the trends observed for the other laminates. The following are the three types of laminates studied (all reinforcement was E-glass, supplied with a polyester-compatible finish for the chopped strand mat, woven roving, and woven fabric):

1. 181-style woven fabric (Uniglass Industries) with Laminac 4155 polyester matrix (American Cyanamid Co.). Laminates were compression molded, then postcured at 100°C for two hours.
2. Five plies of 1.5 oz. chopped strand mat alternated with four plies of style 779 woven roving (both from Stevens Fiberglass Co.) with Laminac 4155 polyester matrix (American Cyanamid Co.). Laminates were fabricated by hand layup, room temperature cure.
3. Scotchply Type 1003 unidirectional ply, epoxy matrix (3M Co.). Compression molded and cured at 350° F according to manufacturer's instructions, 44 alternating 0° (load direction) and 90° (crack direction) plies in the arrangement (90/90/0/90/90/0/.../0/90/90/0/90/90).

Details of the thickness and fiber volume fraction are given for each case in Table 1.

### Test Methods

The test specimens shown in Fig. 1 were machined from the laminates with a diamond-edged wheel and Tensilkut router. Notches were also cut with a diamond-edged wheel. With the exception of a few tests which will be noted individually, all tests were conducted on an Instron Model 1211 dynamic

cycler under load-control conditions. Water immersion was accomplished by surrounding the entire specimen and grip with a containment tank, which resulted in some contamination of the water by rust from the chrome-plated grips. This contamination was minimized by frequent water changes and silicone spray applied to the grips.

The unnotched specimen shapes given in Fig. 1 were determined by trial and error to provide the least reduction in strength due to stress concentrations at the shoulder, while avoiding failure in the grips. The wider specimen was used for the woven roving/mat laminates to offset the effect of increased heterogeneity.

The cleavage specimen used for all of the crack propagation studies has been investigated in detail previously [20]. Figures 2 and 3 indicate that the K-calibration used for the specimen results in a constant value of the fracture toughness,  $K_Q$ , for various crack lengths. These results were obtained on an Instron Universal testing machine at a displacement rate of 0.02 in./min. Figures 2 and 3 (taken from Ref. [20]) indicate that the test specimen may be used to impose a particular value of  $K_I$  on an opening-mode crack for crack growth studies; the damage zone associated with the crack tip clearly remains approximately constant in size as the crack extends. Thus, crack propagation may be studied over a distance of an inch or two under known  $K_I$  conditions and without significant specimen size effects. While the anisotropic elastic constants were considered in determining the K-calibration curve for the woven roving/mat laminates [20], the very similar isotropic K-calibration was used for the other laminates. The value of  $K_I$  in the latter case is given by [21]:

$$K_I = \frac{3.46 P \left( \frac{C}{H} + 0.7 \right)}{BH^{1/2}} \quad (1)$$

where  $P$  is the applied force,  $C$  is the crack length,  $B$  is the thickness, and  $H$  is the half-height of the specimen (1.5 in. in this case). Figures 4 and 5 indicate that crack propagation in the 181 fabric and scotchply laminates also occurred in the expected manner, with crack extension parallel to the original notch, and with a localized damage zone. The cleavage specimen geometry is effective only if the laminate is thick enough to avoid buckling and if the crack tends to propagate along the length direction.

In the course of the tests on the woven roving/mat and 181-style fabric laminates it was necessary to take frequent readings of the crack length. As the photographs in Figs. 3 and 4 suggest, it can be difficult to establish the precise crack tip location, particularly for the woven roving/mat laminates. The methods used to determine the crack-tip position were visual observation followed by graphical smoothing of the data in the case of the 181-style laminates, and observation under cross polarized transmitted light of the woven roving/mat laminates. Only the total specimen lifetime was determined for the Scotchply laminates.

### THEORETICAL PREDICTION

A theory for the crack propagation rate under cyclic loading was presented in Refs [17] and [18]. The theory is based on a model of crack extension involving the ligament by ligament advance of the crack, with each ligament failing according to the S-N curve of the bulk material.

Figure 6 indicates the mode of crack advance observed in the present study as well as in earlier studies [17, 18]: the crack remains stationary for a number of fatigue cycles until a ligament of material at the crack tip fails, then the crack advances to the next ligament. Only those fibers normal to the crack are considered in the model. Ligament widths observed for a variety of laminates range from  $10^{-1}$  to  $10^{-2}$  inches, so that a large number of individual fibers are contained in each ligament [18]. This mode of crack propagation is identical in appearance to that observed in monotonic fracture tests of  $0^\circ/90^\circ$  laminates [1, 2].

For the simple, but commonly observed case where a substantial portion of the S-N curve for the unnotched material can be approximated by a linear relationship, the number of cycles to failure in the linear portion can be represented by

$$\log N = \frac{\sigma - \sigma_f}{S} \quad (2)$$

where  $N$  is the number of cycles to failure,  $\sigma$  is the maximum applied stress,  $\sigma_f$  is the monotonic strength, and  $S$  is the slope of the S-N curve. Such a relationship has been found to give a good approximation to S-N data in 0-tension load cycling for chopped fiber mat, woven roving, woven fabric and  $0^\circ/90^\circ$  unidirectional ply laminates [18] under conditions where  $\sigma_f$  is determined at the same strain rate as is used

in the fatigue tests and the specimen shape is similar to those in Fig. 1.

To apply the S-N relationship to the ligaments at the crack tip it is necessary to obtain an approximation to the local stress tending to fail the ligament. For this purpose, it is assumed that the local stress at the crack tip increases in proportion to  $K_I$ , reaching the local failure stress when  $K_I$  reaches  $K_Q$ , so that the stress on the ligament,  $\sigma_\ell$ , is given by

$$\sigma_\ell = \sigma_f \left( \frac{K_I}{K_Q} \right) \quad (3)$$

This assumption is reasonable since fracture is observed to be synonymous with failure of the ligament at the crack tip in monotonic tests [1]. It may be questionable, however, if the damage zone size varies significantly with the maximum value of  $K_I$  in the test.

Equating  $\sigma$  in Eq. (2) with  $\sigma_\ell$  in Eq. (3) yields the prediction for the crack growth rate under 0-tension fatigue as

$$\frac{dc}{dN} = d / \exp [2.3 \frac{\sigma_f}{S} (1 - K_I / K_Q)] \quad (4)$$

where  $d$  is the experimentally measured ligament width. Since the parameters  $d$ ,  $\sigma_f$ ,  $S$ , and  $K_Q$  in Eq. (4) may be determined directly from the S-N curve, a fracture toughness test, and the observed ligament width, Eq. (4) provides a direct prediction of the crack growth rate,  $dc/dN$ , as a function of  $K_I$ . Although the prediction may be modified to account for cumulative damage effects on ligaments further away from the crack tip [17], these effects have not proven to be significant, and

Eq. (4) has been found to accurately predict the crack growth rate for a variety of laminates [18].

The applicability of the theory to laminates which fail by crack propagation involving fiber fracture appears to derive from the simple, step-wise, ligament by ligament advance of the crack. This contrasts with the mode of crack advance in metals, which usually involves an incremental extension of the crack with every cycle by a complex mechanism. Despite this difference, a similar model to the one described here has been reported to give encouraging crack growth rate predictions for some metals [22].

## RESULTS

### Dynamic Tests

The dynamic tests were initially run on the woven roving/mat laminates only. The loading consisted of a sinusoidal load-time curve between a maximum tensile load and a minimum load which was approximately 5% of the maximum; the frequency was 5-6 cycles per second in all cases. The environment was either ambient (approximately 75°F, 50-70% R.H.) or salt water immersion at room temperature. The salt water was a synthetic 3% NaCl solution. Specimens tested in the salt water environment were presoaked in salt water for ten days prior to the initiation of the test. Slight heating (warm to the touch) was observed for the dry environment crack growth tests, but the temperature effect was not investigated.

Figures 7 and 8 give the S-N curves for unnotched specimens in dry and salt water environments. The data are easily approximated by a straight line over the range of cycles investigated. The lifetimes of the dry samples are generally longer than those for the samples in salt water, but little difference is observed at lower stress levels. Table 2 gives the values for the slopes of the S-N curves (S) and the monotonic strengths ( $\sigma_f$ ). The monotonic strengths determined by extrapolation of the S-N curves to one cycle are significantly lower than the ultimate strengths measured experimentally at the corresponding displacement rate of 60 in/min. Earlier results have shown that the S-N curve is approximately linear including the monotonic strength value for woven and unidirectional ply laminates [17, 18], so the present discrepancy is attributed to some shift in the failure mechanism between monotonic and cyclic tests which is peculiar to laminates containing both woven roving and chopped strand mat. In the prediction of

the cyclic crack growth rate, the extrapolated value of  $\sigma_f$  is used. Additional constants to be used in the theoretical prediction of Eq. (4) are  $K_Q$  measured at 30 in/min displacement rate and the ligament width,  $d$ , taken as an average value from the crack length vs. time data, both of which are also given in Table 2.

Figures 9 and 10 give the theoretical and experimental crack growth results for cyclic loading in dry and salt water environments. The notable features of the results are the good agreement between the theoretical and experimental values, the significant scatter in the data points, and the shift to more rapid crack growth in the salt water environment. The rate of crack extension in salt water averages approximately one half of a decade more rapid than in the dry environment at corresponding  $K_I$  values.

#### Static Tests

The substantial scatter in the cyclic data led to a switch to 181-style fabric reinforced polyester laminates for the static tests, due to the expectation of a greater sensitivity to  $K_I$  in the static case. The static tests were conducted by loading the specimen as rapidly as possible to a predetermined load, and then holding this load constant until failure occurred. The wet specimens were not preconditioned in water prior to testing in most cases, but the effect of preconditioning was investigated separately.

Figures 11 and 12 give the strength vs. time to fail data for the unnotched specimens in dry and distilled water environments. The data are reasonably approximated by a linear relationship, and the limited data for the wet environment indicates a much more rapid decrease in strength with time than for the dry environment.

Figure 13 indicates a typical crack length vs. time curve for the cleavage specimens. The discrete data points were approximated by a smooth curve, and the slope of the curve at each point was determined graphically to obtain a value for the crack growth rate,  $dc/dt$ . Figure 14 indicates that the log time to fail each ligament at the crack tip was a linear function of  $K_I$ ; the average ligament width,  $d$ , was approximately 0.02 in. The crack growth rate vs.  $K_I$  data are plotted in Figs. 15 and 16 for dry and wet environments. The more complete results for the dry environment clearly suggest a power law relationship between  $dc/dt$  and  $K_I$  as

$$dc/dt \propto K_I^n \quad (5)$$

where  $n$  is approximately 24 for the dry environment and 22 for the wet environment

Comparison of Figs. 15 and 16 indicates the surprising result that the crack grows approximately ten times faster in the dry environment than in the wet environment. This is also evident in the total lifetime data for the two environments given in Table 3: the lifetime of the wet samples is 20-40 times longer than that for dry samples.

As noted previously, the results for the static tests do not include a presoak prior to testing. Table 4 indicates that the effect of presoaking the samples for forty days prior to testing is not significant, with only a slight decrease in the lifetime of the presoaked cleavage samples.

#### Scotchply Static and Dynamic Tests

Results from the previous sections indicate that water tends to accelerate cracks under dynamic loading, but to decelerate them under static

loading. However, this finding is complicated by differences in the style of reinforcement, presoak time, and water composition. To clarify the previous results, a set of tests were run on a different material, 0°/90° unidirectional-ply glass/epoxy (Scotchply), with a fixed presoak time (ten days) and a fixed water composition (distilled water). Static and dynamic tests under ambient and water immersion conditions were performed at identical values of maximum applied force; the testing details were unchanged from previous tests.

Rather than recording the rate of crack extension, only the time to complete failure was recorded. The failure time is synonymous with the time to extend the crack 3.5 inches, but the lifetime was consumed almost entirely in the first 0.5 inches of propagation since the constant applied load of 1740 lb. in all cases resulted in a rapidly increasing value of  $K_I$  as the crack extended (see Eq. 1). The specimen lifetime data are, in effect, an average of the crack growth rates at different  $K_I$  values as the crack extends under constant load.

Table 5 gives the results of the Scotchply tests. The specimen lifetime under dynamic loading was almost three times longer in the dry environment, while the wet environment gave a lifetime almost four times as long for static loading. Thus, the earlier finding is confirmed with a significantly different material under invariant conditions. Table 5 also indicates that the damage zone size is larger for the dynamic tests but is unaffected by the environmental conditions (see also Fig. 5).

## DISCUSSION

### Applicability of Crack Growth Model

The simple theoretical model for crack extension described earlier rests on the assumption of a ligament of material at the crack tip which is subjected to fatigue at its local stress level. Failure of the ligament is assumed to occur under the same conditions as failure of an unnotched cupon of the same material, tested at the same stress level. Results from the dynamic tests confirm the applicability of this model for both wet and dry conditions; crack extension is observed to occur in a stepwise, ligament by ligament manner, and the theoretical crack extension rate prediction is shown to be in good agreement with the experimental data over a broad range of loads and crack growth rates. This agreement is anticipated from previous studies of a variety of similar materials [17, 18].

The dominant terms in the theoretical relationship given in Eq. (4) are  $K_I/K_Q$  and  $\sigma_f/S$ . The first term,  $K_I/K_Q$ , simply describes the loading on the specimen relative to its failure condition. The second term,  $\sigma_f/S$ , gives the fundamental fatigue characteristics of the material in tension. Previous studies [18] have shown this ratio to be approximately six for all woven fabric and woven roving laminates over a broad stress range, while the ratio is approximately ten for nonwoven reinforcements including chopped strand mat and Scotchply. The material employed in the dynamic study combines woven roving and chopped strand mat, and the resulting  $\sigma_f/S$  ratio is an intermediate 8.6-8.9 for wet and dry conditions. This intermediate value suggests that neither the woven roving nor the mat dominate the fatigue behavior, but that they both contribute substantially. This is consistent with earlier fracture studies which indicated that the woven roving/mat combinations showed considerably

different damage zone sizes and fracture behavior than did each material separately [2, 23].

The ligament by ligament advance of the crack was also observed for the static loading cases, and, as mentioned, previous dynamic studies have shown the applicability of Eq. (4) for both the 181-style fabric and Scotchply used in the static studies [17, 18]. The implication is that a relationship similar to Eq. (4) should be useful in predicting the static fatigue crack growth rate. Such a relationship for the static case may be derived by substituting  $\sigma_{f1}$  and  $K_{Q1}$ , the strength and fracture toughness at the reference failure time of one minute, for  $\sigma_f$  and  $K_Q$  in Eq. (4). This gives the relationship

$$\frac{dc}{dt} = d/\exp [2.3 \frac{\sigma_{f1}}{S} (1 - K_I/K_{Q1})] \quad (6)$$

where  $d$  and  $S$  are the appropriate values for the statically tested materials. The values of  $\sigma_{f1}$  and  $S$  are given in Figs. 11 and 12, and  $K_{Q1}$  may be taken from Fig. 14 as the value of  $K_I$  corresponding to a one minute failure time for the ligament. Unfortunately, when the correct constants are substituted into Eq. (6), poor agreement is found with the experimental data; in fact, the slope of the ligament strength-time data of Fig. 14 does not correspond to the slope of the unnotched specimen results in Fig. 11. In addition to this, Eq. (6) would predict a higher crack growth rate in water, while a slower rate is observed. It is apparent that this theoretical approach is not directly applicable to the static crack growth phenomenon despite the consistent mode of crack extension. No suitable modification or alternative has yet been discovered

### Effects of Water Immersion

The finding that water immersion tends to decrease the crack growth rate under static loading conditions is contrary to expectations. The strength of unnotched cupons is generally decreased in the presence of water for both dynamic and static loading. Since crack extension clearly occurs in each case by the tensile failure of ligaments at the crack tip, water is expected to result in more rapid failure of the ligaments and a consequent higher crack growth rate. This expectation is realized in the dynamic case, where the crack growth rate is accurately predicted by the theory based on tensile cupon S-N data. However, the opposite trend is clearly and consistently observed for static loading.

There appear to be three general lines of explanation possible for this anomalous finding in the static case: (1) the actual stress at the crack tip is reduced by the presence of water for a given applied load, (2) the value of  $K_I$  given by Eq. (1) is decreased by the presence of water, or (3) the lifetime of the ligaments at the crack tip is increased in the presence of water despite the decreasing unnotched tensile cupon lifetime.

The first proposition would be convincing if water exposure was observed to increase the size of the crack tip damage zone, thus effectively increasing the bluntness of the crack. However, the data in Table 5 do not indicate such an effect, and the damage zone size is insensitive to water for both static and dynamic tests. The stress in the ligament at a particular value of  $K_I$  also depends upon factors other than the damage zone size which may affect the transfer of stress into the ligament [11]. A number of such factors, including a decrease in the shear modulus, increased delamination between plies, and weakening of the

individual fiber-matrix bond, could result in a decreased ligament stress, but none have yet been substantiated.

The second possibility, a change in the K-calibration due to the effect of water, could also be related to the inapplicability of the crack growth theory to the static case. If the modulus of the material were altered by time or environmental effects in those portions of the specimen which are highly stressed, then the effect could be similar to a change in specimen shape. Changes of  $K_I$  in the range of 10-20% would be sufficient to account for the anomalies in the data, and such a change is possible. A K-calibration study to include such effects is feasible [20], but has not yet been conducted.

The last possibility, that the ligament lifetime at a given local stress is actually extended by a water environment, appears doubtful on the basis of available evidence [4, 6, 13]. However, there have been reports of increases in glass strength with water exposure in some cases [24], and some fibers at the crack tip are exposed directly to the environment by the damage zone subcracking and delamination. However, a brief series of yarn strength tests from the 181-style fabric yielded a 10-20% drop in unimpregnated yarn strength with immersion in distilled water, and a further decrease was observed when the yarns were presoaked for one day.

Thus, although conclusive evidence is not available, it seems likely that the water environment has some effect in decreasing the stress on the ligaments, either by an alteration in  $K_I$  or by a relaxation of the stress on the ligament immediately at the crack tip. Any such hypotheses must also address the absence of the same effects in the cyclic tests, which results show no anomaly. The explanation appears to be that such effects may be present in the dynamic tests, but other effects tend

to dominate them. The damage zone is already greatly enlarged by cyclic loading (Table 5) so that water may not greatly increase the effective crack bluntness. Furthermore, the cyclic results are less sensitive to shifts in  $K_I$ , since the effective exponent for cyclic data on 181-style fabric laminates is 2-3 times lower than that given in Fig. 15 [18]. Although the specimen lifetime under cyclic loading does not appear to be severely reduced as compared to the static results in Table 5, it must be realized that the time given for the cyclic tests in the table are total times, only a small fraction of which is spent near the maximum load. Thus, the accumulated time under load is much shorter for the cyclic tests, as the effects of reversing the stress are apparently more severe than the static fatigue effects.

#### Stability of Cracks in Fiberglass

The data given in Figs. 15 and 16 provide useful evidence of the relationship between time and toughness in fiberglass laminates. The data in Fig. 14 may also be interpreted as giving the fracture toughness as a function of time, since the fracture toughness,  $K_Q$ , has been interpreted as the value of  $K_I$  necessary to cause crack advance, crack advance being synonymous with ligament failure. In this interpretation, the effect of time on  $K_Q$  is consistent with earlier findings which considered the effects of loading rate on  $K_Q$  for similar materials [2].

The sharply increasing value of  $K_Q$  with decreasing time suggests that propagating cracks may not readily become unstable. In fact, cracks in typical fracture specimens such as the notched tension configuration are not commonly observed to propagate as rapidly as expected. The terminal velocity for a crack is expected to reach the order-of-magnitude of the

longitudinal stress wave velocity after a short distance of propagation [25]. Using notched tension tests of identical geometry, crack velocities in the expected range were measured for plexiglass and for graphite/epoxy laminates, but the velocity in Scotchply glass/epoxy reached only a few hundred inches/minute, about four orders of magnitude less than expected [9]. Although the graphite and glass reinforcements used in these tests differed by a factor of three in modulus, the reason for the extreme difference in behavior apparently derived primarily from the greatly reduced rate effects in the graphite. Thus, the increasing value of  $K_Q$  with loading rate, and the observation of slow crack propagation velocities in laboratory tests suggested that cracks in fiberglass may never become truly unstable.

The data in Fig. 15 suggest a different interpretation for the stability of cracks. The empirical relationship

$$dc/dt \propto K_I^{24} \quad (7)$$

has certain implications for the crack velocity as a function of the crack length. For a crack in an infinite plate subject to a constant nominal stress  $\sigma$  normal to the crack,  $K_I$  is given by [26]

$$K_I = \sigma \sqrt{\pi C} \quad (8)$$

Substituting (8) into (7)

$$dc/dt \propto \sigma^{24} \pi^{12} C^{12} \quad (9)$$

A stable crack under constant applied stress should propagate at a rate proportional to the 12th power of the crack length. Under these conditions, the crack velocity would increase by a factor of about 4000 as the crack doubled in length, rapidly

bringing the crack under the control of the classical dynamic effects which lead to the predicted terminal velocity. This is hardly an inherently stable situation. The 24th power relationship between  $dc/dt$  and  $K_I$  is substantially greater than the 16th power relationship evident in data from homogeneous soda-lime glass plates for which unstable crack extension is well known [27].

While no conclusive experiments have been conducted to resolve this situation, the contradiction evident in the two preceding paragraphs may be clarified by consideration of the limitations on the available data. Most experiments have heretofore been conducted on relatively small, laboratory-size specimens under controlled displacement conditions. The initial crack size is usually relatively large, and the slow initial crack extension allows unloading of the specimen under controlled displacement conditions. In addition to this, a doubling in size of a 0.5 inch initial crack would only lead to an increase in crack velocity of a factor of 4,000, perhaps from 0.1 to 400 inches/minute, not out of line with measured crack velocities [9]. Laboratory-size notched tension specimens usually bend and unload significantly by the time the crack has doubled in length. Thus, while there is no inherent crack stability, the rate effects in fiberglass may serve to contain the crack velocity in small specimens well below the values observed in many other materials, where a crack would accelerate from 0 to perhaps  $10^6$  inches/minute as it doubled in length.

The increasing value of  $K_Q$  with loading rate does lead to significant advantages for fiberglass in some situations, such as impact loading. The data in Fig. 14 suggest a corresponding disadvantage, as cracks may propagate under relatively low, long duration loading, very slowly at first, but accelerating rapidly as the crack extends. Any cycling of the load under these conditions could lead to much more rapid failure.

### Interpretation of Fracture Toughness Tests

The foregoing discussion contains certain implications for the interpretation and application of fracture test results. While it is generally realized that  $K_Q$ , as other fiberglass properties, is strongly rate sensitive, data such as those in Fig. 15 suggest that  $K_Q$  may be difficult to define properly.

The usual practice of defining  $K_Q$  as the value of  $K_I$  at which unstable crack propagation commences does not seem capable of treating the situation where stable and unstable conditions are ill-defined. Within a broad loading range, the crack is always propagating in fiberglass. The situation is analogous to that observed under fatigue loading in metals, where crack propagation rates and thresholds are the appropriate parameters, rather than instability conditions. A method of accounting for stable crack growth, the R-curve method, has been successfully applied to fiberglass laminates [28]. However, while such a method may appear to provide consistent fracture toughness results, the interpretation of the results still is unclear. The R-curve technique was developed as a means for fixing the instability point of materials which showed some stable crack growth prior to fracture, interpreted as an increasing crack-growth resistance with crack length [29]. However, in the case of fiberglass, the crack would propagate at values of  $K_I$  well below the "critical" value determined in this manner, given sufficient time.

## CONCLUSIONS

Stable crack propagation has been observed in fiberglass laminates over a broad range of cyclic and static loading conditions. Under cyclic loading conditions the rate of crack propagation may be predicted by a simple theory, but the rate of propagation under static conditions was not predictable. A water environment reduces the ultimate tensile strength of unnotched samples for both static and cyclic loading. However, water tends to accelerate cracks under cyclic loading while decelerating them under static loading. The origins of the anomalous effects of water on the rate of crack extension are not clear.

REFERENCES FOR SECTION III

- 1). McGarry, F.J. and Mandell, J.F., "Fracture Toughness Studies of Fiber Reinforced Plastic Laminates," Proc. Special Discussion of Solid Interfaces, Faraday Division of The Chemical Society, Nottingham, England (1972).
- 2). Mandell, J.F., McGarry, F.J., Kashihara, R., and Bishop, W.R., "Engineering Aspects of Fracture Toughness: Fiber Reinforced Laminates," Proc. 29th Reinforced Plastics/Composites Div., SPI, Section 17 D, 1974.
- 3). Owen, M.J., and Bishop, P.J., "Critical Stress Intensity Factors Applied to Glass Reinforced Polyester," J. Composite Materials, Vol. 7 (1973), p. 146.
- 4). Boller, K.H., "Effect of Long-Term Loading on Glass-Reinforced Plastic Laminates," Proc. 14th Technical and Management Conf. Reinforced Plastics Div., SPI, (1959), Section 6 - C.
- 5). Salkind, M.J., "Fatigue of Composites," Composite Materials : Testing and Design (Second Conference), ASTM STP 497, American Society for Testing and Materials (1972) p. 143.
- 6). Bascom, W.B. "The Surface Chemistry of Moisture-Induced Composite Failure," in Composite Materials, Vol 6, L J.Broutrman, R.H. Krock, and E.P. Plueddemann, ed., Academic Press, New York (1974).
- 7). Kelly, A., "Interface Effects and the Work of Fracture of a Fibrous Composite," Proc. Roy. Soc. London, A319 (1970), p. 95.
- 8). McGarry, F.J. and Mandell, J.F., "Fracture Toughness of Fibrous Glass Reinforced Plastic Composites," Proc. 27th Reinforced Plastics/Composites Div., SPI (1972), Section 9 A.
- 9). Mandell, J.F., McGarry, F.J., Im, J., and Meier, U., "Fiber Orientation, Crack Velocity, and Cyclic Loading Effects on the Mode of Crack Extension in Fiber Reinforced Plastics," in Failure Modes in Composites II, TMS/AIME (1974).
- 10). Mandell, J.F. , Wang, S.S. and McGarry, F.J., "The Extension of Crack Tip Damage Zones in Fiber Reinforced Plastic Laminates," J. Composite Materials, Vol. 9 (1975), p. 266.
- 11). Wang, S.S., Mandell, J.F., and McGarry, F.J., "Three-Dimensional Solution for a Through-Thickness Crack with Crack Tip Damage in a Crossplied Laminate," presented at ASTM Symposium on Fracture Mechanics of Composites, Gaithersburg, Md. (1974).
- 12). Gaggar, S., and Broutrman, L.J., "The Development of a Damage Zone at the Tip of a Crack in a Glass Fiber Reinforced Polyester Resin," Int. J. of Fracture, vol 10.(1974), p. 600.

13). Lifshitz, J.M., "Time-Dependent Fracture of Fibrous Composites," in Composite Materials, Vol.5 , L.J. Broutman and R.H. Krock, ed. Academic Press, New York (1974).

14). Owen, M.J., "Fatigue Damage in Glass-Fiber-Reinforced Plastics," in Composite Materials, Vol. 5,L.J. Broutman and R.H. Krock, ed., Academic Press, New York (1974).

15). Broutman, L.J. and Sahu, S., "A New Theory to Predict Cumulative Fatigue Damage in Fiberglass Reinforced Plastics," 24th Annual Tech. Conf. Reinforced Plastics/Composites Div., SPI, Paper 11 D (1969).

16). Waddoups, M.E., Eisenmann, J.R. , Kaminski, R.E., "Macroscopic Fracture Mechanics of Advanced Composite Materials, " J. Comp. Mat., Vol. 5 (1971),p. 446.

17). Mandell, J.F. , and Meier, U., "Fatigue Crack Propagation in 0°/90° E-Glass/Epoxy Composites," Fatigue of Composite Materials, ASTM STP 569,American Society for Testing and Materials (1975),p.28.

18). Mandell, J.F., "Fatigue Crack Propagation Rates in Woven and Non-Woven Fiberglass Laminates, " ASTM/ASME/AIAA/AIME Composite Reliability Conference, Las Vegas, Nevada, 1974 (to be published in ASTM STP 580).

19). Masuda, Y., "Effects of Watery Environment on Fatigue Strength of FRP" in Proc. 17th Japan Cong. on Mat. Res., The Soc. of Mat. Sci., Kyoto, Japan, (1974).

20). Mandell, J.F., McGarry, F.J., Wang, S.S., and Im, J., "Stress Intensity Factors for Anisotropic Fracture Test Specimens of Several Geometries ,"Journal of Composite Materials, Vol. 8 (1974), p. 106.

21). Kanninen, M.F., "An Augmented Double Cantilever Beam Model for Studying Crack Propagation and Arrest," Int. J. Fracture, Vol 9 (1973), p. 83.

22). Majundar, S. , and Morrow, J., "Correlation Between Fatigue Crack Propagation and Low Cycle Fatigue Properties," Fracture Toughness and Slow-Stable Cracking, ASTM STP 559, American Society for Testing and Materials (1974), p. 159.

23). Kashihara, R., "Fracture of Random Chopped Mat and Woven Roving Reinforced Plastics," M.S. Thesis, M.I.T. Dept. of Ocean Engineering (1974).

24). Stockdale, G.F., Tooley, F.V., and Ying, C.W., "Changes in the Tensile Strength of Glass Caused by Water Immersion Treatment," J. Am. Ceram. Soc., Vol. 34 (1951), p. 116.

25). Dulaney, E. N., and Brace, W.F., "Velocity Behaviour of a Growing Crack," J. Appl. Phys. , vol. 31 (1960), p. 2233.

26). Williams, M.L., "On the Stress Distribution at the Base of a Stationary Crack, " J. Appl. Mech. Trans. ASME, Vol 24 (1957),p. 109.

- 27). Wiederhoen, S., Environment-Sensitive Mechanical Properties, ARC. Westwood and N.S. Staff, ed., Gordon and Beach, New York (1966), p.293.
- 28). Gaggar, S.K., and Broutman, L.J., "Strength and Fracture Properties of Random Fiber Polyester Composites," Proc. 30th Reinforced Plastics/Composites Institute, SPI (1975), paper 9 - e.
- 29). Heyer, R.H., "Orack Growth Resistance Curves (R - Curves) - Literature Review," Fracture Toughness Evaluation by R - Curve Methods, ASTM STP 527, American Society for Testing and Materials (1973), p. 3.

TABLE 1 Materials

<u>Material</u>	<u>Specimen</u>	<u>No. Plies</u>	<u>Ave. Thickness (in)</u>	<u>Ave. Fiber Volume Fraction</u>
181 Fabric/Polyester	Unnotched Tension	10	0.10	0.46
	Cleavage	36	0.360	0.43
Woven Roving-Mat/polyester	Unnotched Tension	5-Mat 4-W.R.	0.216	0.31
	Cleavage	"	"	0.31
$0^\circ/90^\circ$ Sctchply	Cleavage	$14-0^\circ$ $30-90^\circ$	0.34	0.55

TABLE 2, Dynamic Fatigue and Monotonic Properties  
for Woven Roving/Mat Laminates.

	<u>Dry</u>	<u>Salt Water</u>
Measured $\sigma_{fm}^*$ (Ksi)	40.0	35.5
Extrapolated $\sigma_f$ from S-N data (Ksi)	31.0	27.0
S (Ksi/decade)	3.48	3.14
$K_Q$ (Ksi $\sqrt{\text{in.}}$ )*	27.8	24.8
Ligament Width, d (in.)	0.125	0.125

\*  $\sigma_{fm}$  measured at 60 in/min. and  $K_Q$  measured at 20 in/min. displacement rate, both consistent with cyclic displacement rates.

TABLE 3. Effect of Water Immersion on the Lifetime of 181-Style  
Fabric/Polyester Cleavage Specimens Under Static Loading.\*

<u>Average Load (lb)</u>	<u>Average Lifetime (min)</u>		<u>Lifetime (wet/dry)</u>
	<u>Dry</u>	<u>Immersed</u>	
1400	33.8	1375.	41
1500	10.4	332.	31
1600	1.4	30.	21

\* Wet : Immersed in Distilled H<sub>2</sub>O ; dry : 50-70% relative humidity ;  
temperature : 70-75° F.

TABLE 4

Effect of Presoaking 181 Style Fabric/Polyester  
Specimens for 40 days Prior to Testing in Distilled Water

<u>Time to Fracture for Immersed Specimens (min)</u>			
		<u>Not Presoaked</u>	<u>Presoaked</u>
<u>Unnotched</u>	<u>Average</u>	19.3	21.5
	<u>Range</u>	14.6 - 28.0	13.1 - 37.5
<u>Cleavage</u>	<u>Average</u>	46.5	36.9
	<u>Range</u>	46.3 - 46.6	17.9 - 46.5

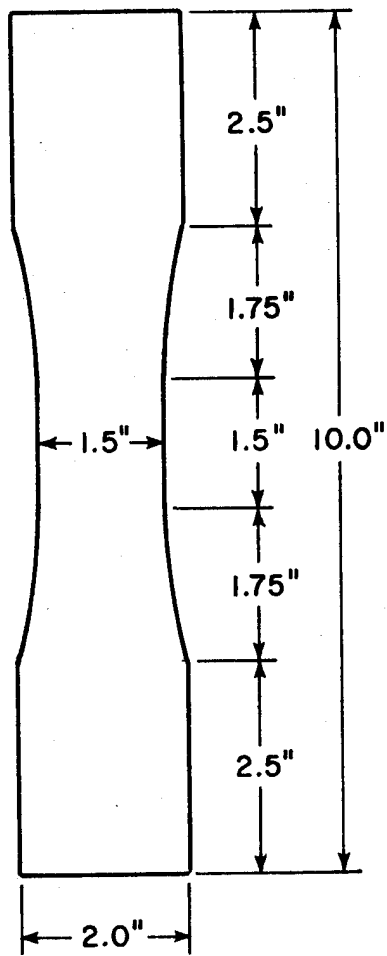
TABLE 5. Effect of Water Immersion on the Lifetime of 0°/90° Scotchply Cleavage Systems Under Static and Dynamic Loading\*

	<u>Static Loading</u>		<u>Dynamic Loading***</u>	
	<u>Dry</u>	<u>Wet</u>	<u>Dry</u>	<u>Wet</u>
<u>Average Lifetime</u> min. or (cycles)	211	877	87.9(10,550)	32.1(3,848)
<u>Range</u> min. or (cycles)	<u>High</u> 240	1,826	91.6(11,000)	39.9(4,770)
	<u>Low</u> 187	324	87.2(10,460)	27.9(3,350)
<u>Average Damage</u>	0.40	0.40	0.70	0.70
<u>Zone Size</u> (in.)**				

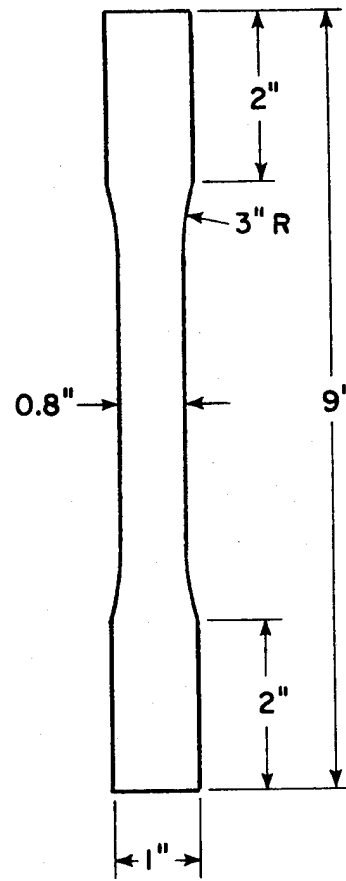
\* Wet : Immersed in distilled H<sub>2</sub>O; dry : 70% relative humidity; temperature : 70-75°F; replication factor 3 (dry), 4 (wet); initial value of  $\sigma_0$  for all tests = 25.3 ksi  $\sqrt{\text{in.}}$

\*\* Average length of subcrack in 0°plies in first 1/2 inch of crack growth.

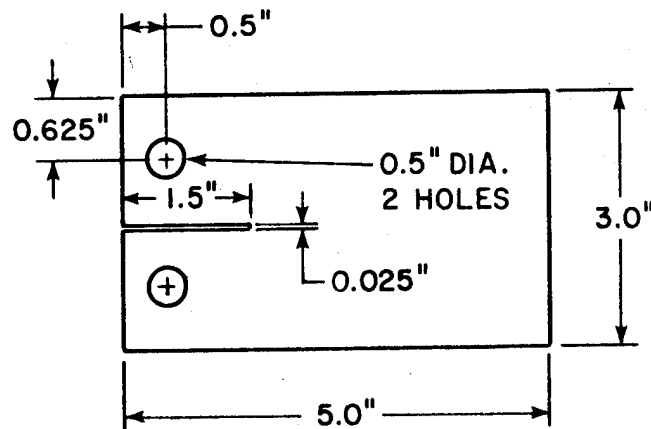
\*\*\* Sinusoidal load vs time, 5 cycle/second.



UNNOTCHED DYNAMIC



UNNOTCHED STATIC



CRACK PROPAGATION

FIGURE 1.  
TEST SPECIMENS.  
-101-

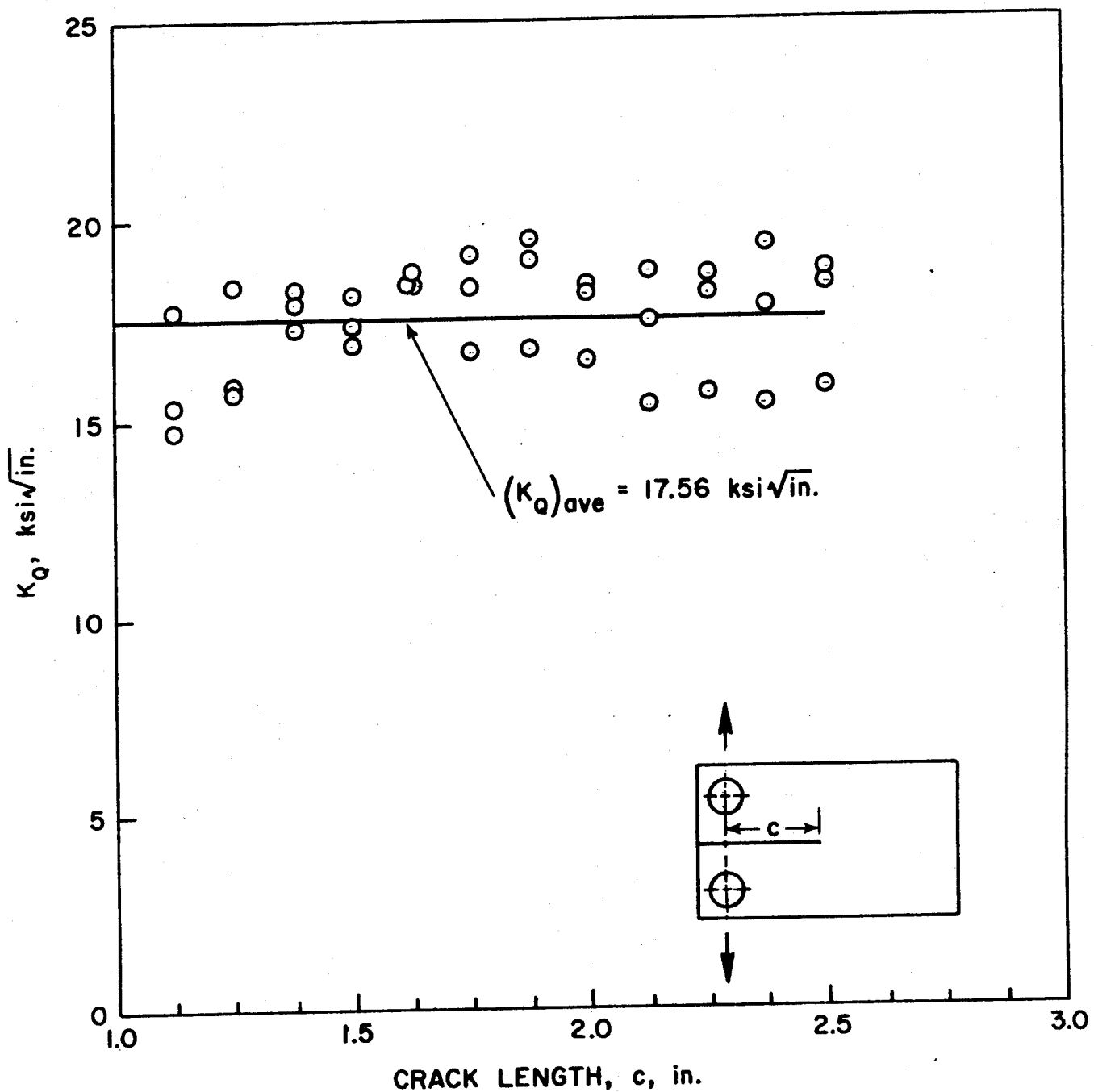
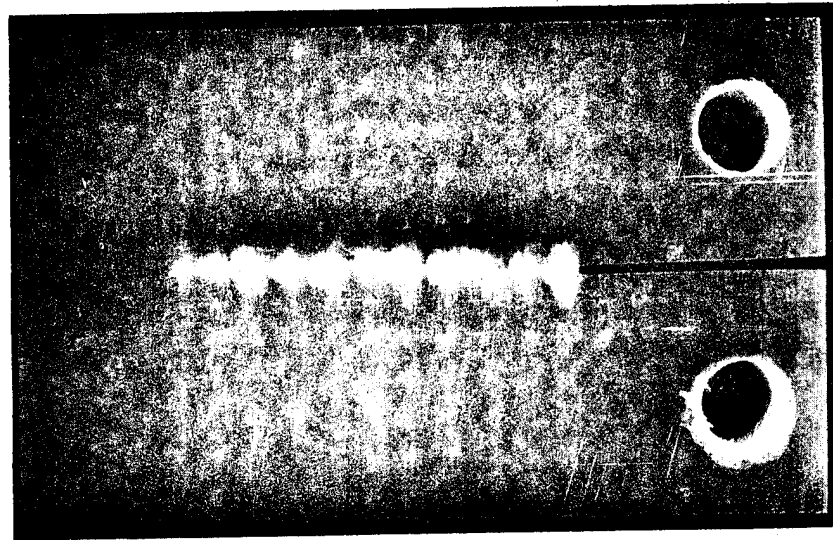
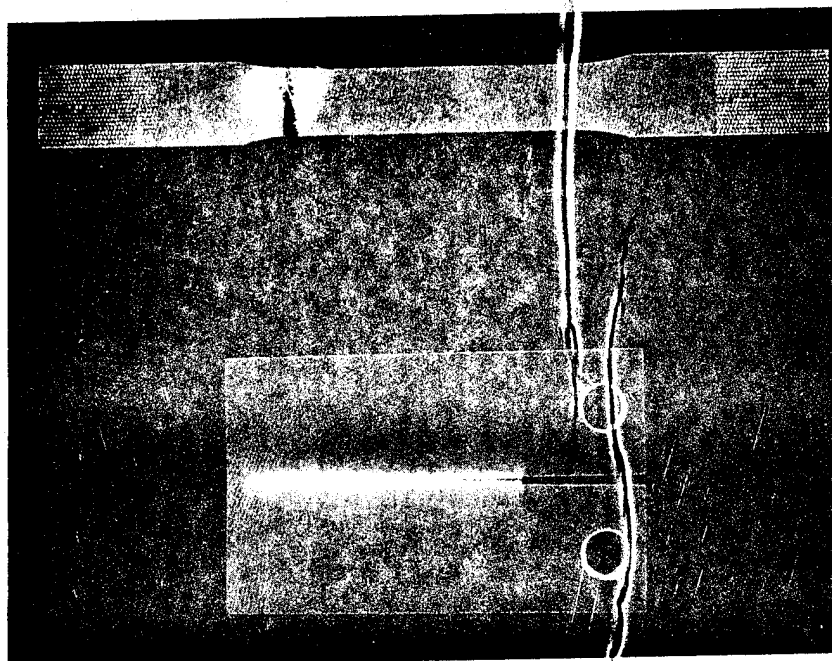


FIGURE 2.  
 $K_Q$  vs. CRACK LENGTH FOR WOVEN ROVING/MAT  
 REINFORCED POLYESTER.



**FIGURE 3.**

**CRACK PROPAGATING IN  $0^\circ/90^\circ$  WOVEN  
ROVING/CHOPPED FIBER MAT REIN-  
FORCED POLYESTER LAMINATE.**



**FIGURE 4.**  
**STATIC FATIGUE SPECIMENS AFTER FAILURE.**

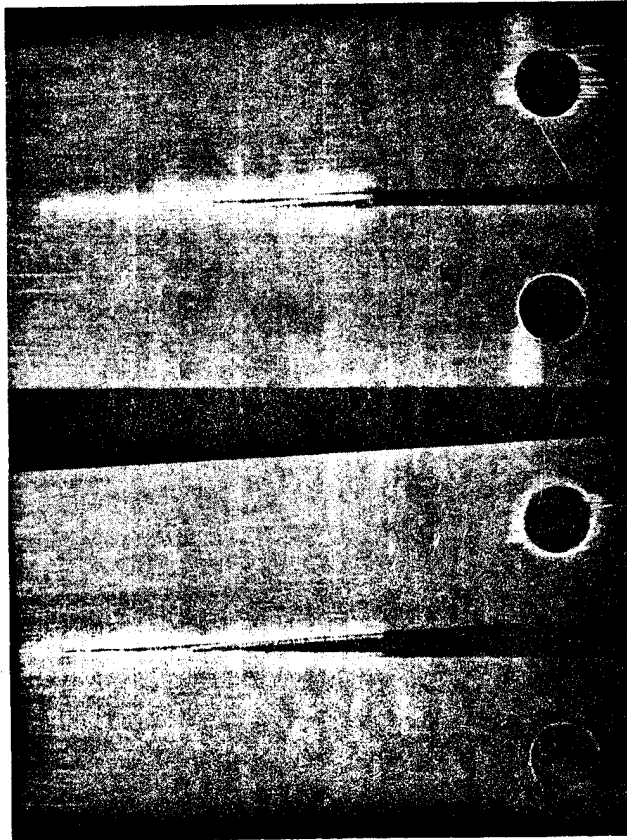


FIGURE 5.

FAILED  $0^\circ/90^\circ$  GLASS/EPOXY FATIGUE SPECIMENS,  
STATIC (TOP) AND DYNAMIC (BOTTOM).

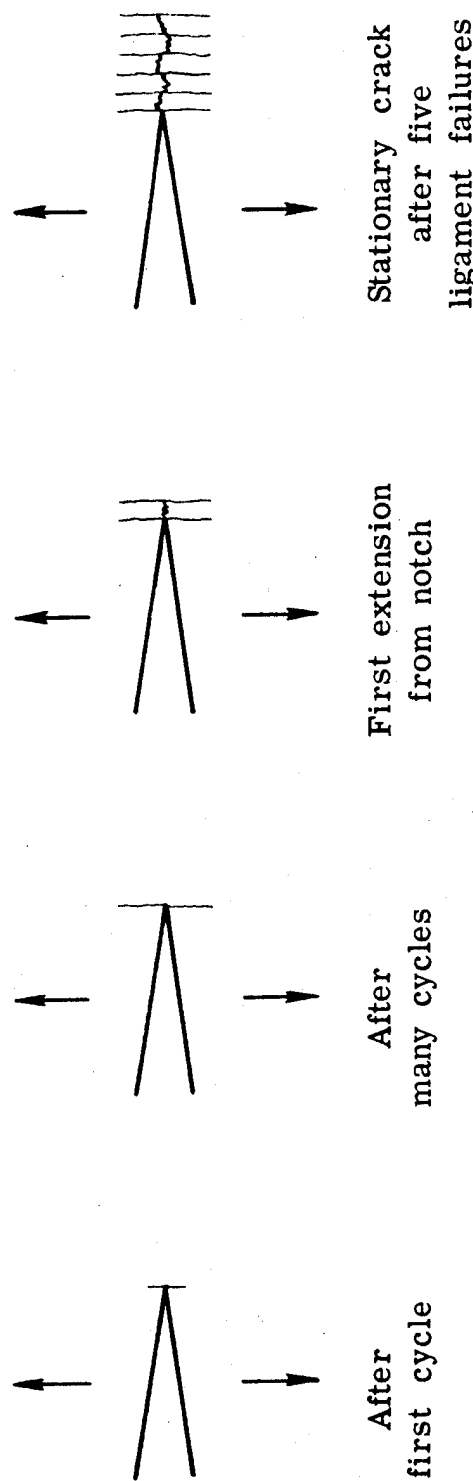


FIGURE 6.

MODE OF FATIGUE CRACK GROWTH IN  $0^\circ$  PLY OF  $(90^\circ/0^\circ/90^\circ/0^\circ/90^\circ)$  LAMINATE, FIBERS PERPENDICULAR TO MAIN CRACK.

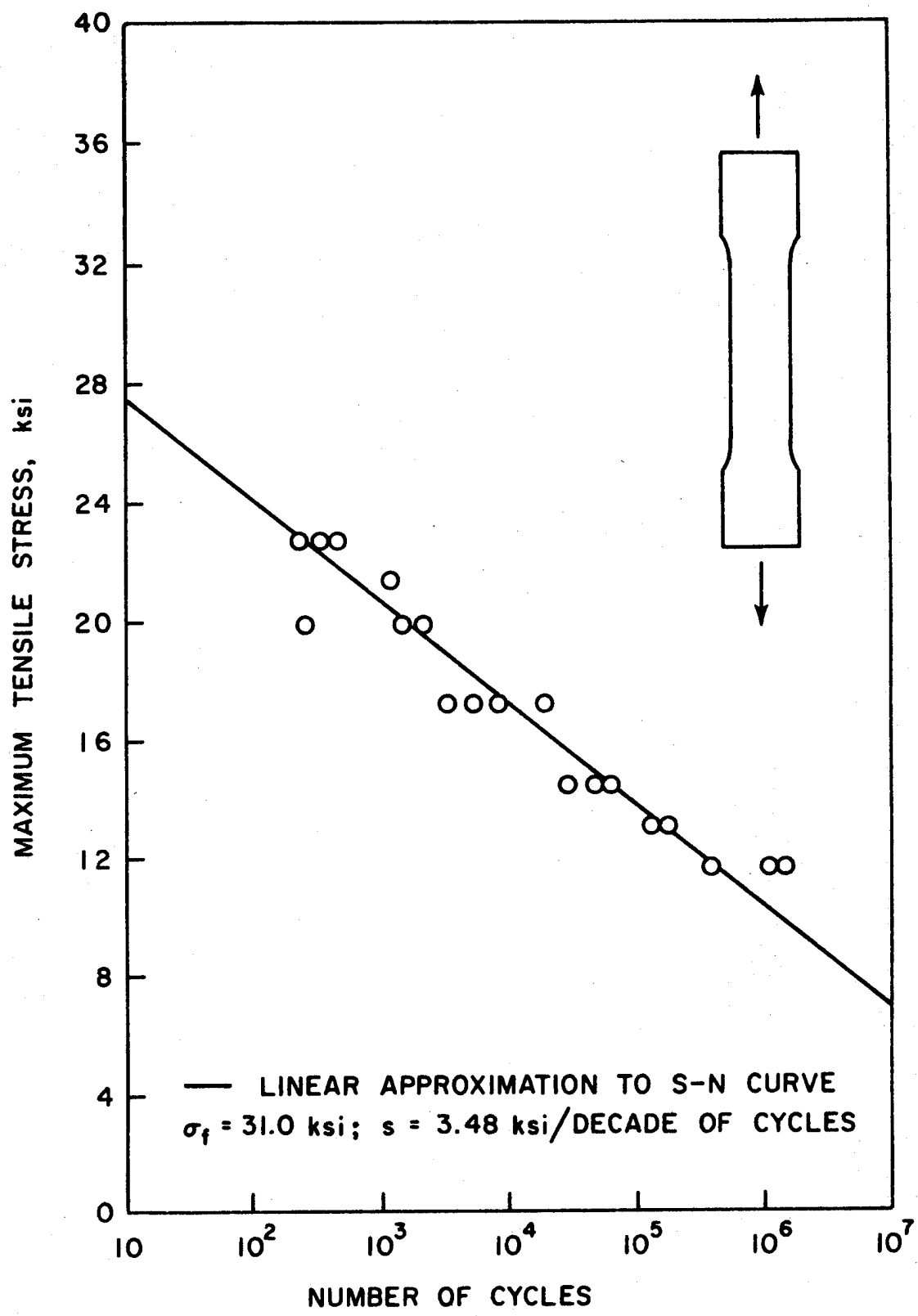


FIGURE 7.  
DYNAMIC S-N CURVE (DRY ENVIRONMENT).

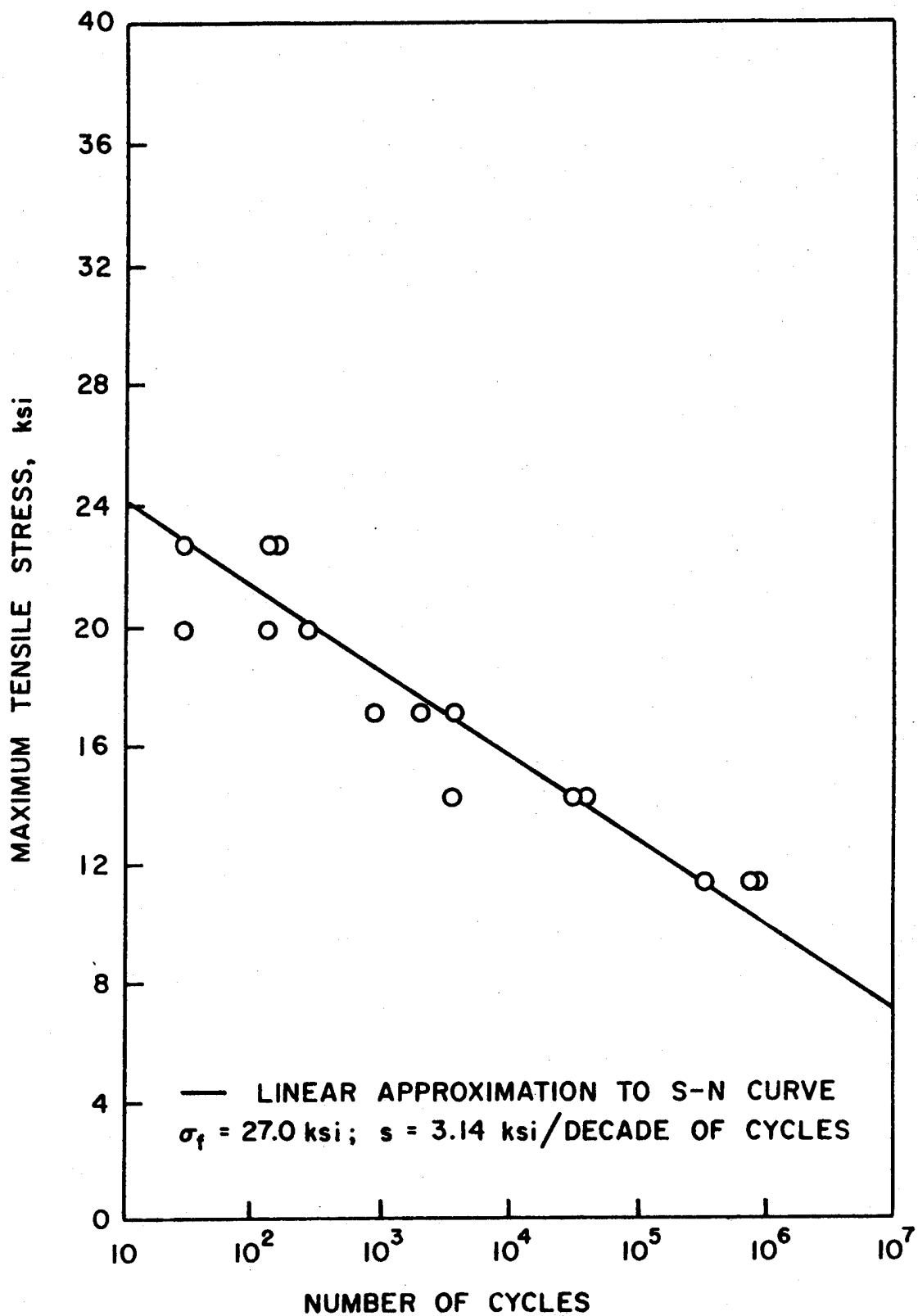


FIGURE 8.  
DYNAMIC S-N CURVE (SALT WATER ENVIRONMENT).

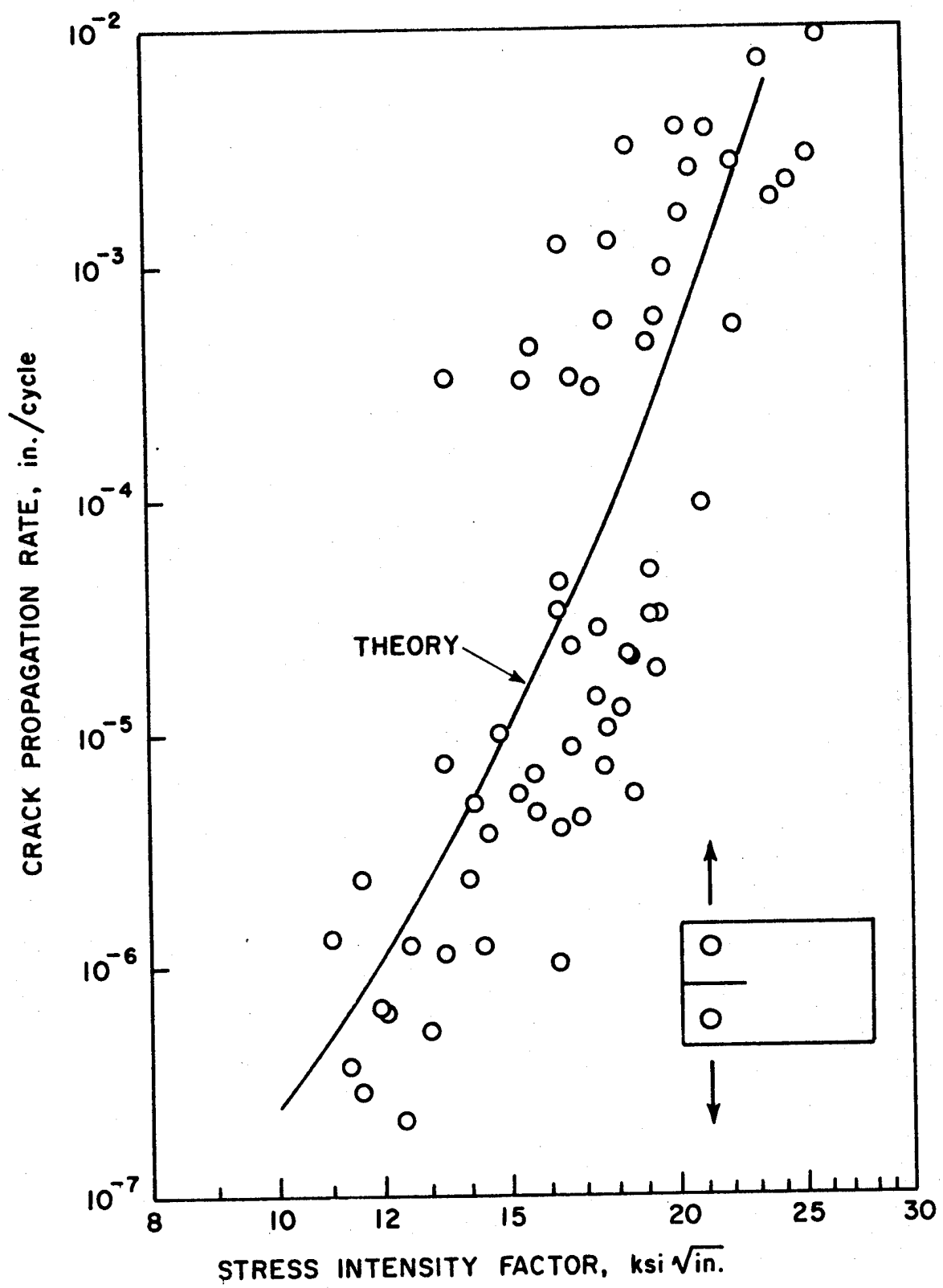


FIGURE 9.

DYNAMIC FATIGUE CRACK PROPAGATION RATE vs. STRESS INTENSITY FACTOR (DRY ENVIRONMENT).

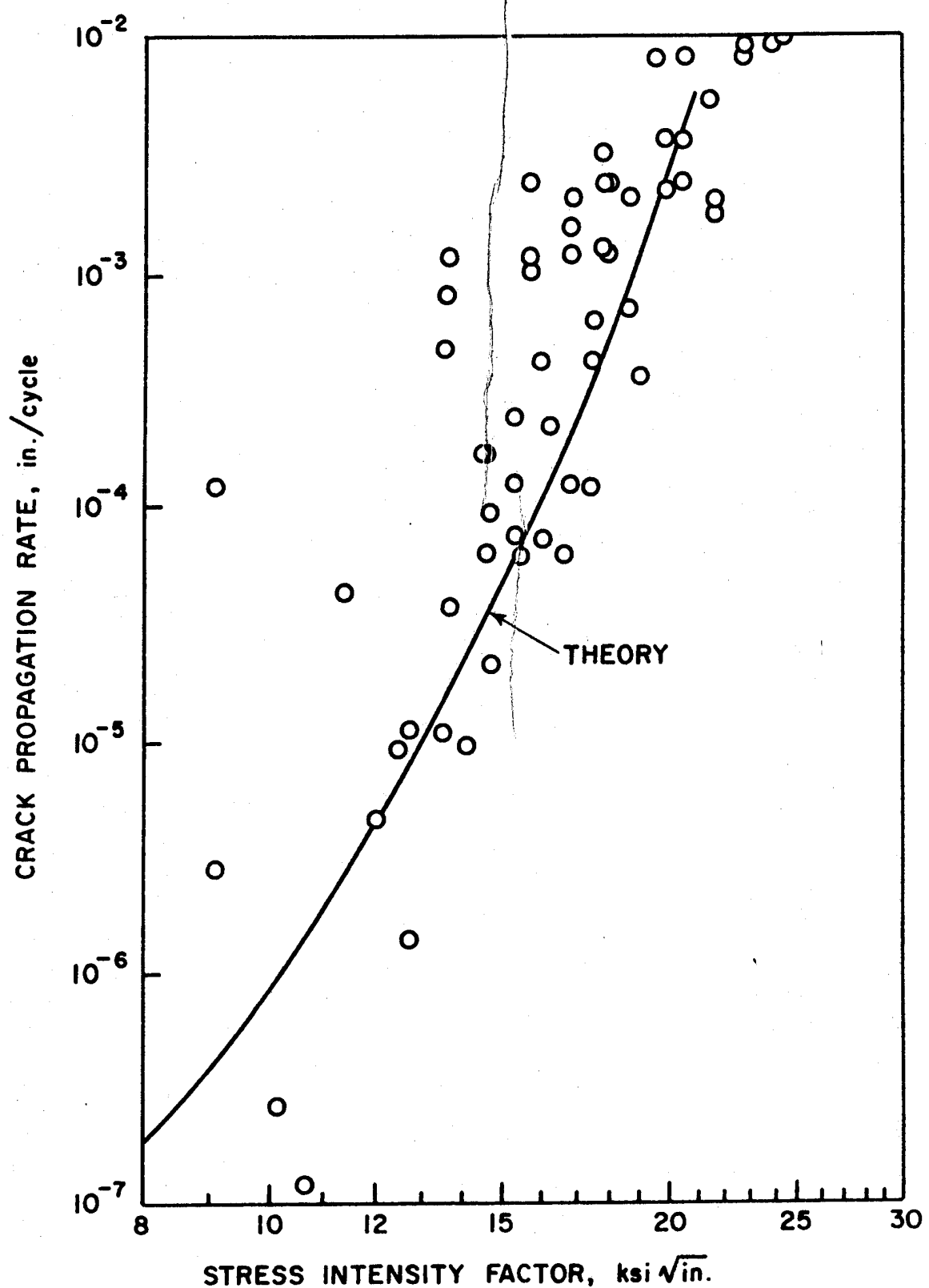


FIGURE 10.

DYNAMIC FATIGUE CRACK PROPAGATION RATE vs. STRESS INTENSITY FACTOR (SALT WATER ENVIRONMENT).

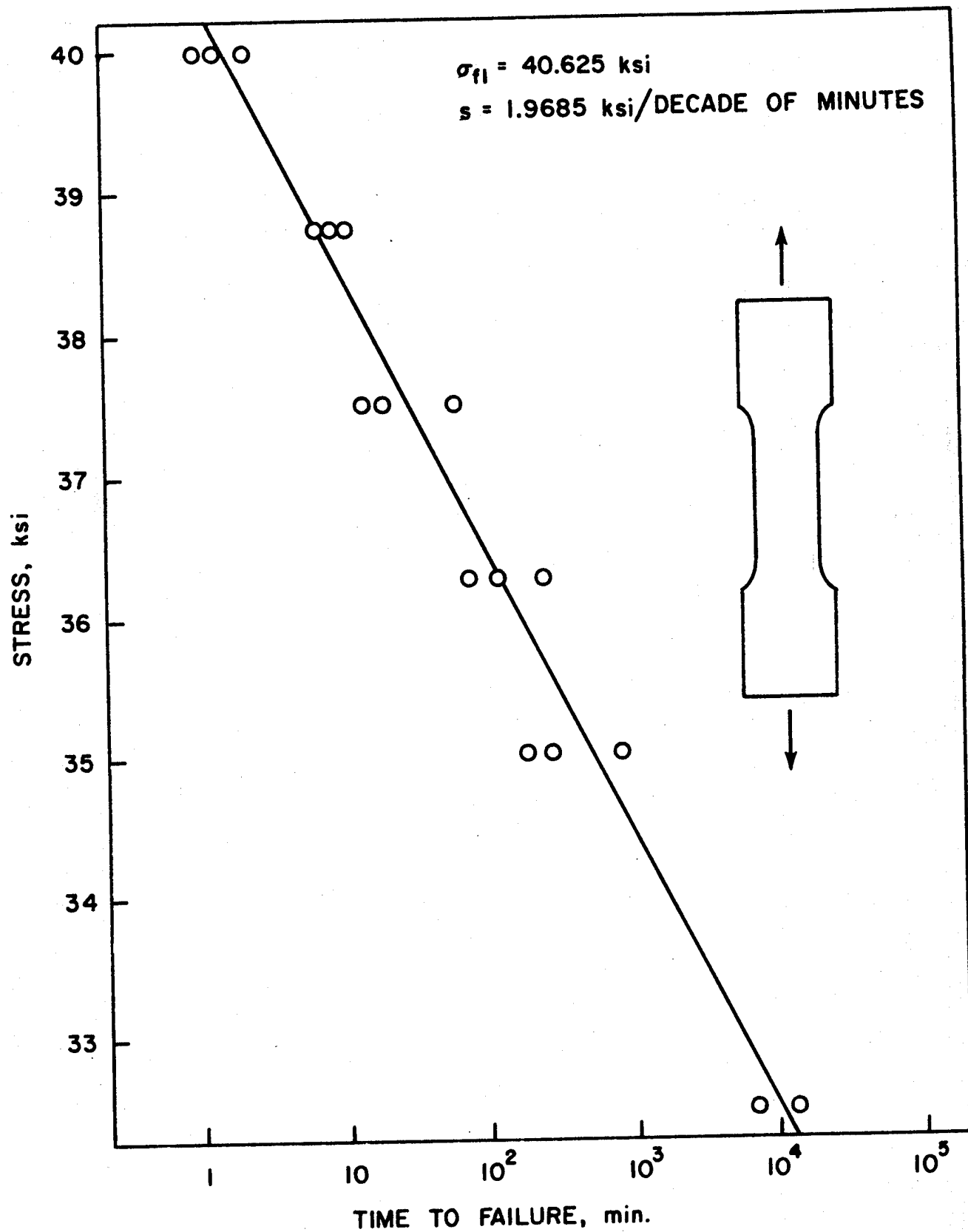


FIGURE 11.  
STATIC STRENGTH-TIME CURVE (DRY ENVIRONMENT).

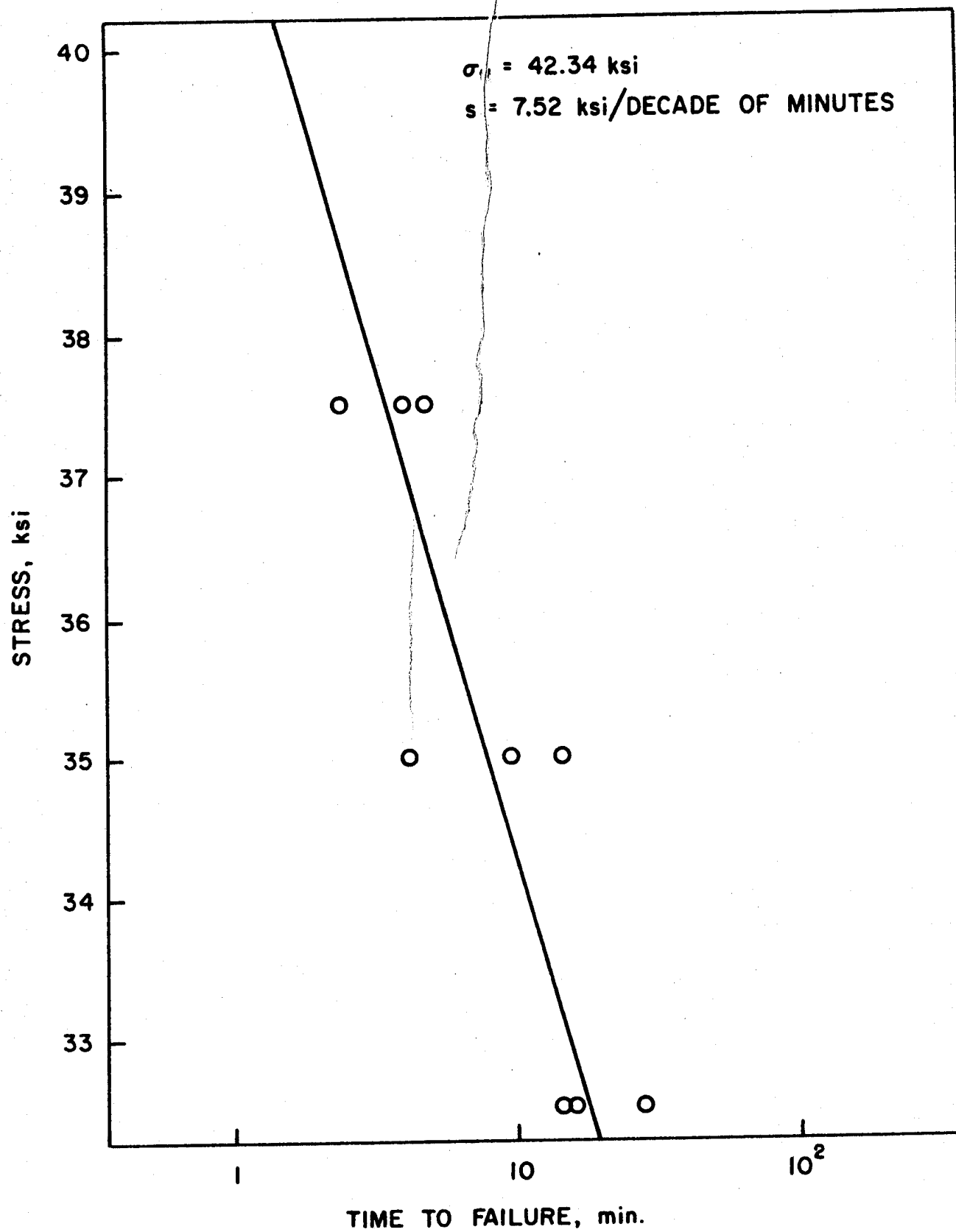


FIGURE 12.  
STATIC STRENGTH-TIME CURVE (WET ENVIRONMENT).

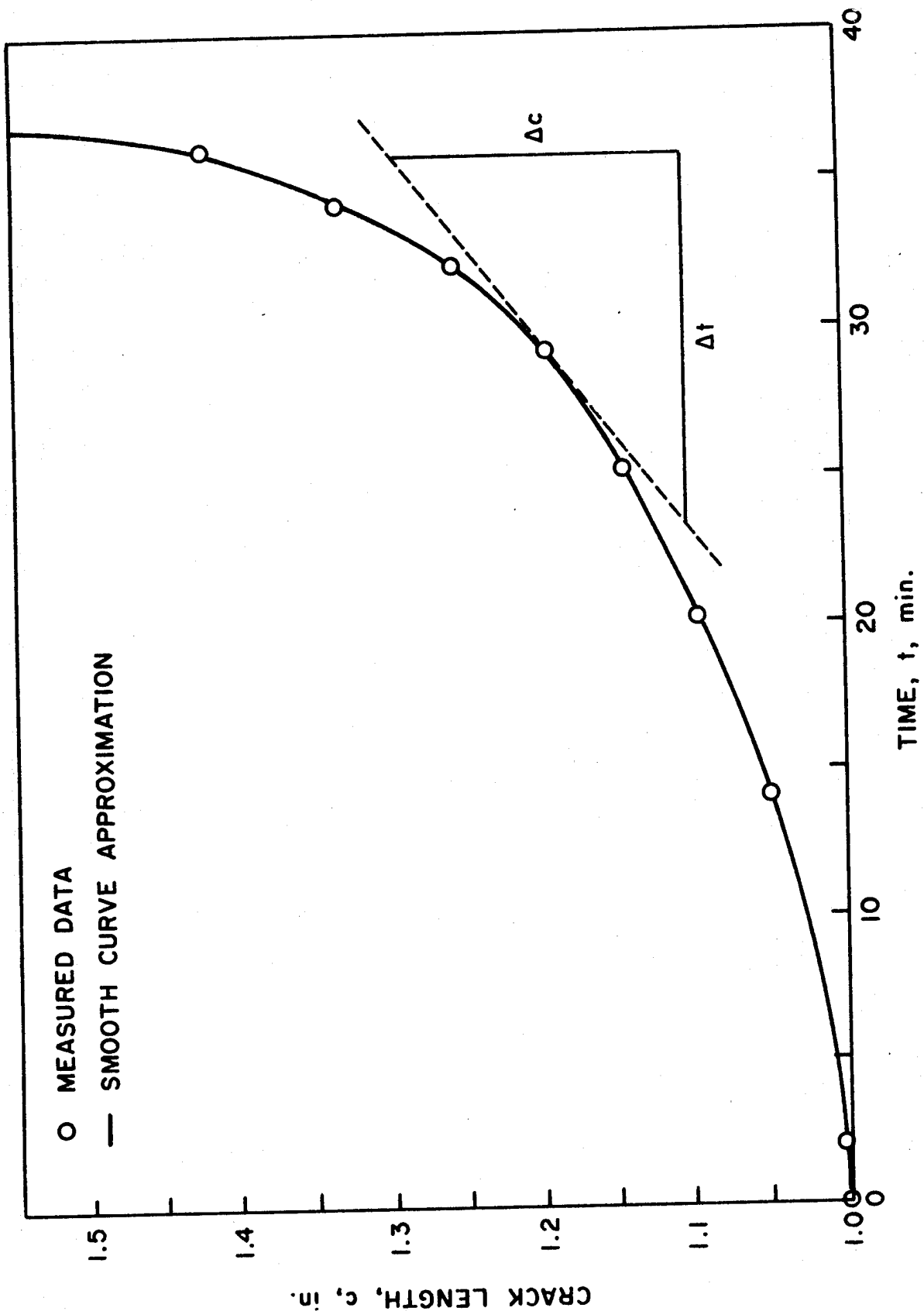


FIGURE 13.  
TYPICAL CRACK LENGTH vs. TIME CURVE, STATIC TEST.

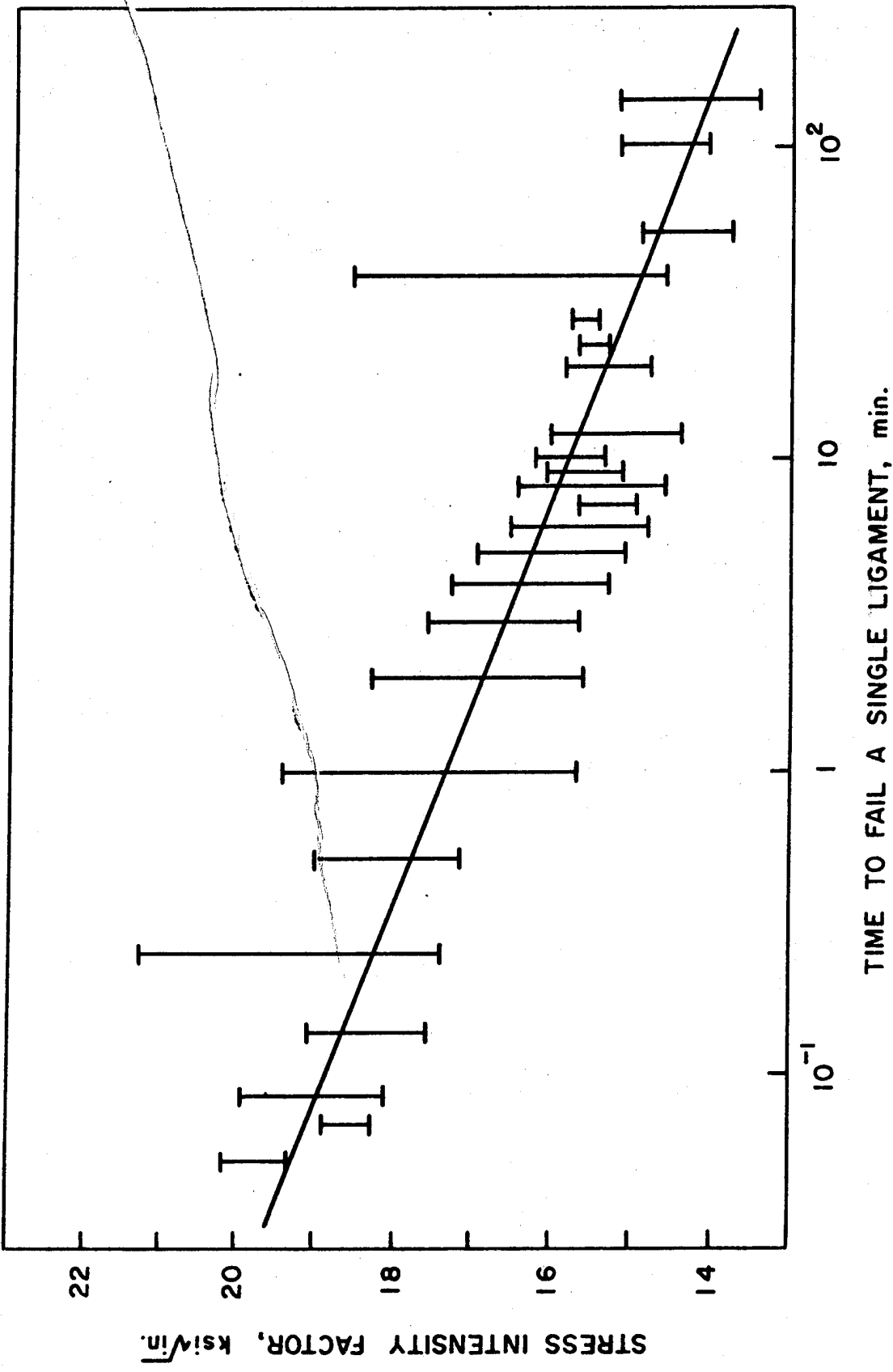


FIGURE 14.  
TIME TO FAIL A SINGLE LIGAMENT vs. STRESS INTENSITY FACTOR, STATIC TEST.

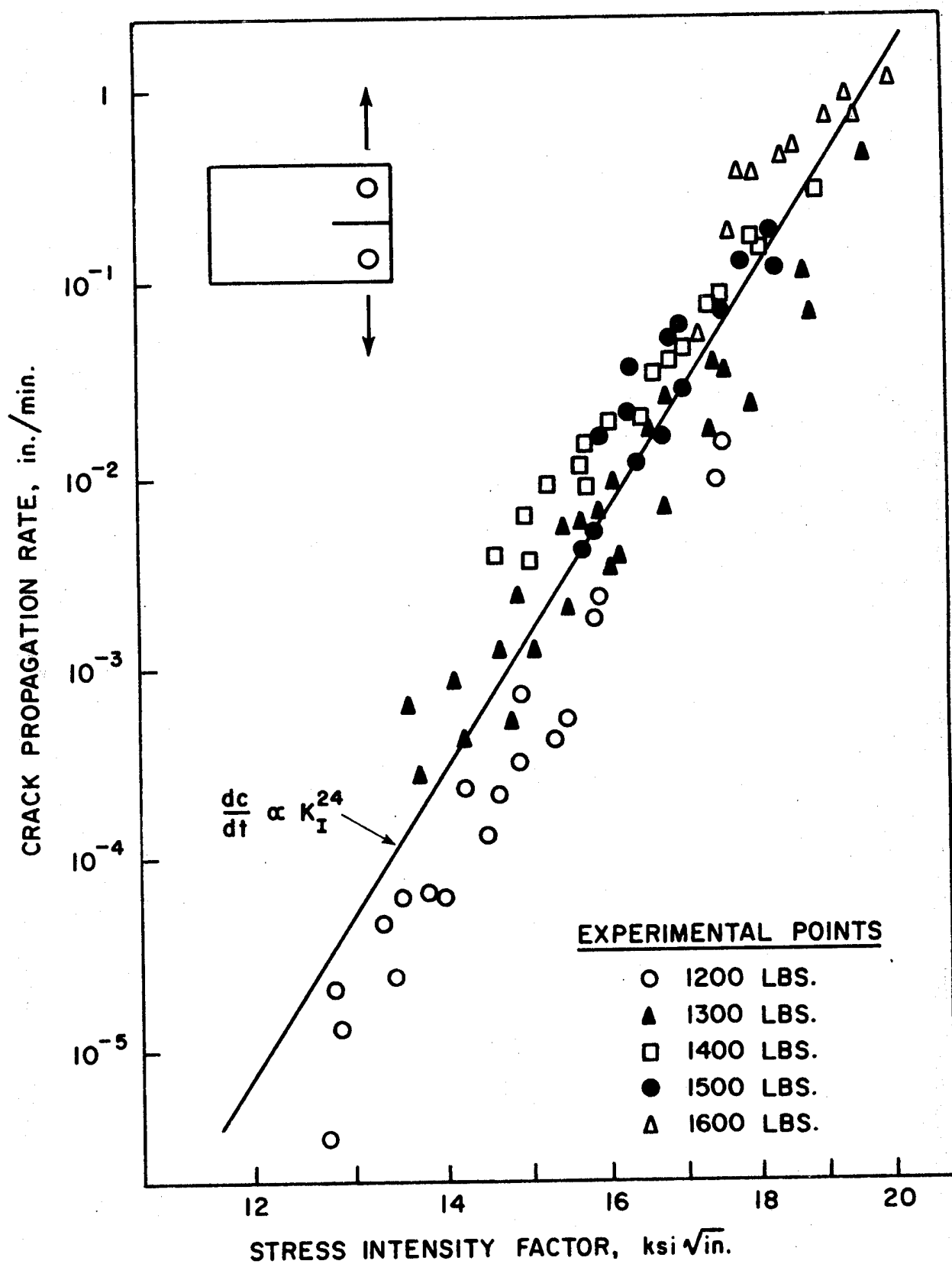


FIGURE 15.

CONSTANT LOAD CRACK PROPAGATION RATE VS.  
STRESS INTENSITY FACTOR (DRY ENVIRONMENT).

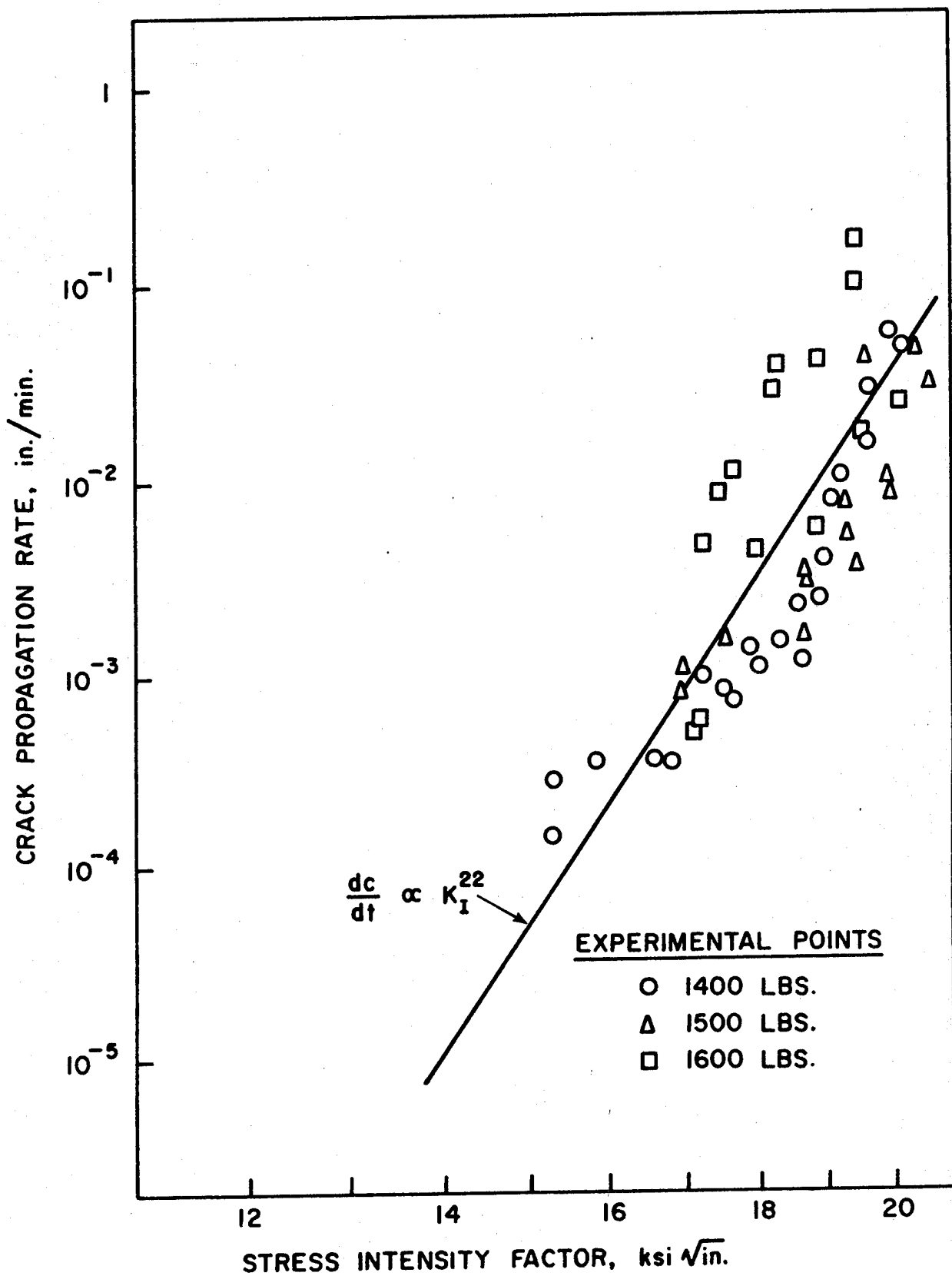


FIGURE 16.  
 CONSTANT LOAD CRACK PROPAGATION RATE vs.  
 STRESS INTENSITY FACTOR (WET ENVIRONMENT).

